THESIS

'FALSE BAKKEN' INTERVAL- SEDIMENT PATTERNS AND DEPOSITIONAL ARCHITECTURE

AT THE FACIES BOUNDARY BETWEEN SILICICLASTIC MUDSTONES AND CARBONATES,

LODGEPOLE FORMATION, MISSISSIPPIAN IN THE WILLISTON BASIN, ND

Submitted by

Joel Spansel

Department of Geosciences

In partial fulfillment of the requirements

Fort the Degree of Master of Science

Colorado State University

Fort Collins, Colorado

Spring 2020

Master's Committee:

    Advisor: Sven Egenhoff

    Sally Sutton
    Joe Von Fischer

ABSTRACT

'FALSE BAKKEN' INTERVAL- SEDIMENT PATTERNS AND DEPOSITIONAL ARCHITECTURE

AT THE FACIES BOUNDARY BETWEEN SILICICLASTIC MUDSTONES AND CARBONATES,

LODGEPOLE FORMATION, MISSISSIPPIAN IN THE WILLISTON BASIN, ND

The lateral facies transition on deep shelves between carbonates and siliciclastic mudstones is largely enigmatic. Based on detailed facies descriptions and interpretations, this study explores which processes have shaped the sedimentary rocks on both sides of this lithological divide, and adds to our understanding of processes operating on deep shelves in general. Both siliciclastic and carbonate rocks of the 'False Bakken' and 'Scallion' intervals of the lower Lodgepole Formation in the Williston Basin, ND, can be grouped into twelve facies: these facies are graded argillaceous mudstone (F1), massive siliciclastic-argillaceous mudstone (F2a), massive calcareous-argillaceous mudstone (F2b), bioturbated pyrtitized bioclast-bearing mudstone (F3), lenticular mudstone (F4), bioclast-rich wavy mudstone (F5), siliciclastic siltstone (F6), glauconitic siltstone (F7), calcareous siltstone (F8), massive to bioturbated carbonate mudstone (F9), nodular skeletal wackestone (F10), and laminated skeletal packstone (F11). These facies are here presented in order of increasing grain size, carbonate content, and bioturbation from F1 to F11. They are arranged in three fining- and coarsening-upward units that can be identified throughout the basin within the succession.

These twelve facies are interpreted to represent distinct processes on a low-inclined shelf system with carbonate occupying the proximal, and siliciclastic mudstones the distal portions of this transect. An overall decrease in energy is reflected from the proximal carbonate to distal siliciclastic facies in this sedimentary system. Nevertheless, most of the mudstone facies still reflect high energy processes operating within the distal portions of the basin; in fact, only one mudstone facies is interpreted to reflect suspension settling under tranquil conditions. Therefore, this study suggests that storm wave base is best placed within the distal siliciclastic mudstones instead of in the proximal carbonates. Carbonate

mudstones, deposited above storm wave base but lacking tempestite deposition are therefore interpreted as having been subject to intense degradation of storm-derived bioclasts. A decrease in oxygen concentration is inferred from proximal carbonates to distal siliciclastics as indicated by the decrease in size and type of burrows; yet, the presence of burrows within the most distal facies belt indicates that at least dysoxic conditions prevailed throughout the Williston Basin during the deposition of the 'False Bakken'.

Three transgressions and regressions are identified within this succession based on laterally correlated facies patterns and indicate an overall increase in sea level from the beginning to the end of 'False Bakken' times. Sediment starvation occurred in the northeastern and/or southwestern portions of the basin as indicated by the presence of glauconitic siltstones and/or lenticular mudstones at various locations within the succession. However, a source of sediment input is interpreted to be located in the northwestern part of the basin based on a high abundance of detrital silt. In addition, a shift in the basin depocenter southwards from Bakken to lower Lodgepole times is reflected in this succession most likely mirroring an increase in subsidence south of Mountrail County during 'False Bakken' deposition.

ACKNOWLEDGEMENTS

TABLE OF CONTENTS

LIST OF FIGURES

INTRODUCTION

The lateral facies transition from carbonates to adjacent siliciclastic mudstones in distal areas remains completely enigmatic and surprisingly underexplored. Most carbonate literature focuses on shallow-marine limestones, be it reefs (e.g., Hubbard et al. 1990; Pomar, 1991; Ritter and Grammer, 2017), lagoons (e.g., Colby and Boardman, 1989; Randazzo and Baisley, 1995; Beanish and Jones, 2002; Klostermann and Gischler, 2015), the shallow shelf (e.g., Nelson et al. 1988; Rankey, 2004), or a ramp system (e.g., Martin et al. 1996; Brandano and Corda, 2002; Pomar et al. 2004). The step from carbonate producing platforms to equivalent facies signatures in adjacent basins is not a far one, so calci-turbidites are similarly well-explored (e.g. Reijmer et al. 1991; Kenter, 1991).

In recent years, siliciclastic mudstones have also received significant attention (Schieber et al. 2007; Schieber and Southard, 2009; Schieber et al. 2010; Macquaker et al. 2010; Wilson and Schieber, 2014), and current-induced processes in these environments once believed to be entirely tranquil have been explored in great detail (e.g. Egenhoff and Fishman, 2013; Borcovsky et al. 2017; Li and Schieber, 2018). However, the intersection where these two rocks, the carbonates and the siliciclastic mudstones, meet has been severely underexplored (e.g. Burchette and Wright 1992). This is insofar surprising as many deep shelves in the world, in the Recent as well as in ancient examples, exhibit this particular transition. This study will therefore propose a model of how such a transition looks in the geological record, and how to unravel sedimentological details to characterize such a facies transition that is likely ubiquitous since carbonates started to form a distinct environment on many shelves worldwide in the Proterozoic (Grotzinger, 1989).

The main unit under study is the 'False Bakken', a siliciclastic mudstone succession intercalated into the lower portion of the Mississippian Lodgepole Formation; in addition, the underlying skeletal wackestones to packstones of the 'Scallion' interval are also assessed (Fig. 1; Mackie, 2013). Based on conodont biostratigraphy, deposition of the lower Lodgepole occurred during the *Siphonodella crenulate*

1

Zone in the Tournasian Stage and is suggested to have commenced prior to the Tournasian-Visean

boundary, although the upper boundary is not well defined due to a lack of conodont data (Holland et al.

1987; Hogancamp and Pocknall, 2018).
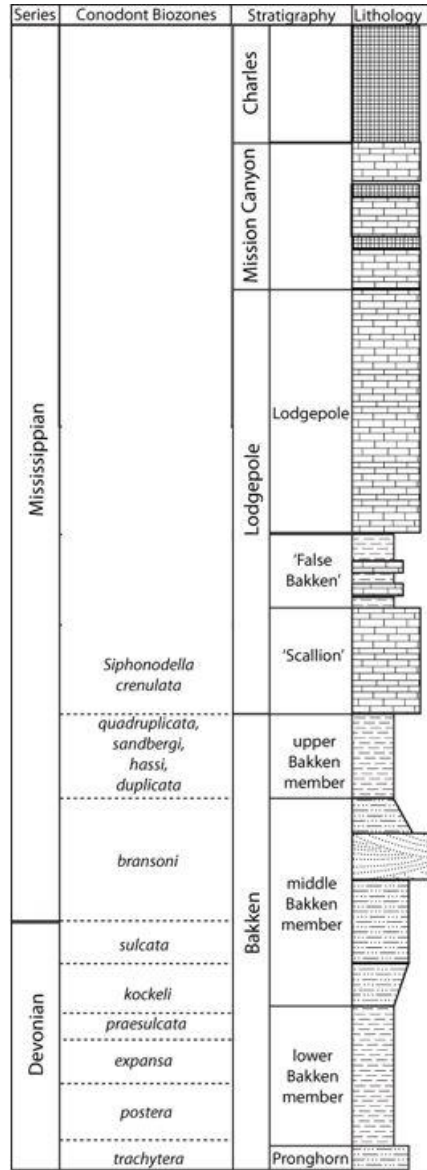
Fig. 1: Stratigraphic column from the Devonian Bakken Formation to the Mississippian Charles Formation modified from Borcovsky et al. (2017). Conodont biozones from Hogancamp and Pocknall, (2018).

GEOLOGIC SETTING

Covering an area of 300,000km^2, the Williston Basin is an intracratonic basin that extends across a large portion of North Dakota, the northwestern portion of South Dakota, the eastern portion of Montana, and the southern portion of Saskatchewan and Manitoba in Canada (Gerhard et al. 1982; Kerr, 1988; Anna et al. 2010). Sedimentation, mainly controlled by sea level fluctuations and episodic, slow subsidence, began in the Cambrian and continued into the Quaternary with the accumulation of about 4,875m of sediments in the deepest section of the basin in northwestern North Dakota (Kerr, 1988; Gaswirth and Marra, 2015). A lack of thick siliciclastic sequences and abundance of carbonates in the Paleozoic indicate the basin was isolated from major orogenic events (Kerr, 1988; Gaswirth et al. 2013), although local structural highs such as the Billings Anticline, Burleigh High, Cedar Creek Anticline, Foster High, and Stutsman High are suggested to have been active highs during the late Devonian-early Mississippian (Ballard, 1963; LeFever and Crashell, 1991; Grover, 1996) in addition to other trends not formerly named (Novak and Egenhoff, 2019; Fig. 2). Paleogeographic reconstructions place the Williston Basin of North America just north of the equator at the end of the Devonian and early Mississippian (Scotese, 1994; Blakey, 2003).

The Mississippian Madison Group reaches a maximum thickness of 610m, conformably overlies the Bakken, and is comprised of carbonates and rare shales of the Lodgepole, anhydrite-bearing carbonates of the Mission Canyon, and evaporites of the Charles Formations (Fig. 1; Carlson and Anderson, 1965; Kerr, 1988). Prior to deposition of the Lodgepole, the Bakken Formation was deposited from Late Devonian to Early Mississippian times (Holland et al. 1987). The Bakken reaches a maximum thickness of 43m and is composed of four units: a basal sand-rich unit, a lower and an upper shale member that are organic rich, and a coarse-grained middle member composed mostly of siltstone and some sandstone (Meissner, 1978; LeFever, 1990; Egenhoff and Fishman, 2013; Egenhoff, 2017).
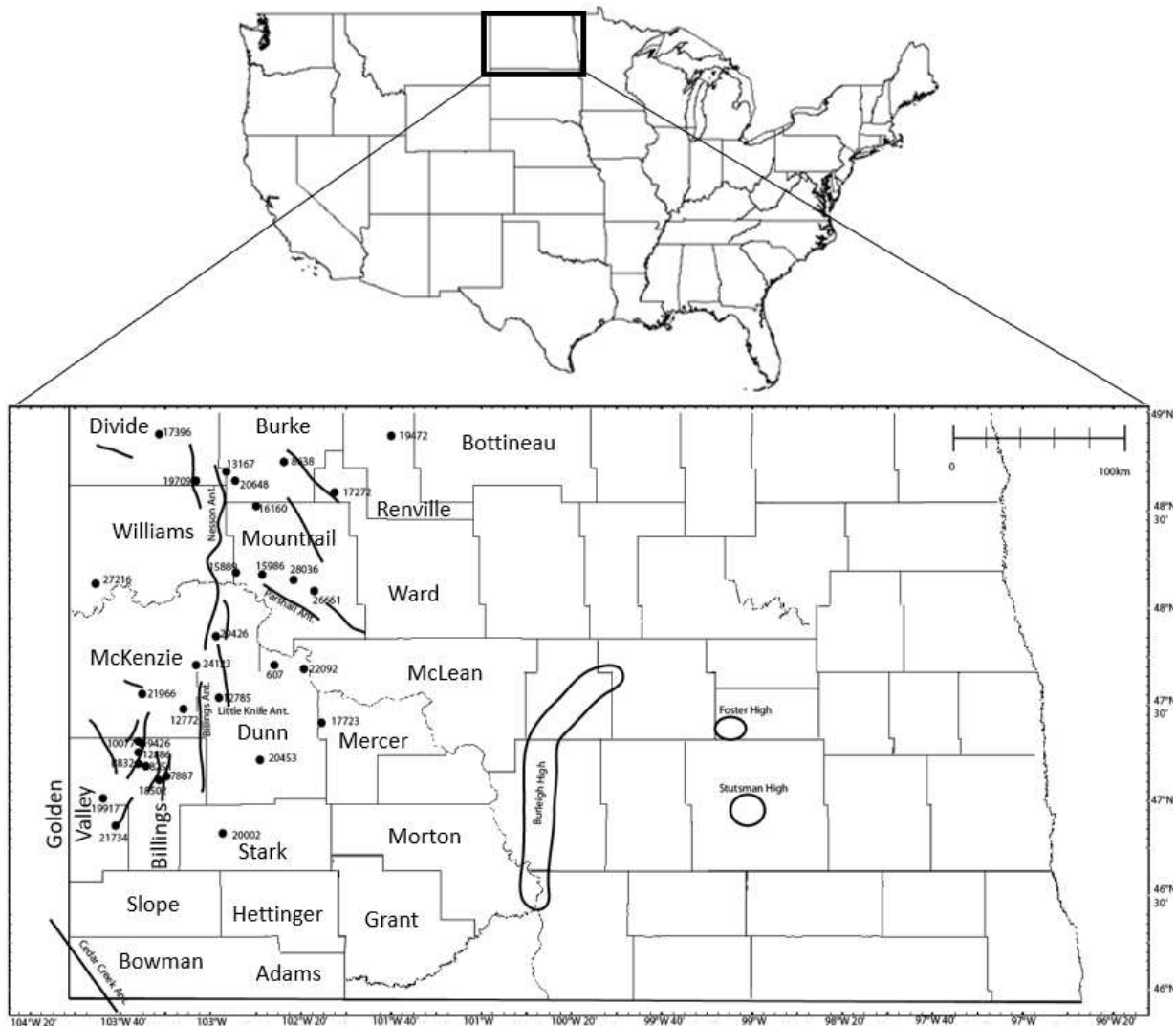
Fig. 2: Location of 33 cores in the western portion of North Dakota. Both core numbers and relevent county names are displayed. Structural highs and anticlines present throughout the Williston Basin at various times. Modified from Novak and Egenhoff (2018) with additional structural highs from Ballard (1963).

The Lodgepole Formation reaches a maximum thickness of 270m in McKenzie County where it consists of mostly limestones with rare shale stringers and thins towards the margins where it is a fossiliferous and oolitic limestone (LeFever and Anderson, 1984; Montgommery, 1996; Stroud, 2011). The 'Scallion' Interval, composed of nodular skeletal wackestones and packstones, conformably overlies the upper Bakken shale member and represents a regression from late Bakken times (Gaswirth et al. 2013; Mackie, 2013; Borcovsky et al. 2017). One to three siliciclastic shales intercalated with carbonate

4

mudstones are informally known as the 'False Bakken' and represent an overall transgression from the 'Scallion Interval' (Montgommery, 1996; Kerr, 1988; LeFever, 1990; Hansen and Long, 1991; Mackie, 2013). The 'False Bakken' is suggested to have been deposited in distal areas on a low-inclined westward dipping carbonate platform and beautifully displays shale-carbonate transitions (Mackie, 2013). The carbonate unit overlying the 'False Bakken' does not have a specific name and is generally just referred to as being part of the "Lower Lodgepole Limestone" (LeFever and Anderson, 1984).

METHODS

Detailed sedimentological analyses were completed for 33 drill cores that penetrated the 'False Bakken' and 'Scallion' intervals of the lower Lodgepole Formation (Fig. 2; see Table 1). All cores are stored at the North Dakota Geological Survey (NDGS) Wilson M. Laird Core and Sample Library in Grand Forks, ND or at the U.S. Geological Survey (USGS) Core Research Center in Denver, CO. Detailed core descriptions on the millimeter to centimeter scale were made with the aid of a hand lens, tape measure, and hydrochloric acid to identify various facies and features. For the purpose of this paper, a facies is best classified as any lamina or bed that reflects a certain composition, grain size distribution, and depositional feature allowing it to be tied to a distinct depositional process.

Ultra-thin thin sections (~20um) were made both perpendicular (n=48) and parallel (n=9) to bedding, as compaction should not impact any depositional features preserved parallel to bedding (i.e., clay clasts and burrows). Additional thin sections (n=16) were borrowed from the USGS to further describe each facies. All thin sections were used for petrographic analyses to identify textures and compositions of various facies identified in core.

Point counting (n=300) was completed on thin sections (n=22) to determine the modal abundance of matrix versus silt grains, as well as the abundance of various grain types within the silt fraction (see Table 2). For other thin sections, modal abundances were determined with the aid of Baccelle and Bosellini (1965) visual diagrams. To determine the mean grain size of the silt-sized fraction of all siliciclastic facies, point counts (n=300) were completed on thin sections (n=26; see Table 3).

An FEI Quanta 450 FEG Scanning Electron Microscope (SEM) equipped with an energy dispersive spectrometer (EDS) at the USGS in Denver, CO, was used to analyze carbon-coated thin sections (n=7) with the most representative siliciclastic facies to identify very small structures and particles (e.g., clay clasts, biogenic grains, burrows, and organic matter; see Appendix III).

6

Table. 1: All wells with geographic locations and core storage locations.						
Number	Well #	Well Name	Latitude	Longitude	County	Location
1	8251	USA #1-24	47.183926	-103.548139	Billings	NDGS
2	18502	TEDDY 44-13TFH	47.111641	-103.415384	Billings	NDGS
3	9426	FEDERAL #12-1	47.30137	-103.54544	Billings	NDGS
4	12886	CONNELL #24-27	47.2567	-103.597082	Billings	NDGS
5	7887	MEE USA #3-17	47.120931	-103.379412	Billings	NDGS
6	10077/E385	FEDERAL 11-4	47.31096	-103.56845	Billings	NDGS/USGS
7	B832	AL AQUITAINE BN 1-23H	47.194467	-103.568295	Billings	NDGS/USGS
8	8638	SLATER #1-24	48.751046	-102.433563	Burke	NDGS
9	20648	GROTE 1-21H	48.663157	-102.834024	Burke	NDGS
10	19773	PRODUCER`S CORPORATION 159-94-17C-8-2H	48.590525	-102.85718	Burke	NDGS
11	13167	SKARPHOL "D" #5	48.708913	-102.898789	Divide	NDGS
12	17396	BLOOMING PRAIRIE	48.879255	-103.438098	Divide	NDGS
13	19709	ROSENVOLD 1-30H	48.661666	-103.132496	Divide	NDGS
14	12785	CARUS FEE #21-19	47.542727	-102.963685	Dunn	NDGS
15	607	ANGUS KENNEDY #F32-24-P	47.711593	-102.522114	Dunn	NDGS
16	22092	MHA 2-05-04H-148-91	47.667005	-102.310361	Dunn	NDGS
17	20453	WALLACE 7-1H	47.213633	-102.635928	Dunn	NDGS
18	21734	OLSON 12-139-104 A 1H	46.863048	-103.749957	Golden Valley	NDGS
19	19917	MAUS 23-22	47.013434	-103.850932	Golden Valley	NDGS
20	24123	MARIANA TRUST 12X-20G2	47.71198	-103.131792	Mckenzie	NDGS
21	12772	AHEL ET AL GRASSEY BUTTE #12-31 H3	47.485595	-103.234115	Mckenzie	NDGS
22	29426	TETON 5-1-3TFSH	47.850828	-102.951089	Mckenzie	NDGS
23	21966	FAIRBANKS 1-20H	47.558227	-103.551635	Mckenzie	NDGS
24	17723	MILLER 34X-9	47.386652	-102.150999	Mercer	NDGS
25	16160	STATE ND 1-11H	48.530775	-102.666355	Mountrail	NDGS
26	26661	WAYZETTA 46-11M	48.094157	-102.212323	Mountrail	NDGS
27	28036	NESS 41-21-2XH	48.152402	-102.375696	Mountrail	NDGS
28	15889	SARA G. BARSTAD 6-44H	48.183932	-102.825858	Mountrail	NDGS
29	15986	J. HORST 1-11H	48.181385	-102.610359	Mountrail	NDGS
30	19472	A TROUT 6H 3-14	48.892306	-101.617541	Renville	NDGS
31	20002	PRAUS 21-28TFH	46.831879	-102.926142	Stark	NDGS
32	17272	IM-SHORTY-159-88- 0805H-1	48.604914	-102.061985	Ward	NDGS
33	27216	LOREN 5303 14-1 2T	48.110300	-103.867388	Williams	NDGS

Facies	Sample #	Matrix	Silt					
			Quartz	Calcite	Bioclast	Mica	PI	AF
Facies 2a	#12886 10505.8	84	9	7	0.0	0.3	0.0	0.0
	#12785 11275	82	12	3	0.3	2	0.0	0.0
	#9426 10782.1	85	9	5	0.3	0.7	0.0	0.0
	#12785 11273.6	85	12	1	0.3	1.0	0.0	0.0
	Average	84	10	4	0	1	0	0
	Std. Dev.	1	2	2	0	1	0	0
Facies 2b	#8251 10375.1	80	6	13	0.3	1.0	0.0	0.0
	#8251 10369.6	84	6	8	1.0	1.0	0.0	0.0
	#18502 10496.7	80	7	13	0.0	0.3	0.0	0.0
	#18502 10500.8	84	5	10	0.7	0.0	0.0	0.3
	#12886 10508.8	75	7	18	0.3	0.0	0.0	0.0
	#15986 10494.1	81	6	13	0.3	0.0	0.0	0.0
	#8251 10377	80	8	11	0.3	1.0	0.0	0.0
	#12785 11276	85	5	9	0.3	0.0	0.0	0.0
	#9426 10785.9	77	7	15	1.3	0.0	0.0	0.0
	#12785 11274.6	87	5	7	0.0	0.3	0.0	0.0
	#18502 10502.1	81	8	9	1.7	1.0	0.0	0.0
	Average	81	6	11	1	0	0	0
	Std. Dev.	4	1	3	1	0	0	0
Facies 3	#12886 10509.7	79	7	12	2	0.0	0.0	0.0
	#15986 10494.5	79	7	10	3	0.7	0.0	0.0
	#12886 10509	85	1	10	4	0.0	0.0	0.0
	#12785 11277.10	91	1	7	0.3	0.0	0.0	0.0
	#20453 10251.6	94	1	4	0.7	0.0	0.0	0.3
	Average	86	3	9	2	0	0	0
	Std. Dev.	7	3	3	2	0	0	0
Facies 5	#9426 10786.6	71	1	10	16	0.0	3	0.0
	#19709 9250.3	67	5	15	13	0.0	0.0	0.3
	Average	69	3	12	14	0	1	0
	Std. Dev.	2	2	4	2	0	2	0

Table 2: Point counts (n=300) to determine modal abundance of various silt grains. PI=Phosphate Intraclast. AF= Agglutinated Foraminifera

Table 3: Silt grain size values from point counting (n=300) siliciclastic facies.					
Thin Section	Facies	Mean	Std. Dev.	Min.	Max.
#12785-11275	1	0.017	0.006	0.006	0.041
#9426	2a	0.018	0.006	0.005	0.046
#12785-11273.6	2a	0.018	0.006	0.007	0.041
#12785-11275	2a	0.018	0.007	0.005	0.051
#12886-10505.8	2a	0.018	0.007	0.006	0.049
#8251-10375.1	2b	0.022	0.007	0.010	0.051
#8251-10377	2b	0.023	0.009	0.008	0.059
#9426-10785.9	2b	0.022	0.007	0.005	0.056
#12785-11274.6	2b	0.022	0.008	0.009	0.060
#12785-11276	2b	0.022	0.007	0.008	0.062
#12886-10508.8	2b	0.022	0.008	0.008	0.061
#15986-10494.1	2b	0.022	0.008	0.008	0.050
#18502-10496.7	2b	0.022	0.008	0.005	0.061
#18502-10500.8	2b	0.022	0.009	0.004	0.062
#18502-10502.1	2b	0.023	0.009	0.005	0.053
#12785-11277.10	3	0.025	0.009	0.009	0.052
#12886-10509.7	3	0.025	0.010	0.010	0.083
#12886-10509	3	0.026	0.012	0.008	0.074
#15986-10494.5	3	0.025	0.008	0.005	0.047
#20453-10251.6	3	0.024	0.008	0.008	0.057
#28036-9698.4	4	0.030	0.009	0.013	0.077
#9426-10786.8	5	0.034	0.013	0.009	0.084
#19709-9250.3	5	0.028	0.010	0.010	0.065
#17396-7942.1	6	0.031	0.010	0.012	0.061
#19709-9251	7	0.036	0.015	0.013	0.109
#17396-7904.8	8	0.056	0.018	0.017	0.122

A total of twelve distinct facies are identified within the 'Scallion' and 'False Bakken' intervals with facies 2a and 2b counting as two facies since they are distinctly different microscopically yet have similar interpretations. These facies were identified from detailed core descriptions, thin section analyses, point counts of grain type and abundance, and/or SEM-EDS analyses. For a summary of these twelve facies see Table 4 and to see the total percentage of facies in each core see Table 5.

Siliciclastic Facies of the 'False Bakken' Interval

Facies 1: Graded Argillaceous Mudstone

Facies 1 accounts for less than 1% of the entire succession and is a dark argillaceous mudstone that occurs as thin, black laminae less than 2mm thick that are laterally continuous across thin sections (Fig. 3a). Macroscopically, this facies can be identified with a keen eye as faint black laminae darker in color than other mudstone facies, but is best described microscopically. Up to 3% of this facies is composed of sub-rounded silt-sized detrital calcite, quartz, and muscovite grains that display normal grading from 0.04mm to 0.005mm in diameter with an average grain size of 0.017mm. The matrix is composed mostly of calcite, quartz, and illite with lesser amounts of potassium feldspar and organic matter. *Phycosiphon incertum* fecal strings up to 0.05mm wide pass through entire lamina in places. A gradual decrease in grain size from the underlying mudstone facies to this facies indicates a gradational basal contact, while an abrupt increase in grain size from this facies to overlying mudstone facies indicates a sharp contact. Diagenetic pyrite, sphalerite, calcite, and apatite are present within this facies.

Facies 1 Interpretation:

The lateral continuity as far as visible in thin section and the fine grain size suggest a very low-energy environment for sedimentation of this facies. Facies 1 laminae were most likely deposited from suspension as no thickness variations are visible in the laminae, and the normal grain size distribution in each of these laminae suggests that these rocks were laid down from a cloud of particles in the water

column that deposited successively finer grains with no additional sediment being supplied to the site of sedimentation. This scenario explains the gradational lower contact of facies 1 laminae recording continued deposition from the underlying rocks; however, its upper, sharp boundary reflects the change in energy during deposition and the onset of a new depositional event, unrelated to facies 1 laminae. It is likely that these fine-grained mudstones were deposited in a dysoxic but not an anoxic environment; this is indicated by the abundance of *Phycosiphon incertum* isp. fecal strings cutting through them. The complete lack of any other burrows in this facies most likely reflects colonization efforts by exclusively an opportunistic life form (cf. Egenhoff and Fishman, 2013). The composition of facies 1 sediments reflects the closeness of these mudstones to a nearby carbonate system yet also shows that some siliciclastic quartz input took place during deposition, most likely introduced into this sedimentary environment by fluvial systems from the nearby Canadian Shield. The composition of the rocks eroded from the Canadian Shield is still reflected in the muscovites that are found in rocks of facies 1.

Facies 2a: Massive Siliciclastic-Argillaceous Mudstone

Facies 2a is a massive, black to dark blue mudstone that shows low effervescence and rare bioclasts in core. The bioclasts, brachiopod fragments, conodonts, and agglutinated foraminifera are in the order of 1mm in length and make up less than 1% of this facies. They are randomly distributed throughout the fine-grained matrix, are generally intact but some being broken, and show various angles relative to bedding. Biotite, muscovite, potassium feldspar, and fecal pellets also occur, are silt-sized and each make up less than 1% of this facies. Mudstones of this facies contain an average of 10% quartz and 4% calcite silt that is 0.018mm in diameter on average and only discernible microscopically (Fig. 3a). The matrix of this facies is dominated by quartz, calcite, micas, and clay minerals, generally with small amounts of organic matter (less than 1%; Fig. 3b). *Phycosiphon incertum* isp. fecal strings up to 0.05mm wide dissect this facies perpendicular to bedding and are best distinguished microscopically by a lack of silt-sized grains and a darker color than the surrounding matrix (Fig. 3c). Diagenetic calcite, sphalerite, apatite, pyrite, and phosphate, the latter in the form of concretions, occur within this facies. This

mudstone can form beds up to 0.5m thick and has a gradational contact with all mudstone facies, but a sharp basal contact with facies 1. In places, dikes from the overlying carbonate facies can be seen intruding into this facies.

Facies 2b: Massive Calcareous-Argillaceous Mudstone

Facies 2b is a massive, black to dark blue calcareous-argillaceous mudstone. It does not differ from facies 2a macroscopically but contains a greater abundance of calcite than quartz silt when compared in thin section, and a coarser silt sized fraction than Facies 2a (see Tables 2 and 3). Sub-angular to sub-rounded silt grains within this facies are 0.022mm in diameter on average and composed of 7-18% calcite (avg., 11%), less than 8% quartz, and a maximum of 1% micas. Intact biogenes and bioclasts of brachiopods (<2mm) and echinoderms (<1mm) make up 1% of this facies or less (Fig. 3d). Agglutinated foraminifera (<1mm) occur in distinct levels of this facies, generally in close stratigraphic proximity (Fig. 3e). All grains and bioclasts are randomly distributed throughout this facies but generally aligned parallel to bedding; nevertheless, they can occur at an angle to bedding in places. *Phycosiphon incertum* isp. fecal strings up to 0.05mm wide are abundant, while *Planolites* isp. burrows are rare. *Planolites* isp. burrows, characterized by a light color, low silt content, and an abundance of calcite and dolomite, are a maximum of 0.2mm high by 0.03mm wide and occur parallel to bedding. Similar to Facies 2a, this mudstone facies usually forms a gradational contact with other mudstone facies, but is intruded by clastic dikes when overlain by carbonate facies.

Facies 2a and 2b Interpretation:

Two processes are most likely responsible for depositing the two mudstone facies (2a & 2b). First, the coarse bioclast and biogenic grains have likely been transported into the environment by high-energy events, probably storms; however, their scarcity indicates that such high-energy events must have occurred relatively rarely in facies 2a and slightly more often in facies 2b settings. Transport of these

grains is reflected in the broken nature of some of the bioclasts; nevertheless, intact shells might not be a good indicator for the absence of transport as many shells do not get abraded much or at all during transport (Miller et al. 1988). The second process indicated by this facies is not easy to identify, and it remains unclear if the bulk of the matrix has been deposited from suspension or as bed load (see Schieber et al. 2007). The large variety of grain sizes in the matrix ranging from clay to silt, however, seems to indicate that these grains were deposited together as marine snow particles. Nevertheless, as no remnants of the marine snow particles are preserved it seems likely that abundant burrowing in facies 2a and 2b probably increased the destruction of the marine snow particles post deposition.

It is likely that the sea-floor was not entirely inhospitable during sedimentation of facies 2a and 2b. Some amount of oxygen must have been present at the sea floor and maybe millimeters into the sediment as indicated by both the agglutinated foraminifera, and the abundance of *Phycosiphon incertum* isp. within facies 2a/b, as well as the rare presence of *Planolites* isp. in 2b. It is therefore assumed here that the environment was most likely dysoxic and not anoxic during deposition.

Facies 3: Bioturbated Pyritized Bioclast-bearing Mudstone

Facies 3 is easily distinguished in core as a massive, brown to black, bioturbated mudstone with pyritized bioclasts (Fig. 4a). Bioclasts make up as much as 4% of this facies and are mostly fragmented and pyritized, but when intact and unaltered can be identified as echinoderms (up to 2.5 by 1mm in size) and brachiopods (less than 3 by 0.1mm in size). Agglutinated foraminifera (0.6 by 0.2mm on average) and conodonts (up to 1mm in length) are rarely found. In most places, these coarse grains are randomly oriented. The silt-sized fraction is mostly sub-angular to sub-rounded, 0.025mm on average in diameter, and composed of up to 12% calcite, 7% quartz, 1% calcispheres, and <1% micas. The matrix is commonly light brown and composed of mostly calcite with lesser amounts of illite, chlorite, and quartz with rare dark patches composed of pyrite (Fig. 4b). *Chondrites* isp. bisects this facies at all angles to bedding from parallel to perpendicular (Fig. 4c). These burrows are identified by a fine grain size, an

13

increase in carbonate or pyrite relative to the surrounding matrix, and are up to 1.5mm across and 0.3mm high. This facies occurs as beds up to 1m thick in most places and often has a gradational contact with overlying and underlying Facies 1 and 2a/b mudstones but may have dikes that come from overlying carbonates.

Facies 3 Interpretation:

The abundance of calcareous fossils and calcite silt reflects a depositional environment that was situated proximal to an area of carbonate production although siliciclastic input is still evident. Coarse bioclasts and detrital grains reflect deposition associated with high energy events (i.e., storms; Borcovsky et al., 2017) with the fine-grained matrix deposited during intermittent tranquil times. Gradational contacts with nearby facies are the result of gradual changes in the depositional environment over significant time periods; however, in some instances carbonate sedimentation on top of this unconsolidated facies may have resulted in the formation of dikes during seismic shocks (Novak and Egenhoff, 2019). After deposition, significant bioturbation by *Chondrites* isp. occurred destroying all potential sedimentary fabrics resulting in the massive bedding. *Chondrites* isp. trace fossils are produced by organisms that can tolerate low oxygen levels (Bromley & Ekdale, 1984). However, the agglutinated foraminifera in this facies indicate the presence of at least some oxygen at the sediment-water interface at times during deposition (Schieber, 2009).

Fig 3a: F1 and F2a

Fig. 3b: F2a
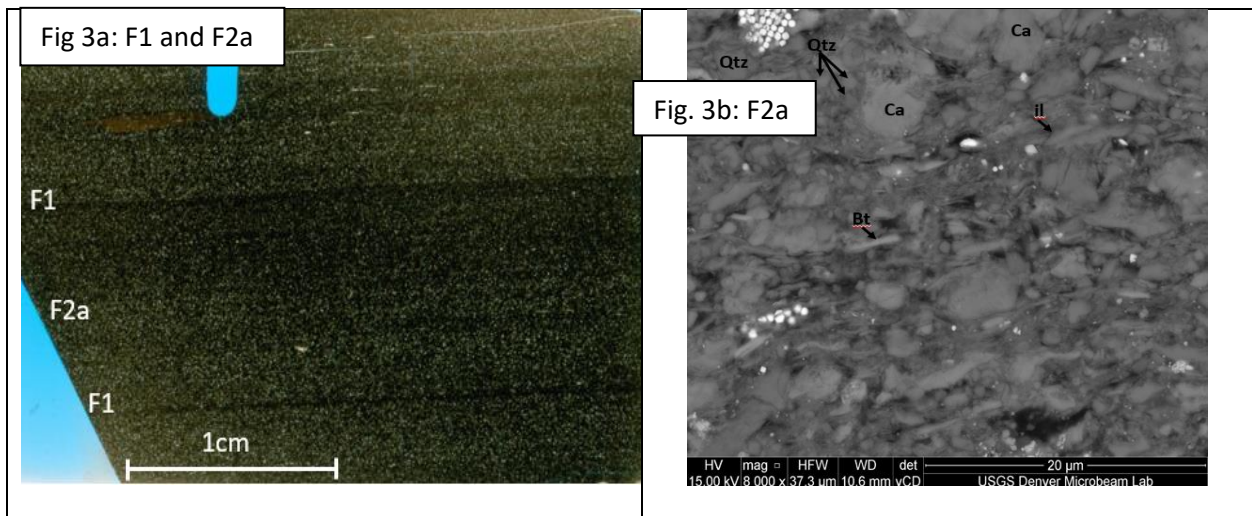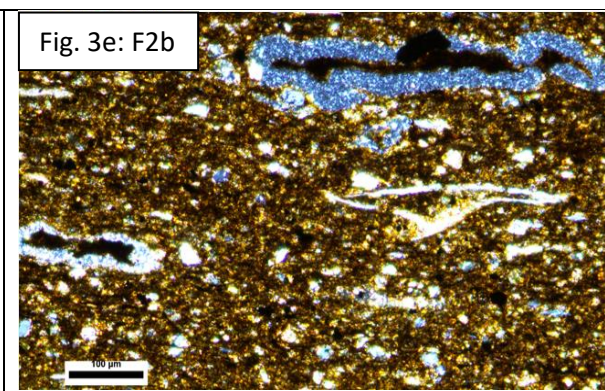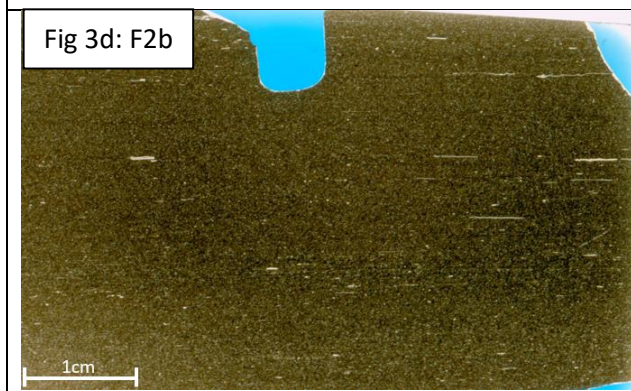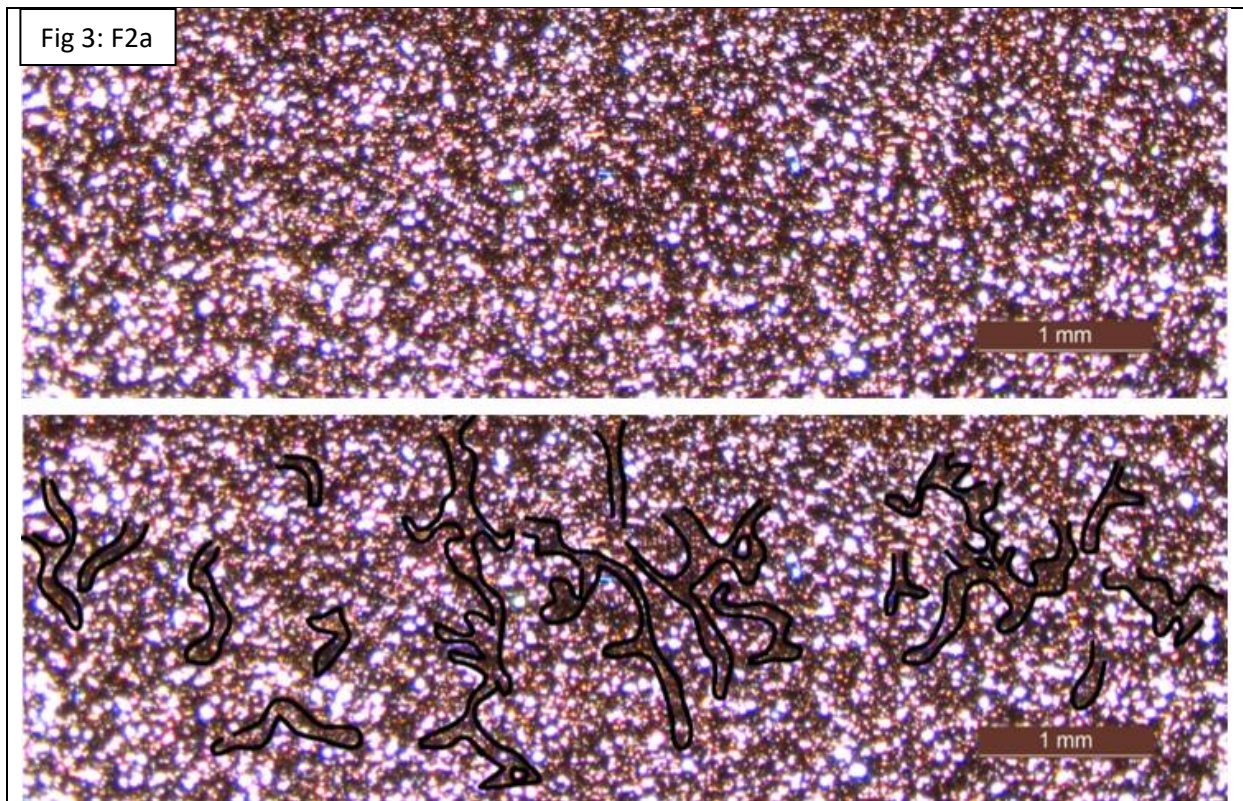
Fig. 3a: Thin section scan of F1 laminae within F2a. F1 laminae are continuous across thin section and contain a low abundance of silt clasts relative to F2a. (#12785-11275)

Fig. 3b: SEM image of F2a matrix with grains labeled. Qtz=quartz; Ca=calcite; il=Illite; Bt=Biotite. (#12785-11275)

Fig. 3c: Two of the same cross-polarized images of *Phycosiphon* isp. dissecting F2a. The top photo displays the burrows without tracks outlined and the bottom photo has some of the burrows outlined in black. (#12785-11275)

Fig. 3d: Thin section scan of F2b that contains bioclasts oriented parallel to bedding and a silt size fraction composed of mostly calcareous silt with some quartz silt. (#8251-10369.6)

Fig. 3e: Cross-polarized image of two agglutinated foraminifera in a brown matrix. In addition, both quartz and calcite silt can be seen distributed throughout this image of F2b. (#12886-10508.8)

Facies 4: Lenticular Mudstone

In core, facies 4 appears as faint brown laminae within other mudstone facies (Fig. 4d) and has a distinct lenticular fabric formed by clay clasts, evident microscopically. Clay clasts are composed of clay sized calcite, quartz, and potassium feldspar, and vary in abundance from 50 to 90% of the volume. Organic matter (<10%) commonly appears as brown to black flakes oriented parallel to bedding and is slightly bent around clay clasts. The silt-sized fraction contains 12% quartz and 5% calcite clasts that are sub-rounded to sub-angular and have an average diameter of 0.031mm. Coarse grains around 1mm in length such as conodonts, agglutinated foraminifera, and brachiopod fragments make up 1% of this facies and are randomly distributed throughout and aligned parallel to bedding. The matrix consists of mostly quartz, calcite, organic matter, and clay minerals with some potassium feldspar and dolomite. *Planolites* isp. burrows occur parallel to bedding, are up to 0.7mm wide and 0.05mm in height, light in color with no silt present, and moderately abundant.

Coarse laminae of this facies, 2 to 5mm thick, are laterally continuous across thin sections and contain a greater abundance of silt (20-40%) and less clay clasts (60-80%) in comparison to thin laminae. Thin laminae (0.2-1.5mm) commonly thicken and thin laterally (Fig. 4e), are continuous across thin sections, contain a great abundance of clay clasts (80-100%), and have low-inclined foresets preserved. Basal contacts are often sharp for both thick and thin laminae, but contacts with overlying facies for thick laminae are gradational and thin laminae are sharp.

Facies 4 Interpretation:

A high energy depositional process is interpreted for this facies based on the presence of clay clasts, coarse silt, bioclasts, and low-inclined foresets. The formation of clay clasts occurs from the erosion of semi-consolidated, water-rich beds on the sea floor by bottom water currents that transport these clasts by traction transport up to 10 km (6mi) (Schieber et al. 2010; Borcovsky et al. 2017). Variability in the abundance of clay clasts versus silt clasts can be attributed to the energy of the flow, the

rate of siliciclastic input into the area of erosion, distance from source, potential reworking, or a combination of those factors. Thin laminae composed almost entirely of clay clasts are interpreted to have originated from an area of sediment starvation with clay clasts being moved by bed load transport during high-energy events, probably storms (cf. Schieber et al. 2010); however, it is unlikely that the currents containing exclusively clay clasts reworked other sediment as no remnants of such sediment has been found in lenticular mudstones. Similarly, thick laminae with 20 to 40% silt and 60-80% clay clasts are associated with high energy events; however, as such currents were capable of transporting both clay clasts and silt together, it is most likely that they reworked the silt from the sea-floor during transport of the clay clasts. However, these clay clasts may have originated from an area of the basin that was not sediment starved allowing for silt and clay clasts to be reworked and transported together. Reworking would also explain why laminae containing clay clasts and silt grains are often thicker than laminae exclusively consisting of clay clasts considering that sediment must have been added in order to increase grain diversity in the laminae.

The presence of agglutinated foraminifera and *Planolites* isp. burrows suggests that at least dysoxic conditions, rather than anoxic conditions, prevailed on the sea-floor during deposition and may have extended several centimeters into the substrate. However, this facies has a high abundance of preserved organic matter attributed to it having a short residence time on the seafloor and/or deposition as organomineralic aggregates (Macquaker et al. 2010; Passey et al. 2010).

Facies 5: Bioclast-rich Wavy Mudstone

Facies 5 is a bioclast-rich mudstone forming laminae and beds that range in thickness from 1mm to 5cm (Figs. 5a, 5b, and 5c), but occurring commonly as beds thicker than 1cm. Disarticulated echinoderms (0.5-1.5mm) and brachiopods (<1.2cm) account for 14% of this facies on average. Rugose corals, agglutinated foraminifera, conodonts, and phosphate intraclasts are up to 1mm in length and compose a maximum of 1% of this facies. The silt-sized fraction makes up to 20% of this facies and is

dominated by calcite (10-15%) and up to 5% quartz grains that are mostly sub-angular to sub-rounded and 0.03mm in diameter on average. The matrix is light brown to dark brown and composed of quartz, clay minerals, micas, calcite, and potassium feldspar. *Planolites* isp. burrows bisect this facies parallel to bedding and are up to 1.5mm in length and 0.2mm in height. This facies commonly has a sharp wavy contact with the underlying mudstone facies, and displays a slight decrease in grain size and abundance up-section within a single bed; in places, bioclasts are intermixed with matrix in these normally graded beds and also decrease in size and abundance up-section. In places, this facies occurs as thin laminae less than 2mm thick composed mainly of brachiopods or echinoderms that are aligned parallel to bedding within a dark brown matrix (Fig. 5c).

Facies 5 Interpretation:

An abundances of bioclasts, coarse detrital silt, and a sharp erosional basal contact all indicate that this facies represents deposition from high energy events capable of transporting up to sand-size material. The volume of bioclasts relative to matrix is interpreted to reflect lag deposition (e.g. storms and/or bottom currents; cf. Schieber, 2017) concentrating large particles such as bioclasts, phosphate intraclasts, and conodonts at the base of event beds. The fine-grained material most likely settled in-between the large components during waning of the depositing flow; the same waning is also reflected in the normal grading observed in individual beds of this facies. The small bioclasts intermixed with matrix overlying the lags are thought to have also been deposited during the waning stages of these high-energy events. The fact that the bioclasts decrease in size and abundance is interpreted to directly reflect the waning stages of the flow. Where exclusively lags occur it is envisioned that only the lowermost part of the event deposit was preserved. *Planolites* isp. forming organisms and agglutinated foraminifera indicate that the environment at the sediment-water interface contained at least some free oxygen to enable them to survive.
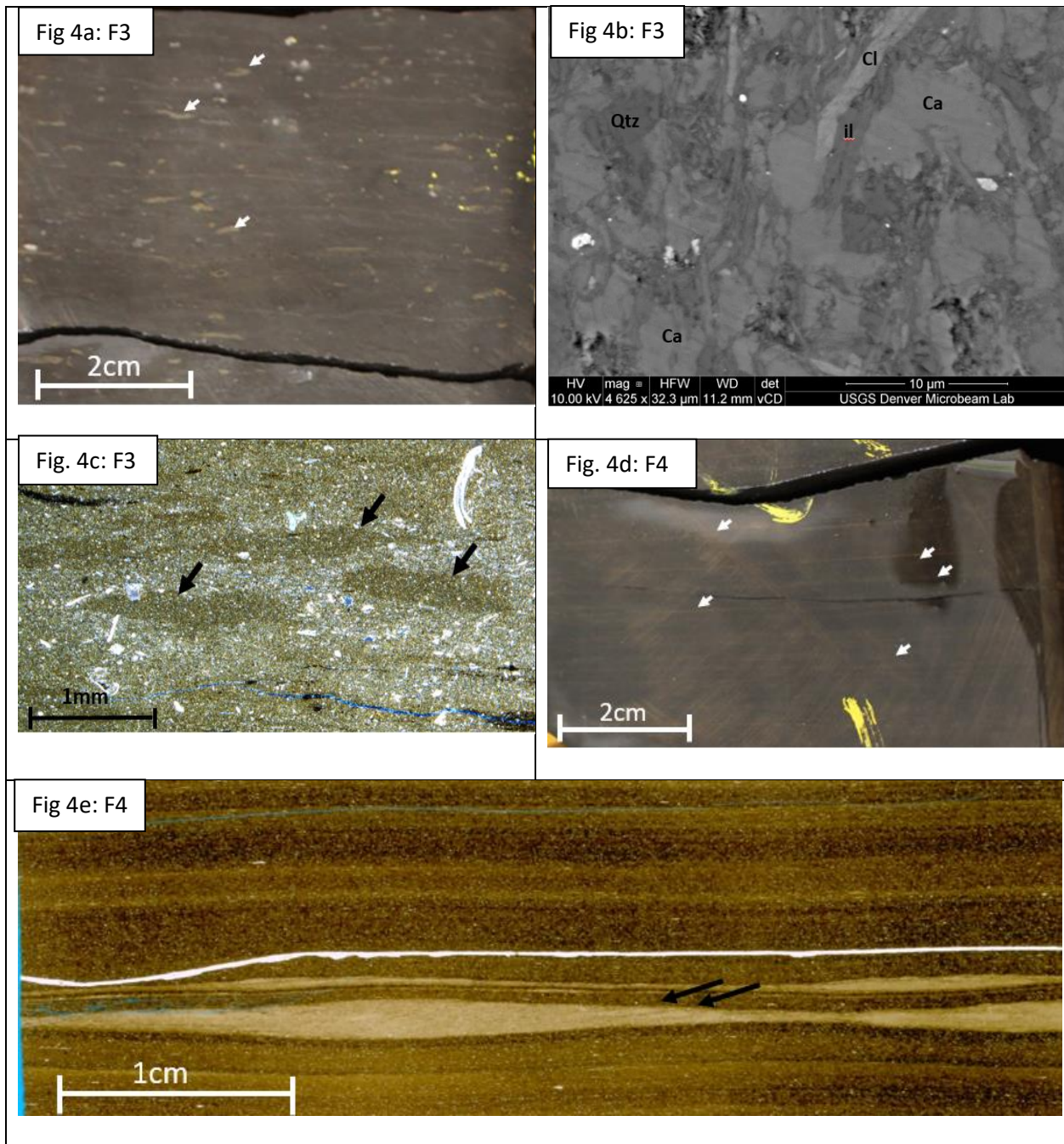
Fig. 4a: Core image of F3 that is easily identified by the abundance of pyritized bioclasts (pointed out by white arrows) in a dark grey matrix. (#20002)

Fig. 4b: SEM image of the calcite rich matrix in F3. Qtz= quartz; Ca= calcite; il=Illite; Cl=Chlorite. (#12886-10509)

Fig. 4c: Plane polarized thin section image with arrows pointing at *Chondrites* isp. burrows in F3. Silt-sized clasts around burrows are predominantly calcite. (#12886-10509)

Fig. 4d: Core image showing faint brown lenticular mudstone laminae (F4) indicated by white arrows. (#21734)

Fig. 4e: Thin section scan displaying lenticular mudstone (F4) laminae composed of entirely clay clasts that thicken and thin laterally.Two black arrows point at low-inclined foresets within individual laminae and the arrows are at the same inclination as foresets (#21734-10369.9)

Facies 6: Siliciclastic Siltstone

Facies 6 is a faintly laminated, black to dark brown, siliciclastic siltstone. This facies occurs as beds up to several centimeters thick and laminae (Figs. 5d and 5e) with a maximum of 55% sub-rounded silt that is on average 0.031mm in diameter. Individual laminae vary in thickness laterally in thin sections. The silt grains are composed of less than 35% quartz and 20% calcite in a matrix made up of calcite, quartz, clay minerals, and rutile. Rip-up clasts are made up of mudstone and are dark brown with silt-sized quartz and calcite grains, clay-sized clay minerals, and organic matter. Phosphate grains, rip-up clasts, conodonts, and bioclasts are a maximum of 1mm in length, oriented parallel to bedding, and distributed evenly throughout. *Planolites* isp. burrows are present with a light brown color and fine grain fill dominated by quartz and calcite. Basal contacts are sharp and planar with other siltstone and mudstone facies, and sharp and wavy with overlying siltstone facies.

Facies 6 Interpretation:

The abundance of quartz silt grains in this facies and the scarcity of matrix indicates a relative high-energy setting for the deposition of siliciclastic siltstones (F6). Rip-up clasts confirm a high-energy setting for these sediments as well as the bioclasts and conodonts which are interpreted to represent lag deposits. These rip-up clasts with coarse silt are interpreted to be from a similar facies as the composition and grain size is equivalent to these siliciclastic siltstones. The fact that many of the laminae show distinct changes in thickness at the microscope scale indicates that bed-load processes were responsible for the deposition of these rocks. Sharp contacts likely reflect rapid changes in the depositional environment associated with pulses of siliciclastic input from a nearby source. The presence of *Planolites* isp. indicate that enough oxygen was present to sustain life within this setting.

Facies 7: Glauconitic Siltstone

Facies 7 contains about 20% glauconite (0.5mm) within laminae up to 8mm thick (Fig. 5d). Brachiopods, echinoderms, and bioclasts are up to 4% of this facies and often less than 1mm in length.

Sub-rounded quartz silt accounts for a maximum of 25% of this facies and is 0.036mm in diameter on average. The matrix is light brown and composed of quartz, clay minerals, and calcite. Both glauconite and bioclasts are randomly oriented in most places but can be aligned parallel to bedding. This facies often has a sharp, wavy contact with underlying and overlying siltstones and varies in thickness laterally.

Facies 7 Interpretation:

The detrital quartz silt and bioclasts within this facies suggests that high energy processes were responsible for depositing both silt and sand-sized grains in this setting. Bed load transport of these coarse grains is indicated by laminae that thicken and thin laterally. The high energy events that transported the silt and bioclasts were strong enough to erode into the underlying beds as indicated by the presence of a sharp wavy basal contact of beds containing facies 8 deposits. After deposition, individual laminae were exposed at the sea floor long enough for glauconite to form (Amorosi, 1995) suggesting that sediment was not continuously supplied to this area. Although bioturbation is not evident, it is likely the cause for the random orientation of coarser grains within this facies

Facies 8: Calcareous Siltstone

Facies 8 is a dark grey calcareous siltstone that appears as faint laminae up to 2cm thick but more commonly forms laminae up to 8mm thick containing rare bioclasts and phosphate intraclasts identifiable in core. Microscopically, silt that is 0.056mm in diameter on average and sub-rounded makes up to 65% of this facies with bioclasts and the matrix accounting for the other 35% (Fig. 5e). Silt grains are composed of a maximum of 35% calcispheres (0.05mm), 15% calcite, and 15% quartz (0.025mm). Brachiopods, phosphate intraclasts, and conodonts are commonly up to 1mm in length and are located at the bottom of laminae or concentrated together in lens-like structures that are laterally discontinuous within laminae; however, calcispheres and quartz silt occur throughout this facies. The matrix is light brown and comprised of mainly quartz and calcite with lesser amounts of clay minerals, dolomite, and rutile. Light brown *Planolites* isp. burrows (<1.5 by 0.2mm) occur in this facies and are often filled

21

with mostly mud sized calcite, quartz, and clay minerals. Beds of this facies vary in thickness laterally and have a wavy, sharp basal contact with underlying facies.

Facies 8 Interpretation:

The coarse silt-sized fraction, bioclasts, phosphate intraclasts, and rip-up clasts in this facies reflect sedimentation by high energy processes. As coarse bioclasts often occur at the base of this facies, it is thought that these are transported by high energy events (i.e. bottom currents induced by storms, e.g. Schieber, 2016) that show a waning stage reflected in the decrease of grain sizes. Bed load processes are indicated by the laminae that thicken and thin laterally in addition to a wavy, likely erosional basal contact. High abundances of bioclasts within laterally discontinuous laminae are interpreted as lag deposits also associated with high energy events capable of scouring into the underlying sediment and depositing coarse-grained material. The great abundance of calcispheres suggests that algal organisms were present within this area or nearby, deposited within this environment and replaced by calcite (Hart, 1991; Scholle & Ulmer-Scholle, 2003). The presence of burrows indicate that oxygen was available in this setting.

Fig. 5a: F5

Fig. 5b: F5

Fig. 5c: F5

Fig. 5d: F7 and F8

Fig 5e: F6 and F8
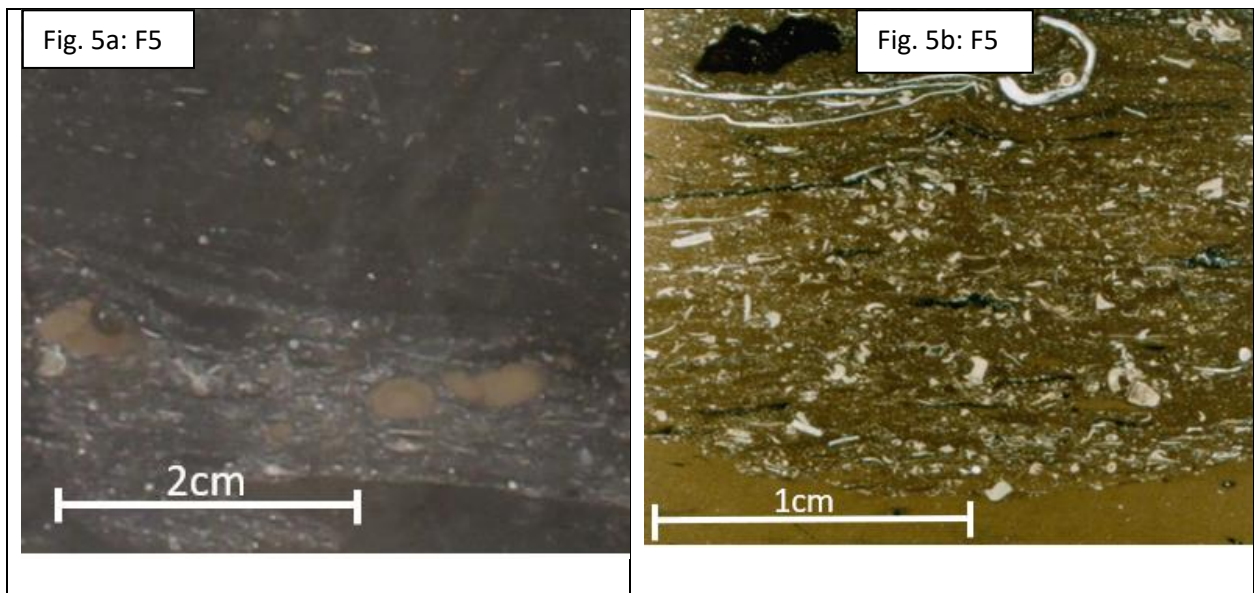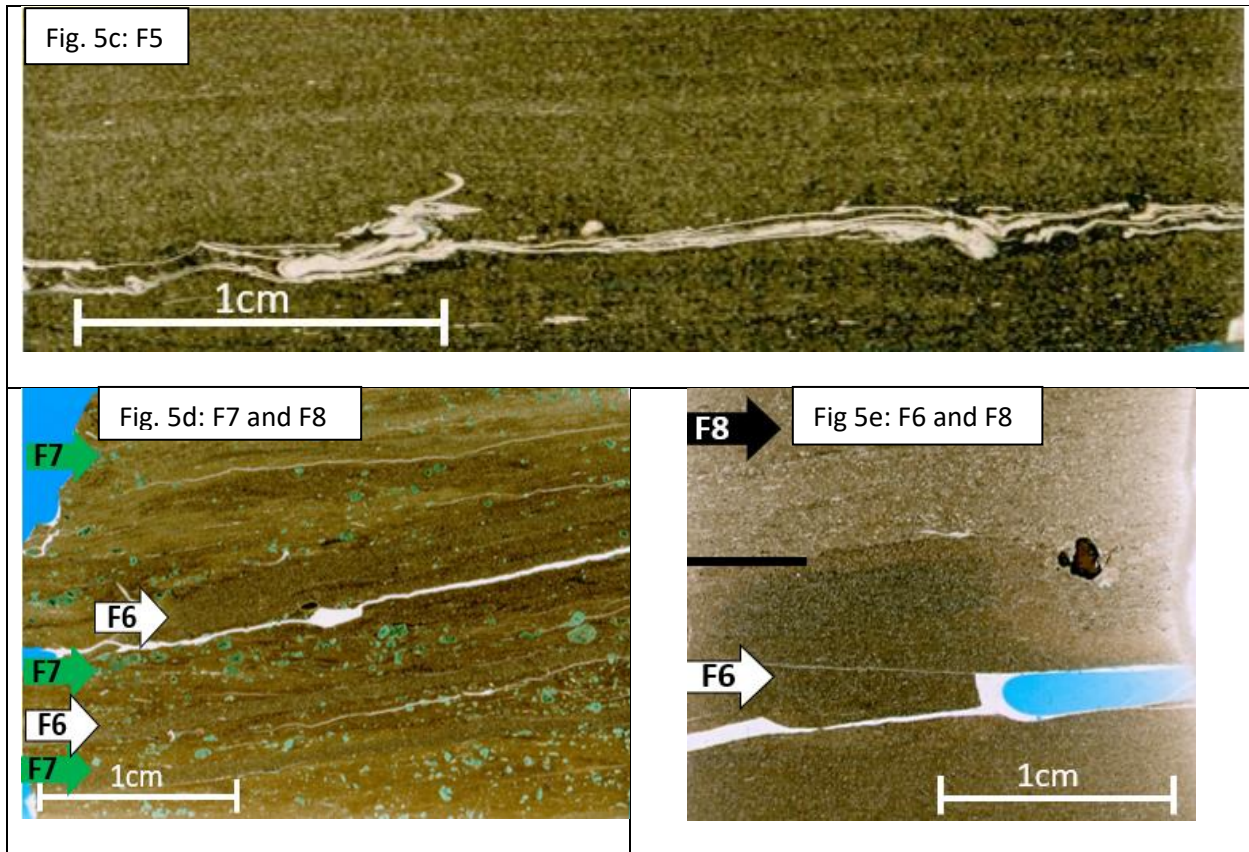
Fig. 5a: Core image of F5 lamina within F3. A great abundance of white bioclasts and some brown phosphate intraclasts are present within the lamina. (#12785)

Fig. 5b: Thin section scan that displays the wavy contact between a thick bioclast mudstone lamina (F5) and the underlying mudstone (F2b). An abundance of bioclast debris is present within this facies in addition to a dark black phosphate intraclast. (#92426-10786.6)

Fig. 5c: Thin section scan of a thin bioclast lamina (F5) composed entirely of brachiopod shell fragments in a dark brown matrix. (#9426-10783.1)

Fig. 5d: Thin section scan of F6 and F7 laminae interbedded with one another and irregular way contacts with laminae that thicken and thin laterally. Can see green glauconite within F7 laminae and an abundance of quartz silt within F6 laminae. (#19709-9251)

Fig. 5e: Thin section displaying the irregular wavy contact between F8 and the underlying F6. F8 is lighter in color and contains more calcite than the underlying finer grained quartz rich siltstone (F6). Notice the wavy contact with a brown phosphate intraclast at the base of F8. (#17396-7915.8)

Carbonate Facies of the 'False Bakken' Interval

Facies 9: Massive to Bioturbated Carbonate Mudstone

This facies is easily identified in core as a light to dark grey, massive or heavily bioturbated carbonate mudstone with up to 3% bioclasts in a matrix composed of carbonate mud (Figs. 6a and 6b). Biogenes, such as echinoderms, brachiopods, gastropods, and ostracods, are randomly distributed and

oriented throughout this facies when present. Calcispheres and detrital quartz account for less than 2% of this facies and are about 0.05mm in diameter. This facies is often massive with skeletal material randomly oriented and distributed throughout, and is bisected by burrows in places. *Zoophycos* isp. burrows cut through this facies at any angle to bedding; these burrows are less than 1cm in diameter, devoid of bioclasts, and display clear back filling spreiten structures (Fig. 6a). This facies can form beds up to several meters thick, and most commonly has a gradational contact with underlying mudstone and carbonate facies.

Facies 9 Interpretation:

This facies is dominated by fine grained carbonate mud suggesting a fairly low depositional energy allowing the fine grained carbonate mud to be deposited. Nevertheless, previous experimental work suggests that carbonate mud floccules can be transported via bed load transport in the same manner as clay clasts (Schieber et al. 2013) and therefore this facies may represent bed load transport despite its fine-grained nature. The coarse fraction of bioclasts, although rare, suggests that some high energy processes capable of transporting bioclasts may have operated within this depositional environment. The presence of quartz silt indicates siliciclastic input reached this setting but was not abundant. Bioturbation has reworked the sediment destroying any potential sedimentary fabrics (i.e., floccule ripples and/or bioclast lag deposits) that may have been preserved resulting in the massive nature of this facies. The large *Zoophycos* isp. burrows suggest high oxygen levels and an overall hospitable environment allowing for relatively large organisms to thrive.

Carbonate Facies of the 'Scallion' Interval

Facies 10: Nodular Skeletal Wackestone

Facies 10 is a nodular, grey to greyish brown wackestone with up to 25% bioclasts and thin shell-rich lamina in places (Figs 6c and 6d). It occurs as massive beds up to several meters thick with 15-20% biogenes and 5-10% bioclasts that are randomly distributed throughout a matrix dominated by calcareous

mud with nodular concretions in places. Skeletal material is 0.5-1mm in length and composed of mostly intact and disarticulated echinoderms (<15%) and brachiopods (<10%) with ostracods, trilobites, and conodonts accounting for less than 3% of this facies each. In addition, detrital calcite silt (0.05mm on average) makes up to 10% of this facies and is distributed throughout. Nodular carbonate concretions are commonly up to 5cm in diameter and are easily distinguished by a dark grey material around the concretions.

Facies 10 Interpretation:

A high abundance of biogenes and bioclasts indicate that these organisms most likely lived in or very close to this depositional environment. The concentration of biogenes and bioclasts in laminae, nevertheless, indicates that high energy storm events operated frequently within this facies allowing for the bed load transportation and abrasion of the bioclasts. The carbonate mud was likely deposited either during more tranquil times or perhaps in a similar manner to the carbonate mudstone facies by bedload transport as floccules (Schieber et al. 2013). Intact biogenes likely lived within the substrate, implying that oxygen levels were high enough within this environment to support a large fauna. Nodular concretions formed from the precipitation of carbonate cements along bedding planes (Mackie, 2013).

Facies 11: Laminated Skeletal Packstone

Facies 11 is a grey to dark grey packstone with biogenes and bioclasts (0.75 to 1.25mm in length on average) generally aligned parallel to bedding (Fig. 6e). Echinoderms (<45%) and brachiopods (<15%) are the most common biogenes in addition to rare gastropods, trilobite fragments, ostracods, conodonts, and phosphate intraclasts (Fig. 6f). Calcite fragments and quartz make up the silt sized fraction (0.06mm on average) of this facies and contain a brown matrix dominated by calcite, clay minerals, and quartz. Shells often align horizontal or at a slight angle to bedding forming laminations up to several centimeters thick. These laminations often occur as packages forming beds up to 25cm thick. Irregularly shaped dark brown clay lenses or thin laminae with low abundances of bioclasts occur within this facies and are

laterally discontinuous (Fig. 6f). In core, a wavy, sharp contact with underlying carbonate facies is often observed, and the contact with overlying mudstone or carbonate facies is generally gradational.

Facies 11 Interpretation:

The high abundance of bioclasts within this facies and erosional contact indicates that this facies was deposited by high energy processes. Biogenes are often found intact likely indicating that they were either transported short distances or lived within the environment. The great abundance of bioclasts and their orientation parallel to bedding reflects strong high-energy events (e.g. large storms) that transported and deposited bioclasts and biogenes via bed load processes. Erosion of the underlying facies occurred from the high energy event resulting in the sharp wavy contact. Large clay lenses within the bioclastic fraction are interpreted as rip-up clasts from nearby that were transported and deposited with the coarse bioclasts. When thin laminae of fine-grained silt and clay occur within this facies it may be a result of more tranquil times between storm events allowing for the deposition of this fine-grained material.

Fig 6a: F9
2cm

Fig 6b: F9
1cm
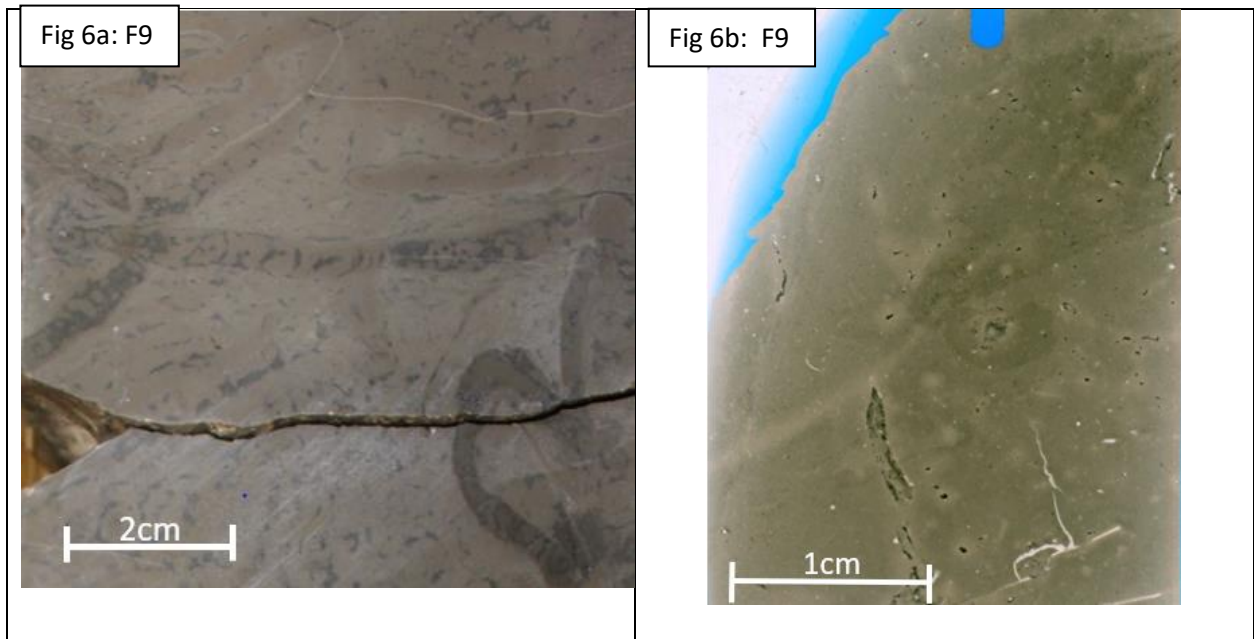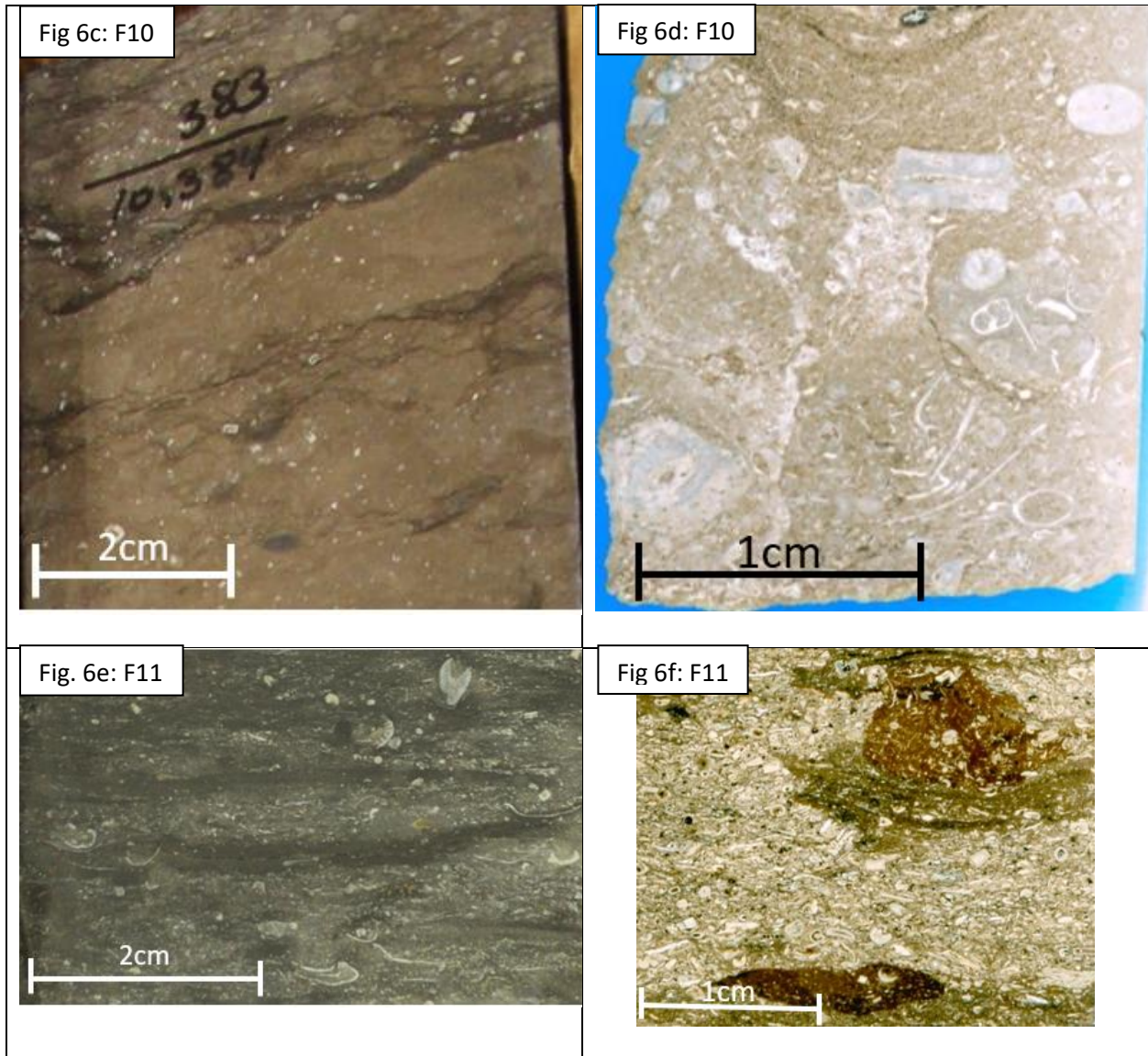
Fig. 6a: Core image of F9 dominated by grey carbonate mud with rare bioclasts. *Zoophycos* burrows seen dissecting this facies at all angles. (#16160-9412)

Fig. 6b: Thin section scan of F9 composed almost entirely of carbonate mud. (#12785-11271.5)

Fig. 6c: An image of F10 in core, a nodular greyish wackestone with bioclasts evenly distributed throughout and irregular dark brown laminae. (#8251-10384')

Fig. 6d: A thin section scan of F10 with an abundance of bioclasts suspended in a brown matrix. (#16160-9420.5)

Fig. 6e: A core image of the laminated skeletal packstones (F11) that contain a high abundance of bioclasts within irregular laminae. (#12785-11278')

Fig. 6f: A thin section scan of laminated skeletal packstones with an abundance of bioclasts distributed throughout. Several clay lens that are brown in color occur within this thin section. (E385-10759.1)

Facies	Thickness and Sedimentary Structures	Upper and Lower Contact	Silt Grains	Mean Silt Grain Size (mm)	Biogenes, Bioclasts, and/or Other Sand-Sized Grains	Burrows
Table. 4: This table lists all facies in order with the main distinguishable features present for each facies.						
F1: Graded Argillaceous Mudstone	Laminae (2mm); Normal Grading	Upper-Sharp; Lower-Gradational	Quartz (2%), Calcite (1%), and Micas (<1%)	0.017	n/a	*Phycosiphon incertum* isp. (<0.05mm)
F2a: Massive Siliciclastic-Argillaceous Mudstone	Beds (5cm to 50cm)	Upper-Gradational; Lower-Sharp	Quartz (8-12%), Calcite (1-7%), Micas (<1%), and Potassium Feldspar (<1%)	0.018	Bioclasts, Brachiopods, Conodonts, Agglutinated foraminifera are about 1mm and make up less than 1% of facies	*Phycosiphon incertum* isp. (<0.05mm)
F2b: Massive Calcareous-Argillaceous Mudstone	Beds (5cm to 50cm)	Upper-Gradational; Lower-Sharp	Calcite (7-18%), Quartz (<8%), and Micas (<1%)	0.022	Bioclasts, Brachiopods, Echinoderms, and Agglutinated foraminifera are <2mm and make up less than 2% of this facies	*Phycosiphon incertum* isp. (<0.05mm) and *Planolites* isp. (<0.2 by 0.03mm)
F3: Bioturbated Pyritized Bioclast-bearing Mudstone	Beds (5 to 100cm)	Upper-Gradational; Lower-Gradational	Calcite (<12%), Quartz (<7%), and Micas (<1%)	0.025	Bioclasts may be pyritized, Echinoderms, Agglutinated foraminifera, and Conodonts are <3mm and make up less than 4% of this facies	*Chondrites* isp. (<1.5mm by 0.3mm)
F4: Lenticular Mudstone	Laminae thicken and thin laterally (0.2 to 5mm)	Upper-Sharp; Lower-Sharp and Wavy	Clay clasts (50-90%), Quartz (<12%), Organic	0.030	Bioclasts, Brachiopods, Conodonts, Agglutinated foraminifera	*Planolites* isp. (<0.7 by 0.05mm)

			Matter (<10%), and Calcite (5%)		make up to 1% of this facies.	
F5: Bioclast-rich Wavy Mudstone	Laminae (1mm to 5cm); Faint grading	Upper-Gradational; Lower-Sharp and Wavy	Calcite (10-15%%) and Quartz (<5%)	0.031	Echinoderms and Brachiopods (10 to 20%); Rugose corals, Agglutinated foraminifera, Conodonts, and Phosphate intraclasts make up less than 1% of this facies	*Planolites* isp. (<1.5 by 0.2mm)
F6: Siliciclastic Siltstone	Laminae (1cm) to Beds (5cm)	Upper-Sharp; Lower-Sharp	Quartz (35%) and Calcite (20%)	0.031	Phosphate grains, Rip-up Clasts, Conodonts, Bioclasts are <1mm in length and make up <2% of this facies	*Planolites isp.* (<1.5 by 0.2mm)
F7: Glauconitic Siltstone	Laminae (~8mm)	Upper-Sharp; Lower-Sharp and Wavy	Quartz (25%)	0.036	Glauconite (20%), Brachiopods (2%), Echinoderms (2%), and Bioclasts (2%) are <1mm in length	n/a
F8: Calcareous Siltstone	Laminae (0.8 to 2cm)	Upper-Sharp; Lower-Sharp and Wavy	Calcispheres (35%), Calcite (15%), and Quartz (15%)	0.056	Brachiopods, Phosphate intraclasts, and Conodonts are <1mm	*Planolites* isp. (<1.5 by 0.2mm)

Facies	Bedding	Contacts	Minor Components	Grain Size (mm)	Skeletal Components	Trace Fossils
F9: Massive to Bioturbated Carbonate Mudstone	Beds (<3m)	Upper-Gradational; Lower-Gradational	Calcispheres (1%) and Quartz (1%)	0.05	Echinoderms, Brachiopods, Gastropods, and Ostracods are <0.5mm and make up < 3% of this facies	*Zoophycos* isp (<1cm)
F10: Nodular Skeletal Wackestone	Beds (<1m)	Upper-Gradational; Lower-Gradational	Calcite (10%)	0.05	Echinoderms (<15%), Brachiopods (<10%), Bioclasts (5-10%), Ostracods (<3%), Trilobites (<3%), and Conodonts (<1%)	n/a
F11: Laminated Skeletal Packstone	Laminae (<5cm)	Upper-Gradational; Lower-Sharp and Wavy	Calcite (10%) and Quartz (<1%)	0.06	Echinoderms (<45%), Brachiopods (<15%), Gastropods (<1%), Trilobites (<1%), Ostracods (<1%), Conodonts (<1%), and Phosphate Intraclasts (<1%)	n/a

Table 5: Wells organized by county with the total thickness of each core from the base of the Scallion to the last siliciclastic False Bakken shale. The percentage of each facies present in each core is displayed. In addition, at the bottom is the number of thin sections that have each facies.

Well #	County	F1 %	F2a / F2b %	F3%	F4 %	F5 %	F6 %	F7 %	F8 %	F9%	F10 %	F11 %	Absent Core%	Core Thickness (in)
8251	Billings	0	17	38	0	0	0	0	0	0	40	1	4	225
18502	Billings	2	17	35	0	3	0	0	0	0	41	2	0	177
9426/E383	Billings	0.5	14	21	0	3	0	0	0	0	60	1	0	221
12886	Billings	0	12	34	0	0.9	0	0	0	0	27	3	23	212
7887/B659	Billings	1	9	23	0	0.5	0	0	0	0	39	2	24	193
10077/E385	Billings	0	17	19	0	0	0	0	0	0	62	2	0	167
B832	Billings	0	18	24	0	0	0	0	0	0	55	3	0	176
8638	Burke	0	4	2	1	0	1	2	0	3	84	3	0	141
20648	Burke	0	2	3	0	0	0.7	1	0	3	90	0	0	136
19773	Burke	0	0	0	0	0	0.8	2	0	3	94	0	0	125
13167	Divide	0	2	4	0	0	1	4	0	4	80	4	0	145
17396	Divide	0	0	0	0	0	28	0	48	0	23	0	0	1138
19709	Divide	0	3	0	0	3	0.8	2	0	3	88	0	0	128
12785	Dunn	2	21	9	0	2	0	0	0	0	58	9	0	194
607	Dunn	0	4	25	0.7	0.7	0	0	0	1	65	0	3	295
22092	Dunn	0	0.9	6	2	0.9	0	0	0	4	82	4	0	228
20453	Dunn	0	5	20	0	3	0	0	0	13	39	1	19	197
21734	Golden Valley	0	7	15	1	0	0	0	0	55	20	2	0	413
19917	Golden Valley	0	17	39	2	0.5	0	0	0	26	12	3	0	195
24123	Mckenzie	0	4	7	0	0	0	0	0	41	43	1	3	308
12772	Mckenzie	0	9	8	0	0.7	0	0	0	0	81	1	0	151
29426	Mckenzie	0	8	12	0	0.6	0	0	0	0	74	3	3	154
21966	Mckenzie	0	3	6	0	0.7	0	0	0	7	80	4	0	135
17723	Mercer	0	0.8	20	0	0.4	0	0	0	12	67	0	0	256
16160	Mountrail	0	5	3	0	0	1	3	0	0	80	8	0	150
26661	Mountrail	0	5	13	0.3	0	0	0	0	36	45	2	0	376
28036	Mountrail	0	3	7	0.8	0.3	0	0	0	21	62	2	4	364
15889	Mountrail	0	2	6	0	0	0	0	0	22	68	2	0	176
15986	Mountrail	0	2	5	0	0	0	0	0	8	82	3	0	196
19472	Renville	0	2	6	0.7	0	0	0	0	9	79	3	0	303
20002	Stark	0	11	40	0	0.5	0	0	0	0	47	1	0	190
17272	Ward	0	5	8	0.5	0	1	2	0	4	71	8	0	191

27216	Williams	0	12	3	0	0	0	0	0	13	71	1	0	152
Total Facies Thickness in all cores		11	489	1,002	22	39	335	24	548	822	4168	167	181	7808
Total Facies Percentage in all cores		0.1	6.3	12.8	0.3	0.5	4.3	0.3	7.0	10.5	53.4	2.1	2.3	100
Total Facies observed in thin section		2	6\16	15	6	6	3	1	2	1	3	4		

FACIES ARCHITECTURE

The 'False Bakken' interval consists of mostly siliciclastic mudstones, and towards the North, East, and West also intercalated limestones in its upper portion, and varies in thickness between about 0.1 to 20m with an average thickness of 1.9m (see Table 5). The "Scallion interval", composed of coarse-grained carbonate facies, has a sharp contact with the underlying upper Bakken mudstone or Three Forks dolomitic limestone, and a gradational contact with the overlying 'False Bakken' (Mackie, 2013). The transition from coarse bioclastic limestones of the "Scallion interval" to fine-grained siliciclastic and carbonate mudstones of the 'False Bakken' indicates an overall decrease in grain size for the entire succession. Three alternating small-scale (0.5-1.5m thick) fining- and coarsening-upward packages are evident in the 'False Bakken' interval that can be mapped throughout the basin. These packages increase in areal extent from the first to third package (Fig. 7) and can be correlated across the basin (Fig. 8).

Vertical facies transitions and stacking patterns are similar in cores of close proximity to one another but vary when further apart spatially. The lowermost fining-upward unit of the succession is indicated by the gradual transition from coarse bioclastic limestones (F10-F11) of the uppermost 'Scallion' interval to bioturbated pyritized bioclast-bearing mudstones (F3) of the lower 'False Bakken' in all areas south of Renville County. Further to the north, this facies transition shows a gradual contact from the 'Scallion' coarse bioclastic limestones (F10 and F11) to glauconitic siltstones (F7), the latter constituting the basal 'False Bakken' facies. The bulk of this first fining-upward succession is made up of siliciclastic mudstones (F1-F4); its uppermost portion is represented by massive siliciclastic mudstones (F2a and F2b) in Billings, Stark, and Dunn Counties, bioturbated pyritized bioclast-bearing mudstones (F3) in areas outside of these counties, and glauconitic siltstones (F7) in the very northeast of the study area.
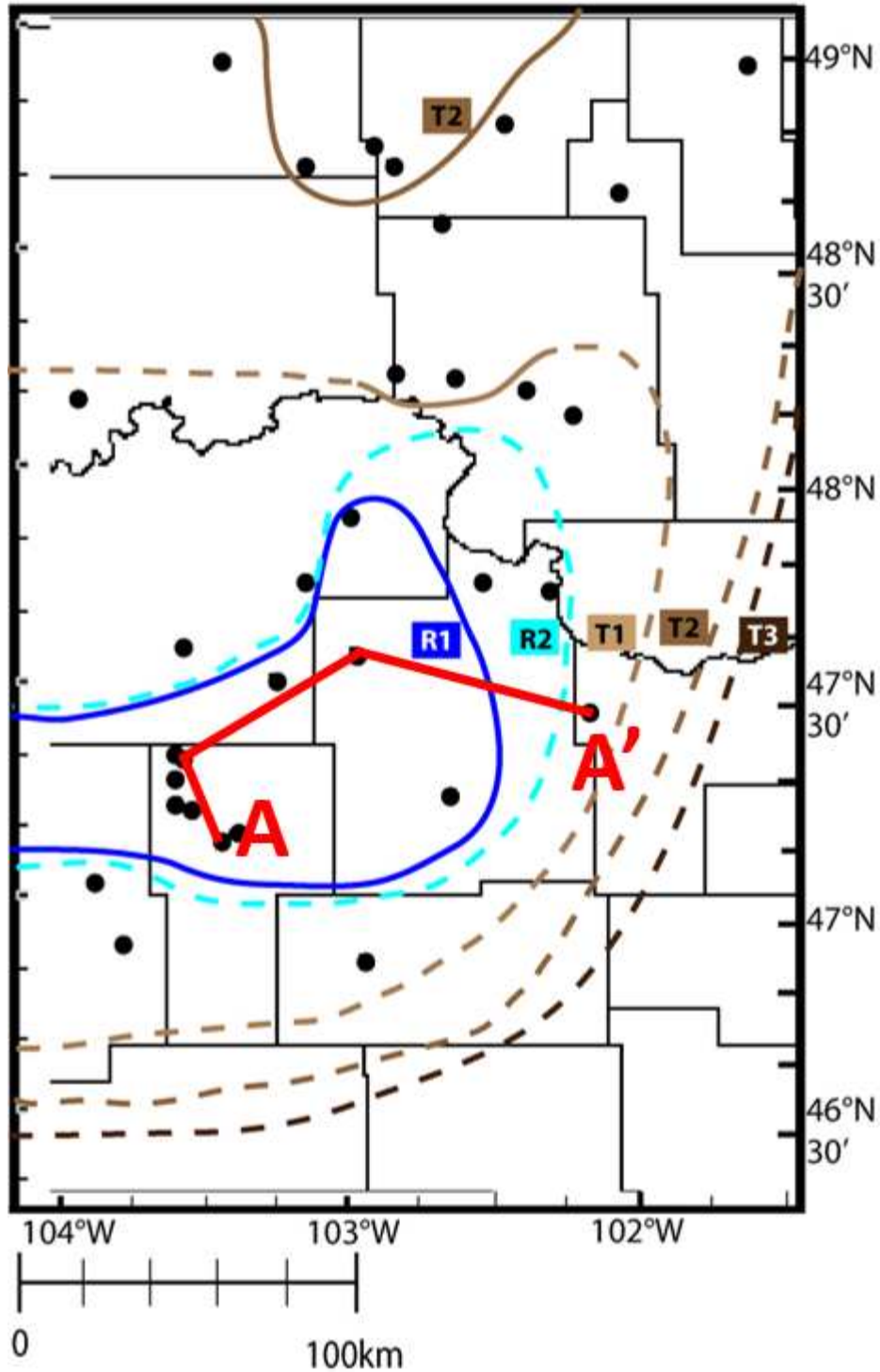
Fig. 7: Individual lines represent the contact between shales and carbonates for the coarsening and fining upward units, when dashed the contact is inferred. Three contacts between the siliciclastics and carbonates within the fining-upward units are indicated by brown lines labeled T1, T2, and T3. In addition, two coarsening upward units are represented by lines shaded blue and labeled R1 and R2. T1 occurs in the lowermost part of the succession and T3 at the top.

34
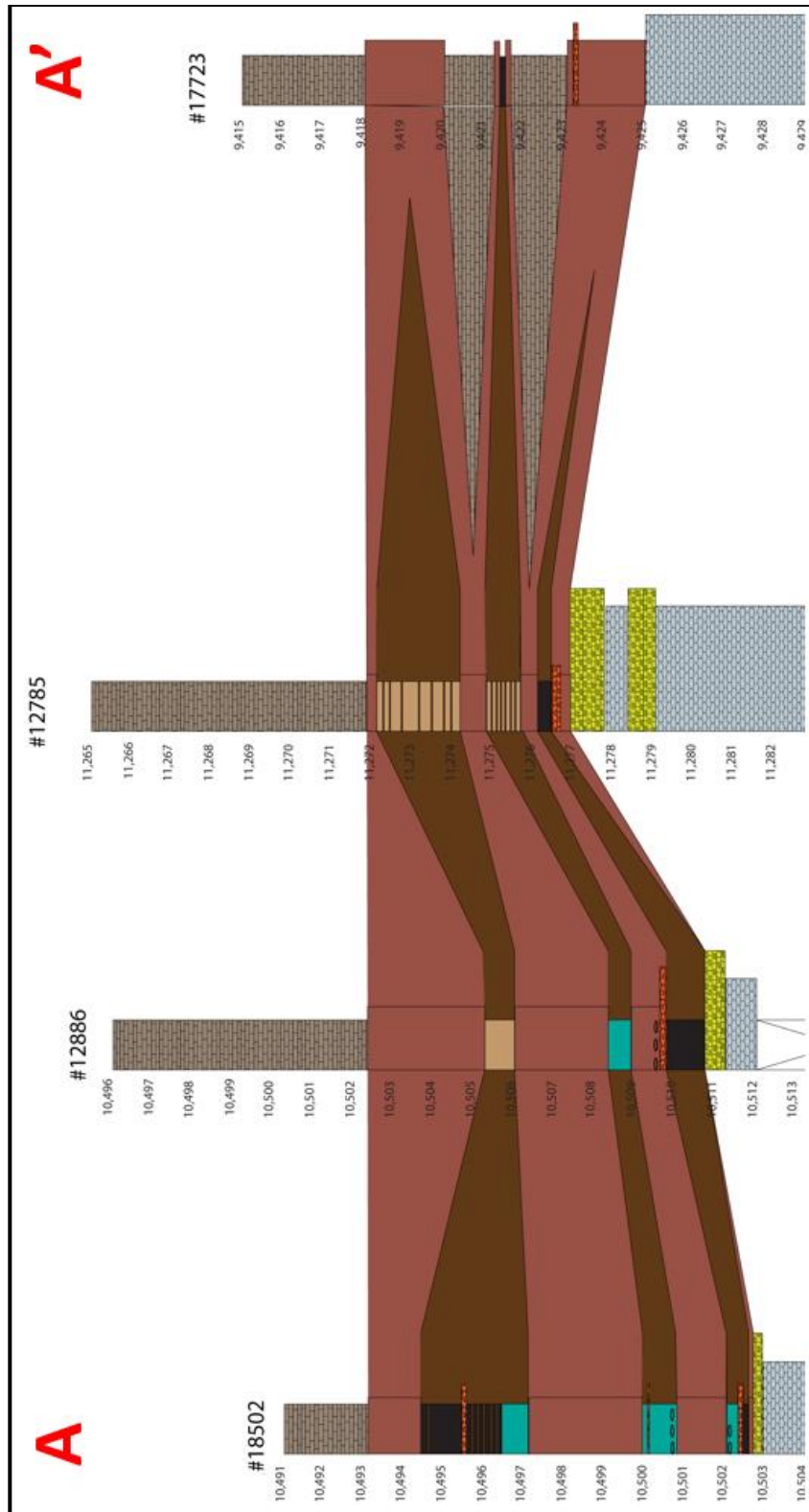
Fig. 8: Cross-section from core #18502 to #17723 in which these fining- and coarsening-upward units are correlated across the basin. Brown=F1, F2a, F2b, F4, and F5; Red=F3, F4, F5; and Grey=F9. See Fig. 7 for cross-section line.

Overlying the first fining-upward package are three coarsening- and two fining-upward units that alternate with one another and display similar facies changes up-section based on location within the basin. In the northern, eastern, and western parts of the study area, the typical fining-upward packages are composed of carbonates mudstones (F9) at the base, overlain by pyritized bioclast-bearing mudstones (F3), and massive fine-grained siliciclastic mudstones (F2a and F2b) at the top. However, in Billings County and nearby the characteristic fining-upward packages show basal pyritized bioclast-bearing mudstones (F3) overlain by massive fine-grained siliciclastic mudstones (F2a and 2b). Characteristic coarsening-upward packages in the northern, eastern, and western parts of the basin have massive fine-grained siliciclastic mudstones (F2a and F2b) at their bases which are overlain by pyritized bioclast-bearing mudstones (F3) and carbonates mudstones (F9) at the tops. Within and near Billings County, carbonate mudstones are absent and the coarsening-upward successions are composed of massive fine-grained siliciclastic mudstones (F2a and F2b) that are overlain by pyritized bioclast-bearing mudstones (F3).

The three fining- and overlying coarsening-upward packages forming the 'False Bakken' interval show some distinct facies differences throughout the study area in northwestern North Dakota: graded argillaceous mudstones (F1) and lenticular mudstones (F4) occur only in the second and third fining- and coarsening-upward packages and are absent in the basal fining- and coarsening-upward unit; bioclast-rich wavy mudstones (F5), in contrast, occur in all three packages. Nevertheless, not every core necessarily shows all of the facies that generally make up the fining- and coarsening-upward packages so the occurrence of graded argillaceous mudstones (F1) and lenticular mudstones (F4) may be restricted to distinct cores. For example, graded argillaceous mudstones (F1) are only present in four cores within and around Billings County (Fig. 9a) while lenticular mudstones (F4) occur exclusively in the northeast and southwest portions of the basin outside of Billings County (Fig. 9b). Bioclast-rich mudstones (F5) occur throughout the basin in general but are more abundant within Billings and adjacent Counties (Fig. 9c). Core #17396 in the northwest of the study area is an anomaly as it contains a 22m thick succession of silt-

rich siliciclastics (F6; F8) while this thick succession is absent east of this core; instead, several cores in that area contain glauconitic siltstones (F7; Fig. 9d) that are in places interbedded with siliciclastic siltstones (F6), and this facies generally forms the basal portion of the 'False Bakken' section.

Within this succession, various facies occur as laminae intercalated into other facies. Laminated skeletal packstones (F11) occur within nodular skeletal wackestones (F10); however, carbonate mudstones (F9) have no additional facies present within them. Within the bioturbated pyritized bioclast-bearing mudstone facies (F3) and massive calcareous-argillaceous mudstones (F2b), lenticular (F4) and bioclast-rich (F5) mudstones can occur as laminae in these facies; however, the abundance of these laminae (F4 and F5) is greater within facies 3. Finally, graded argillaceous mudstones (F1) only occur within the massive siliciclastic-argillaceous mudstones (F2a).
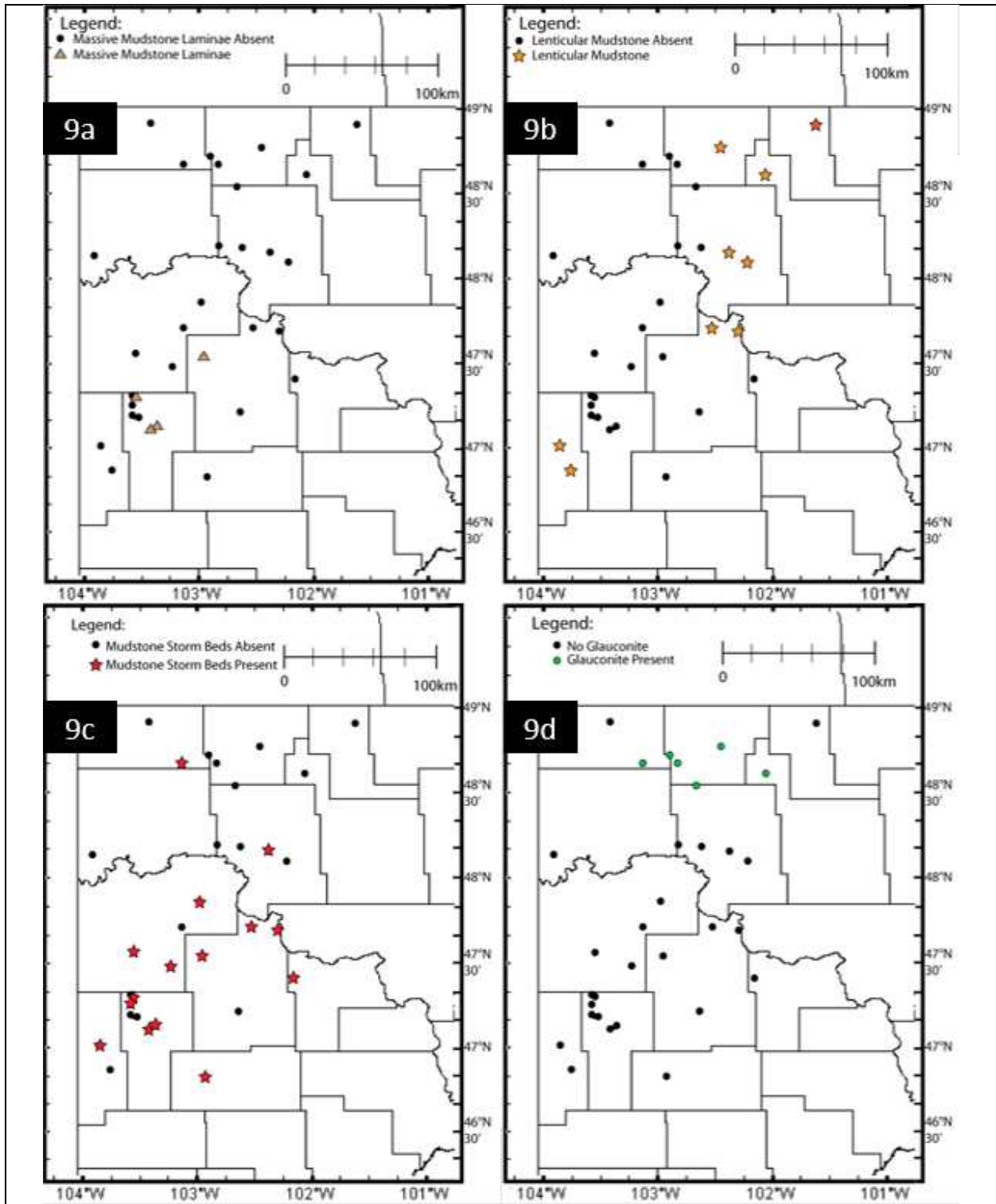
Maps above show the distribution of graded argillaceous mudstone facies (F1) indicated by a brown triangle (Fig. 9a), lenticular mudstones (F4) by orange stars (Fig. 9b), bioclast-rich wavy mudstones (F5) by red stars (Fig. 9c), and glauconitic siltstones (F7) by green circles (Fig. 9d).

DEPOSITIONAL MODEL

The 'False Bakken' succession shows a subdivision into two distinctly different depositional zones, the more proximal one characterized by carbonate deposition, and the distal one by sedimentation of siliciclastic mudstones similar to facies models in recent and ancient carbonate systems (Burchette and Wright, 1992). Within these depositional zones, the facies are arranged following an energy gradient which assumes overall high energy in proximal, and low energy in distal settings (Fig. 10); this energy gradient is reflected in the overall grain size of facies: high-energy deposits show large maximum grain sizes and low-energy facies overall small grain sizes. The carbonate depositional zone consists of two distinct facies belts which are here defined as areas of deposition of similar facies: a proximal zone of carbonate wacke- to packstone sedimentation (FB1) consisting of dominantly wackestone facies (F10) with intercalated packstone laminae (F11), and a distal carbonate mudstone (F9) dominated facies belt (FB2) containing only minor isolated bioclasts and no other facies types (Fig. 11). The siliciclastic mudstone depositional zone is subdivided into three facies belts: a proximal dominantly siliciclastic mudstone facies belt (FB3) with abundant carbonate in the matrix and pyritized fossil debris (F3) which in places contains lenticular siliciclastic mudstones (F4) and bioclast wavy siliciclastic mudstones (F5), a massive siliciclastic mudstone facies belt (FB4) with calcareous debris and quartz grains (F2b) that also shows lenticular siliciclastic mudstones (F4) and bioclast wavy siliciclastic mudstones (F5), and a massive siliciclastic mudstone facies belt (FB5) with quartz grains and rare calcareous debris (F2a) that shows laminae of intercalated very fine-grained siliciclastic mudstones (F1). The size, abundance, and type of burrow varies between the various facies belts with large *Zoophycos* isp. tracks exclusively found churning through the carbonate mudstones (FB2); *Chondrites* isp. and *Planolites* isp. are found mainly within the most proximal siliciclastic facies belt (FB3); and small *Phycosiphon incertum* isp. are the only tracks within the most distal massive siliciclastic facies belt (FB5).
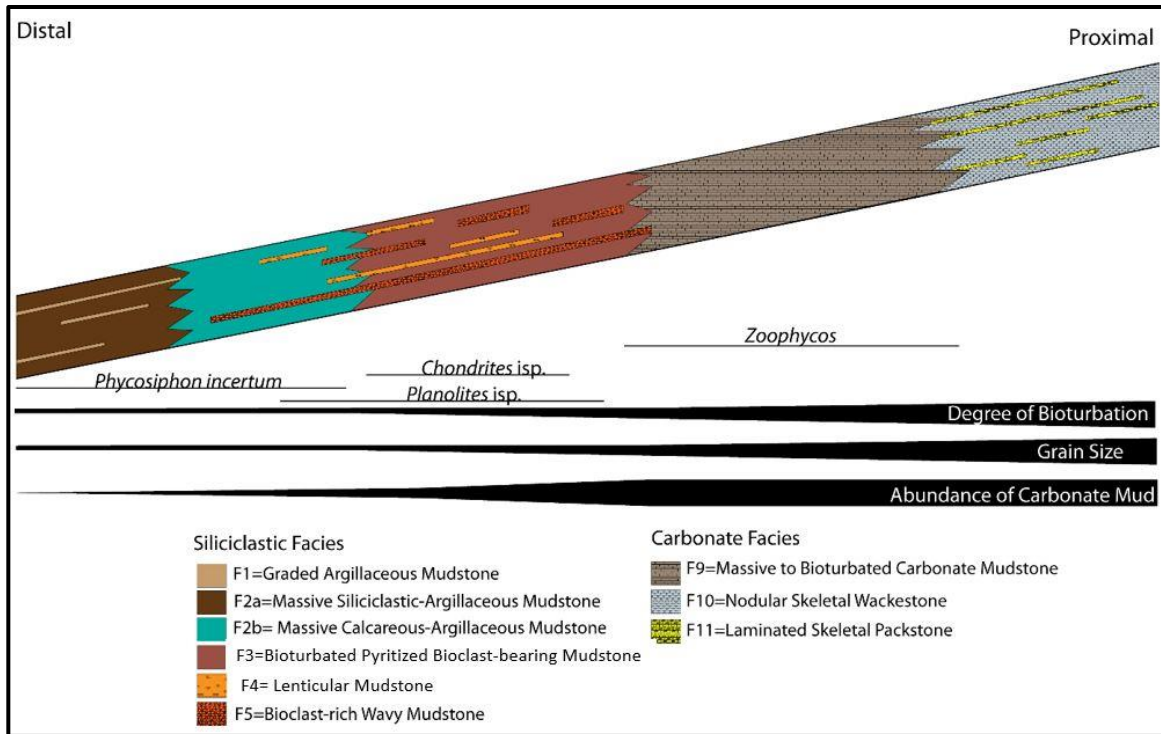
Fig. 10: Idealized depositional model that displays where each facies belt and the intercalated laminae occur from distal to more proximal settings on the low inclined ramp. This model is representative for both transgressions and regressions as all facies belts are thought to be present throughout the succession. A decrease in bioturbation, grain size, and carbonate occurs from proximal carbonates to distal siliciclastics. Types of burrows are labeled where they occur on this model.

Following this general facies distribution (Fig. 10), the five facies belts represent distinct positions on the low-inclined margin of the Williston epicontinental basin that most likely reflect different depths of deposition, distances from the shoreline which influenced the potential delivery of grains to any given location within the basin, and oxygen concentrations limiting infaunal and benthic life. Starting at the proximal end of what is preserved in the lowermost Lodgepole Formation, the carbonate wackestones (F10) with intercalated packstone laminae (F11) show an alternation of fair-weather and storm influence on deposition, and therefore likely represent sedimentation in a mid-ramp position (Burchette and Wright, 1992) above storm wave base as indicated by the packstone laminae (F11) interpreted as tempestites. Further basinwards, a lack of packstone laminae (F11) and low abundances of bioclasts within the carbonate mudstones (F9) indicate little storm influence on deposition, and an abundance

40

of *Zoophycos* isp. burrows up to 1cm in diameter reflect that oxygen concentrations were significant enough to support numerous large organisms. However, crossing the threshold from carbonates to siliciclastic mudstones, the siliciclastic facies belt adjacent to the carbonate mudstones (mainly F3 with laminae of F4 and F5) again reflects high-energy influence on deposition, most likely by storms or similar currents (see Schieber 2016). It is therefore likely that also the carbonate mudstones (F9) were subjected to storm deposition. The facies belt basinward of the most proximal siliciclastic mudstones, the massive calcareous-argillaceous mudstone (F2b), still records the influence of storm waves with the presence of some intercalated bioclast-rich wavy mudstones (F5). Nevertheless, other indicators of high-energy events also occur in places such as lenticular mudstones (F4). The most distal facies belt consisting of massive siliciclastic-argillaceous mudstones (F2a) with some intercalated graded argillaceous mudstone laminae (F1) shows mostly enigmatic sedimentary conditions based on its nearly completely bioturbated nature with only the fine grain size of the graded argillaceous mudstones (F1) showing deposition from suspension. The bulk of the succession, though, is thought to be deposited by bed-load transport based on its grain size that is coarser than the suspension laminae; it is therefore interpreted to be largely deposited by storm events and associated bed-load depositional processes (see Li and Schieber 2018) prior to bioturbation. The deepest of the siliciclastic facies belts exclusively shows sub-millimeter *Phycosiphon incertum* fecal strings reflecting that most likely dysoxic conditions prevailed during deposition allowing for small organisms to move through the muddy substrate (Egenhoff and Fishman, 2013).
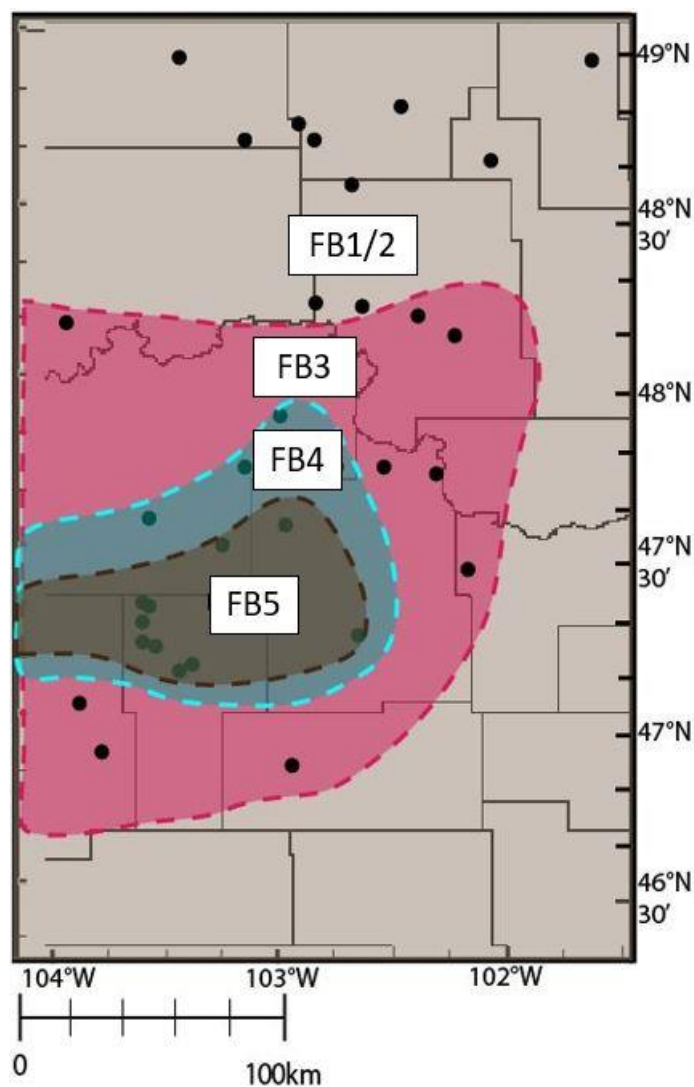
Fig. 11: A schematic map of where facies belts occur relative to one another within the basin. The aerial extent of each facies belt changes for each sequence and the distribution presented here is based on the location of each facies belt for the first sequence.

In this study, the 'False Bakken' is interpreted to consist of three transgressive and regressive sequences based on grain-size trends throughout measured sections in this particular stratigraphic interval (Figs. 7 and 8). Nevertheless, these three sequences are not made up of exactly the same facies. The fact that lenticular mudstones occur only in the upper two but not in the lowermost sequence indicates that sediment starvation did not occur throughout the entire succession. As lenticular mudstones (F4) are generally interpreted to reflect condensation (Schieber et al 2010; Borcovsky et al. 2017), their distribution almost entirely in the eastern portion of the study area reflects sediment starvation mostly in

42

this part of the basin and not in most of its western portion (Fig. 9b). However, the two sections to the extreme southwest in Golden Valley County containing lenticular mudstones (F4) indicate a locally different starved environment, either on a basin high, or in an otherwise sheltered setting that is confined to this part of the basin. Similarly, the graded argillaceous mudstone laminae (F1) are restricted to exclusively the central portion of the basin (Fig. 9a) and do not occur in any of the other sections as they are deposited only in the most distal settings. This seems reasonable as suspension laminae will be easiest formed and best preserved in distal settings, and the center of the basin during 'False Bakken' deposition seems adequate for conserving these sediments. Glauconitic siltstones (F7) are restricted to the very northeastern portion of the basin and exclusively occur in the first sequence (Fig. 9d) indicating condensation of the depositional environment (e.g. Amorosi 1995) during this time, however, only in this particular location of the basin. Although glauconitic siltstones (F7) are only present within the first sequence unlike lenticular mudstones (F4), both occur in the northeastern portion of the basin suggesting this part of the basin was even more sheltered from sedimentation than the east in general, leading to extreme condensation during 'False Bakken' deposition exclusively in that area.

The elevated thickness of the siltstone facies (F6; F8) as well as high amounts of quartz silt exclusively in the central portion of Divide County (in the very northwest of the study area) indicates a nearby source of siliciclastic input. While this one well (#17396) is located close to the basin area where glauconite is abundant (Fig. 12), its characteristics indicate rather high amounts of sedimentation and not condensation like the adjacent wells that contain glauconite facies. It is therefore assumed that the central part of Divide County was located close to a sediment input area, likely representing a distal delta environment (cf. Angulo and Buatois, 2012, for the underlying upper Bakken shale). Nevertheless, the glauconite-bearing succession must have been completely sheltered from its neighbors further in the northwest not allowing any sediment to be transported to these glauconite-bearing successions during the first cycle. This could either indicate a barrier (see Fig. 12), e.g. a tectonic element, subdividing the northern Divide County well from its eastern neighbors by blocking any sediment flow to the east, or be

43

caused by the Coriolis force preferentially transporting sediment to the right in the northern hemisphere (Duke, 1990). Some tectonic influence on facies distribution seems, however, likely as the northeastern most well (#19472) in the study area, located east of the glauconite-bearing wells, does not contain any glauconite, and was therefore likely not sediment-starved.

The distribution of facies throughout the 'False Bakken' clearly shows this unit to be overall transgressive (Fig. 7). This is shown in the maximum extent of the transgressive siliciclastic mudstones (cf. Loutit et al. 1988) that cover an increasingly larger area starting with the transgressive siliciclastic mudstones of sequence 1 (T1) which are overstepped by the siliciclastic mudstones of sequence 2 (T2) showing a wider areal distribution, and the siliciclastic mudstones of sequence 3 which are present in all wells used in the present study. The maximum regressions, however, are not as well defined as the transgressions. The data suggest, though, that the two regressions reflected in the succession seem to show the position of the carbonate-siliciclastic mudstone transition in a similar place for sequence 1 and sequence 2. The sea-level fall during sequence 3 must have been of major amplitude as it terminated black shale deposition in the North Dakota portion of the Williston Basin for the lower Mississippian succession and therewith defined the end of the 'False Bakken'.

The 'False Bakken' facies study also shows an interesting aspect of basin geometry reflected in the distribution of carbonate and siliciclastic mudstone facies: throughout 'False Bakken' deposition the basin center was located in western Dunn and northern Billings Counties and may have extended westwards through Golden Valley County into Montana. The basin center remained stable during 'False Bakken' sedimentation yet presents a southwards shift of the basin center from the underlying Bakken Formation where it was near the borders of Williams, McKenzie, and Mountrail Counties (Borcovsky et al. 2017, and references therein). It is unclear what caused this shift. However, throughout Bakken times the Williston Basin was connected to the Elk Point Basin in southern Saskatchewan (Gerhard et al. 1982; LeFever and Anderson, 1984; Gaswirth et al. 2013) and tectonic subsidence in the middle Lodgepole caused the Williston Basin to gain access to the Cordilleran sea to the west through the Central Montana

trough and abandon its previous connection to the Elk Point Basin (Bjorlie, 1979; Gerhard et al. 1982; Gaswirth et al. 2013). It is therefore inferred that this tectonic subsidence thought to occur in the middle Lodgepole actually occurred during sedimentation of the 'False Bakken' interval of the lower Lodgepole causing a southward shift of the basin depocenter from Bakken to lower Lodgepole times.

DISCUSSION

Facies in Siliciclastic Mudstones

This study assumes that there are six different siliciclastic mudstone facies that make up the succession of the 'False Bakken' in the Williston Basin in contrast to merely two described before (Mackie 2013; Stroud, 2011). The question remains whether these additional facies are warranted, and what they achieve in order to describe the sedimentology of the 'False Bakken' in better detail.

In this contribution, the siliciclastic mudstone facies are grouped into three facies belts that are placed adjacent to two carbonate facies belts but in waters deeper and further away from land than the carbonates. These three siliciclastic mudstone facies belts, are characterized by decreasing grain sizes further distally but at the same time also differ significantly in their biogenic and carbonate content. The further away from the shoreline a facies is the less carbonate mud it contains as the carbonate is thought to be produced in shallow water (e.g. Schlager 2003) and then transported downslope, probably preferentially during storms. The identification of three siliciclastic mudstone facies belts and three intercalated facies allows for a much more detailed and precise look at the 'False Bakken' succession in comparison to previous models that identified only two siliciclastic facies. Therefore, this more detailed approach provides a way to easily differentiate proximal from distal siliciclastic sediments within the succession. Furthermore, the proximal portion contains many more high-energy features not displayed in distal siliciclastic mudstones: the bioclast-rich wavy mudstones (F5) interpreted as storm laminae get less prominent further downslope and are not found in the most distal massive siliciclastic-argillaceous mudstones (F2a). Suspension-derived graded argillaceous mudstones (F1) occur exclusively in the most distal facies belt (FB5-massive siliciclastic-argillaceous mudstones) thereby highlighting its deep-shelf nature and it being out of reach of some of the storm waves during deposition. All in all, the mudstone subdivision proposed in this contribution therefore invites a much more detailed look at the 'False Bakken' interval, and the proposed model allows for predictions of facies occurrences throughout the

study area that would not have been possible otherwise. It is therefore suggested that a detailed documentation of siliciclastic mudstone facies, as similar as they may seem macroscopically, can elevate the understanding of any succession from being merely fine-grained to reflecting significant shifts in depositional energy, and associated sedimentary structures and grains.

Carbonate-Shale Transitions

During 'False Bakken' deposition, the boundary between carbonate mudstones (F9) and siliciclastic mudstones (F2a, F2b, and F3) are observed in two of the three cycles documented for this stratigraphic interval. Both facies belts, not only the carbonates (e.g. Burchette and Wright, 1992), are well documented in core and thin section. It therefore seems reasonable to compare the processes interpreted for both sides of this shale-carbonate transition, and highlight differences and similarities in order to get an idea for the preservation and expression of e.g. storm-induced structures in the sedimentary record.

In the carbonates, storm beds are only preserved in the wackestone facies belt, here interpreted to be the most proximal (Fig. 10), but not in the adjacent carbonate mudstone facies belt. Consequently, it is assumed that the lack of storm beds in carbonate mudstone facies reflects a lack of storm wave reworking for the carbonate mudstones, and therefore storm wave base should have been placed at the top of the carbonate mudstone facies belt; yet, most models place it at the transition from carbonates to siliciclastic mudstones assuming that the mudstones, following an antiquated view, have been deposited from suspension whereas carbonates are thought to have formed in shallow water (see above). Close examination of the siliciclastic mudstone facies present in the 'False Bakken' interval, however, contradicts this concept of suspension deposition in nearly all of the mudstones: suspected suspension-derived sediments are in fact quite rare and restricted to exclusively the most distal facies belt. The most proximal two siliciclastic facies belts, however, show abundant bioclast lags that are here (and in Mackie 2013) interpreted to represent storm beds characterized by shells and other bioclast debris.

The problem highlighted by this work is that storms are evident in siliciclastic mudstone facies in the 'False Bakken' of the Williston Basin until at least its second deepest facies belt (Fig. 10), and the carbonate mudstones which do not reflect any storm activity are bordering facies belts with abundant storm indicators on both sides, the deep and the shallow end. This indicates that the carbonate mudstones most likely do not preserve storm-formed structures, e.g. shell lags present in both of the adjacent facies belts, and the question remains why this is the case.

It may be suggested that carbonate mudstones were deposited on structural highs; therefore, storm deposits may not have been preserved. However, there is little evidence for this as carbonates occur mostly in areas that are not associated with structural highs. It is well known that carbonate mud can be transported by bed load processes (Schieber et al. 2013) and form e.g. ripples. These bed load processes may be masked by subsequent intense bioturbation from organisms that entirely burrowed through the fine-grained carbonate and destroyed any sedimentary structures originally present in the sediment. However, carbonate particles of mostly bioclastic debris are present in greater abundances in siliciclastic mudstones than in the carbonate mudstones; therefore, it seems reasonable to assume that the carbonate facies belt originally contained a greater abundance of bioclastic debris.

Up to centimeter-size carbonate grains, biogenic in origin, can be completely corroded by biogenic processes governing micritization (bioerosion, e.g. Hallock, 1988; Peterhänsel and Pratt, 2001) and has been shown to occur for the Palliser Platform and several other examples in the rock record (e.g. the Prague Basin, Vodráqková et al. 2013; Adriatic Carbonate Platform; Zamagni et al. 2008; Ándara Massif; Merino-Tomé et al. 2009). Although not yet suggested to have taken place within the Williston Basin, micritization is suspected to occur within the carbonates of the 'False Bakken' interval and likely in other places with carbonate-siliciclastic mudstone transitions.

The process most likely works in the following way: the carbonate mudstones are generally seen as the most distal carbonate facies belt (e.g. Burchette and Wright, 1992). The further distal an environment is the less sediment will likely be transported to that location as it is deeper and requires

higher energy to be delivered that far from the shoreline. Carbonate mudstones therefore represent the area where low amounts of bioclastic debris will be delivered. Nevertheless, based on the facies characteristics of adjacent facies these carbonates most likely also contained more bioclasts. Because of the low sedimentation rates in this distal setting the carbonate grains remain at or near the sea floor, where bioeroding organisms thrive from the influx of river-borne nutrients (Hallock, 1988; Peterhänsel and Pratt 2001). This increase in nutrient availability is confirmed by the abundance of calcispheres, suggested to be of algal origin, that form blooms associated with high nutrient concentrations in the water column (Hart, 1991; Scholle and Ulmer-Scholle, 2003). The bioclasts are degraded at the sea floor thereby producing the carbonate mud that is so characteristic for this facies belt. The storm beds degrade from this process and the newly produced mud will be mixed in with the carbonate mud already in place. Only silt-size bioclastic remnants in the carbonate mudstones still reflect that this facies was originally not exclusively a mudstone but most likely contained some coarser-grained storm beds. It is therefore assumed that in similar settings with terrestrial input and its associated nutrient influx, as indicated by the presence of e.g. biotite and calcispheres, more distal carbonate mudstones likely contained storm events that were not preserved due to an increase in bioerosion of bioclastic grains exposed on the sea floor.

Position of Storm Wave Base and Implications for Carbonate Facies Models

This study shows that distinct storm beds are still detectable in the siliciclastic mudstones in the second deepest facies belt of the Williston Basin (Fig. 10). The classical position of the storm wave base at the lower boundary of the carbonate facies belts is therefore not corroborated by this study as at least two of the siliciclastic mudstone facies belts have distinctive storm beds and other indicators of erosional processes (e.g. erosion of clay clasts from the sea floor, see above). Commonly, storm wave base, the depth at which storms frequently influence sedimentation on the seafloor, is used to define the transition from mid- to outer-ramp depositional settings and can vary significantly in depth depending on the basin type (Burchette and Wright, 1992). During deposition of the 'False Bakken', many of the siliciclastic

mudstone facies are thought to reflect storm deposition, and therefore the position of the storm wave base has to be significantly deeper than the carbonate-siliciclastic mudstone facies boundary.

In the Recent, the storm wave base is located as deep as 250m in the open Atlantic, and even in the "sheltered" Gulf of Mexico around 200 m based on buoy measurements (Peters and Loss, 2012). It is suspected that the intracratonic Williston Basin in the Mississippian was much more sheltered than the Gulf of Mexico today and most likely experienced a much shallower storm wave base; however, where that was located is not clear. Based on comparisons with the modern Persian/Arabian Gulf (Purser and Seibold, 2012) which is also a sheltered setting, the carbonate-siliciclastic mudstone transition is approximately at 70 m water depth. It can therefore be assumed that the Williston Basin may have possessed this facies transition at a similar water depth or, because of its even more protected nature, even further up in the water column. In any case, this facies transition cannot have been much deeper than some tens of meters, and the Williston Basin as a whole was probably not deeper than about 100m considering that the inclination of an intracratonic basin is significantly less than 1° (Burchette and Wright, 1992).

The findings of this study therefore have important implications even for carbonate facies models: it is suspected that there are more examples in the rock record that will contain bioclast storm horizons in the shales adjacent to and more distal than the carbonate mudstones. Consequently, storm wave base should not be placed at the carbonate-siliciclastic mudstone facies boundary but is most likely located somewhere in the siliciclastic mudstones if it is not below the deepest point of the basin center, and therewith not within a given succession at all. Storm wave bases as deep as 250m in open ocean settings seem to limit identifying this boundary in many successions in the rock record, and it clearly will be located significantly deeper than is assumed for many carbonate units throughout geological time, and all climatic zones.

Glauconite

This study assumes that the glauconite in facies 7 defines a part of the basin that is very restricted, and found exclusively in sequence one of the three sequences that make up the 'False Bakken' succession. However, as the 'False Bakken' is shown to be overall transgressive as indicated by the overstepping of transgressive fine-grained strata in the three sequences (Fig. 7), condensation should be common in the transgressive portions of all three sequences and not just in the first one. The exclusivity of glauconite in only the lower 'False Bakken' sequence therefore remains enigmatic.

Nevertheless, there are other sedimentary features that are indicative of sedimentary starvation, e.g. the clay clasts (Schieber et al. 2010; Borcovsky et al. 2017). These features are common in both the 'False Bakken' sequences two and three indicating that sediment starvation was indeed still a major factor during the middle and upper part of 'False Bakken' deposition. Alternatively, the distribution of glauconitic sediment may be patchy so that certain areas, e.g. where the drill cores were taken, may not show glauconite even though it may be present in the sediments. Nevertheless, the abundance of glauconite in sequence one of the 'False Bakken' interval seems to reflect that starvation was strongest in this part of the succession, and it is worth exploring why.

Sedimentation of the Lodgepole Formation started with carbonates throughout North Dakota, showing a distinct coarsening towards the boundary of the 'False Bakken' interval, interpreted as a lowering of sea-level. Sea-level change must have been significant in order to transition from the 'Scallion' carbonate wacke- to packstones underlying the 'False Bakken' to the siliciclastic mudstones characterizing this last black shale interval in the lower Mississippian succession. The two subsequent sea-level changes of the 'False Bakken' interval reach an overall larger area than the first one; however, they did not show such a significant change in basin configuration as the first sea-level fluctuation. The glauconite may therefore be a result of strong sediment starvation related to a very prominent sea-level rise during sequence one.
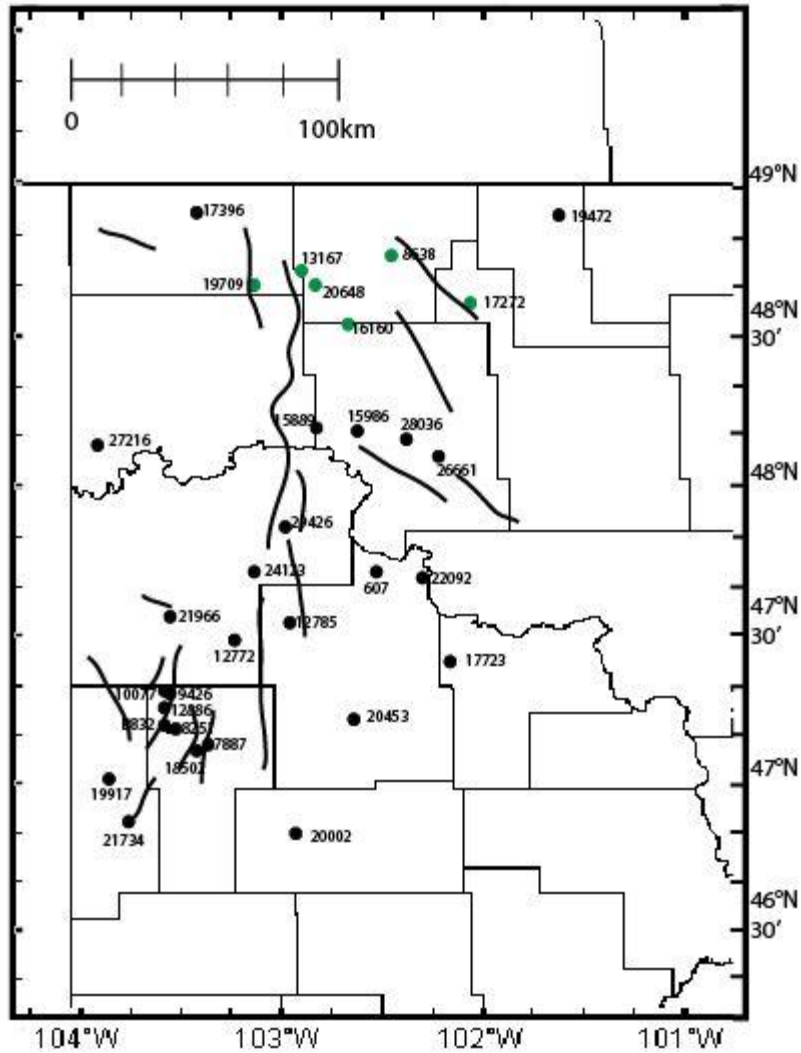
Fig. 12: All cores are labeled and any cores with a green dot contain glauconitic siltstones (F7). Anticline structures from Novak and Egenhoff, (2018) are overlain onto this map.

Nevertheless, another factor may have influenced glauconite to be entirely restricted to the northeast of the study area. The initial sea-level rise during sequence one formed a gulf extending eastwards and then northwards into the central and northern-central part of the study area. The glauconite is only occurring at the very end of this gulf when it was newly formed, and in an area especially isolated from the rest of the Lodgepole Sea. It is therefore likely that the isolated position of sediments containing glauconite has added to this area being especially sediment-starved.

Finally, tectonic structures mapped out in the basin for middle Bakken times may have influenced sediment patterns during 'False Bakken' deposition, too. The two northwestern-most wells in Divide County (17396 and 19709; Fig. 12) are separated by a lineament that could have been forming a barrier during 'False Bakken' deposition and thereby altering sediment delivery to areas now occupied by glauconitic-siltstones. Alternatively, as the Williston Basin was situated on the northern hemisphere during Lodgepole Formation deposition, the main sediment flow was likely preferentially shedding sediment to the west thereby starving areas located towards the east of well 17396. Either one of these factors, or a combination of any or all of them was likely responsible for glauconitization during the initial sequence of 'False Bakken' deposition. Glauconite sediments therefore represent not only a testimony to strong sediment starvation but at the same time indicate a distinct stratigraphic level within 'False Bakken' stratigraphy.

Oxygen Availability in the Water Column and Sediment during 'False Bakken' deposition

Burrows of several types and/or fecal strings are present in the 'False Bakken' interval throughout all facies. Nevertheless, the abundance of burrow types and the intensity of burrowing change from more proximal to distal settings with proximal sediments showing high and distal low to moderate abundances of burrows and burrowing (Fig. 10). It is well known that carbonate facies are generally well oxygenated (Wilson, 1975). However, siliciclastic mudstones are generally not seen as strongly bioturbated, yet some ichnospecies exist (e.g. Schieber 2003; Borcovsky et al. 2017): *Planolites* isp. have been identified in a number of siliciclastic mudstone units (e.g. Alum Shale, Egenhoff et al. 2015; upper Bakken Shale, Egenhoff and Fishman 2013, Borcovsky et al. 2017), and *Chondrites* isp. is also known from several shale units (e.g. Greenhorn and Niobrara Formation, Archer and Hattin, 1984; Posidonienschiefer Formation, Bromley and Ekdale, 1984; Upper Kellwasser interval, Boyer et al. 2014). Nevertheless, transitioning from carbonates to siliciclastic mudstones, diameters of burrow structures become smaller, from several millimeters in the carbonates to about 0.05 millimeters in the siliciclastic mudstones. This size reduction is interpreted to reflect a decrease in oxygen availability at the sediment-water interface

(Bottjer and Gorsline, 1984; Savrda and Bottjer, 1987). This deficit in oxygen availability is also reflected in the decrease of burrow types within the sediment: in the most distal depositional facies belt, only *Phycosiphon* fecal strings (Egenhoff and Fishman, 2013) are present yet they indicate that the environment could not have been completely anoxic as an opportunistic fauna was able to survive. It is therefore concluded that the carbonate-siliciclastic mudstone transition most likely represents a reduction in oxygen level reflected in smaller faunas whereas oxygen values decreased dramatically towards the deepest portions of the basin. Yet, they most likely never reached anoxic levels as shown by the presence of fecal strings in the distal most facies.

CONCLUSIONS

The 'False Bakken' interval of the lower Lodgepole Formation in the Williston Basin is comprised of 9 siliciclastic facies and 3 carbonate facies: these are graded argillaceous mudstone (F1), massive siliciclastic-argillaceous mudstone (F2a), massive calcareous-argillaceous mudstone (F2b), bioturbated pyrtitized bioclast-bearing mudstone (F3), lenticular mudstone (F4), bioclast-rich wavy mudstone (F5), siliciclastic siltstone (F6), glauconitic siltstone (F7), calcareous siltstone (F8), massive to bioturbated carbonate mudstone (F9), nodular skeletal wackestone (F10), and laminated skeletal packstone (F11). Grain size, carbonate content, and bioturbation increase successively from F1 to F11 throughout the succession.

The 'False Bakken' shows three fining- and coarsening-upwards units : (1) a fining upward trend from carbonate mudstones (F9) to bioturbated pyritized bioclast-bearing mudstones (F3) to massive siliciclastic mudstones (F2a and F2b) and (2) a coarsening upward trend from carbonate mudstones (F9) to bioturbated pyritized bioclast-bearing mudstones (F3) to massive siliciclastic mudstones (F2a and F2b).

Bioclast-rich wavy mudstones (F5) and lenticular mudstones (F4) are commonly intercalated within bioturbated pyritized bioclast-bearing mudstones (F3) and massive calcareous-argillaceous mudstones (F2b), while graded argillaceous mudstones (F1) are only found within massive siliciclastic-argillaceous mudstones (F2a). These facies (F1, F4, and F5) are not always present within the three coarsening- and fining- upward units and only occur locally within the basin. Bioclast-rich wavy mudstones (F5) are present within all three coarsening- and fining- upward units and distributed throughout the basin. Lenticular mudstones (F4) and graded argillaceous mudstones (F1) are only present within the upper two coarsening- and fining- upward units; however, the graded argillaceous mudstones (F1) are exclusive to Billings County while lenticular mudstones (F4) occur mostly in the northeastern portion of the study area. With each successive fining upward unit, siliciclastic mudstones occupy increasingly larger areal extents. Siltstone facies are restricted to the northern part of the basin with a

thick succession of siltstones present only in core #17396 in the very northwest of the study area. Just east of this core, however, are several cores that contain glauconitic siltstones (F7).

From these coarsening- and fining- upward units, five facies belts were identified based on similar depositional characteristics: the (FB1) nodular skeletal wackestone, (FB2) the carbonate mudstone, (FB3) the pyritized bioclast-bearing mudstone, (FB4) the calcareous-argillaceous mudstone, and (FB5) the siliciclastic-argillaceous mudstone. The five facies belts are interpreted to represent a transect from proximal to distal settings during 'False Bakken' sedimentation with the carbonates being deposited in more proximal settings and siliciclastics in distal settings. These facies belts are consequently arranged along a depositional transect that shows a decrease in grain size and carbonate abundance from proximal to distal basin locations and is accompanied by a decrease of bioturbation abundance and diversity in the same direction. The most distal facies shows normally-graded fine-grained laminae (F1) that reflect suspension settling in quiet waters, intercalated into massive siliciclastic-argillaceous mudstones (F2a). High-energy reworking and deposition of fine-grained sediment, in contrast, is represented by bioclast-rich wavy mudstones (F5) and lenticular mudstones (F4) thought to show storm reworking and bed-load transport. The distribution of these features in all but the most distal facies belts shows how far storm waves could reach during 'False Bakken' deposition. Storm wave base therefore has to be placed either between the lowermost two siliciclastic mudstone facies belts or could have reached down even to the deepest basin position as suspension settling laminae are rare within the distal facies belt.

The burrowing trends detected in the 'False Bakken' succession show that siliciclastic mudstone deposition did not occur in an anoxic environment as proposed for many black shale successions. Instead, the presence of burrows and fecal strings even in the more distal basin areas show most likely dysoxic conditions throughout 'False Bakken' deposition, with the increase in burrow diversity and abundance up-dip most likely reflecting an increase in oxygenation of the basin towards proximal areas.

The three fining and coarsening-upward successions are interpreted to reflect three transgressions and regressions in the 'False Bakken' succession. Each of the transgressions occupied a successively larger area showing that the 'False Bakken' interval was overall transgressive. These transgressions flooded a carbonate-dominated shelf in western North Dakota with the first transgression resulting in the largest amount of change in facies distribution interpreted to reflect the highest amount of sea-level rise. Nevertheless, all three transgressions resulted in sediment starvation with only the first one leading to the local development of glauconitic siltstones (F7) at the most sediment-starved end of a newly developed gulf in northwestern North Dakota. Lenticular mudstones (F4) deposited during the two later transgressions are interpreted as resulting from the local reworking of siliciclastic mudstones because of sediment starvation in the eastern portion of the basin. The limited extent of siltstone facies (F6; F8) in the northwestern most part of the basin is thought to indicate local sediment input into the basin. It is suspected that structural elements confined sediment distribution to the east; however, the local occurrence of siltstone laminae in glauconitic siltstones (F7) seems to reflect that at times of major sediment input these tectonic barriers could be overcome.

REFERENCES

Amorosi, A., 1995. Glaucony and sequence stratigraphy: A conceptual framework of distribution in siliciclastic sequences. J. Sediment. Res. 65, 419–425.

Angulo, S., Buatois, L.A., 2012. Ichnology of a Late Devonian-Early Carboniferous low-energy seaway: The Bakken Formation of subsurface Saskatchewan, Canada: Assessing paleoenvironmental controls and biotic responses. Palaeogeogr. Palaeoclimatol. Palaeoecol. 315–316, 46–60. https://doi.org/10.1016/j.palaeo.2011.11.007

Anna, L.O., Pollastro, R., Gaswirth, S.B., 2010. Williston Basin Province — Stratigraphic and Structural Framework to a Geologic Assessment of Undiscovered Oil and Gas Resources, in: US Geological Survey Williston Basin Province Assessment Team, Assessment of Undiscovered Oil and Gas Resources of the Williston Basin Province of North Dakota, Montana, and South Dakota. pp. 1–17. https://doi.org/10.1306/M971332

Archer, A.W., Hattin, D.E., 1984. Trace fossils in upper Cretaceous argillaceous marine facies of the U.S. Western interior. Palaeogeogr. Palaeoclimatol. Palaeoecol. 45, 165–187. https://doi.org/10.1016/0031-0182(84)90039-7

Baccelle, L., Bosellini, A., 1965. Diagrammi per la stima visiva della composizione percentuale nelle rocce sedimentarie. Annali dell' Università di Ferrara, IX, 1 (3), 59-62

Ballard, F. V, 1963. Structural and stratigraphic relationships in the Paleozoic rocks of eastern North Dakota. North Dakota Geol. Surv. Bull. 40.

Beanish, J., Jones, B., 2002. Dynamic carbonate sedimentation in a shallow coastal lagoon: Case study of South Sound, Grand Cayman, British West Indies. J. Coast. Res. 18, 254–266. https://doi.org/10.7939/R3125QR09

Bjorlie, P., 1979. The Carrington Shale Facies (Mississippian) and its Relationship to the Scallion. North Dakota Geol. Surv.

Blakey, R.C., 2003. Carboniferous – Permian paleogeography of the assembly of Pangaea. Proc. XVth Int. Congr. Carbonif. Permian Stratigr. 443–456.

Borcovsky, D., Egenhoff, S., Fishman, N., Maletz, J., Boehlke, A., Lowers, H., 2017. Sedimentology, facies architecture, and sequence stratigraphy of a Mississippian black mudstone succession-The upper member of the Bakken Formation, North Dakota, United States, AAPG Bulletin. https://doi.org/10.1306/01111715183

Bottjer, D., Gorsline, D., 1984. Development of a Comprehensive Oxygen-deficient Marine Biofacies Model- Evidence from Santa Monica, San Pedro, and Santa Barbara Basins, California Continental Borderland, AAPG Bulletin. 68, 1179-1192.

Boyer, D.L., Haddad, E.E., Seeger, E.S., 2014. The Last Gasp: Trace Fossils Track Deoxygenation Leading Into the Frasnian-Famennian Extinction Event. Palaios 29, 646–651. https://doi.org/10.2110/palo.2014.049

Brandano, M., Corda, L., 2002. Nutrients, sea level and tectonics: Constrains for the facies architecture of a Miocene carbonate ramp in central Italy. Terra Nov. 14, 257–262. https://doi.org/10.1046/j.1365-3121.2000.00419.x

Bromley, R., Ekdale, A., 1984. Chondrites : A Trace Fossil Indicator of Anoxia in Sediments. Adv. Sci. 224, 872–874.

Burchette, T.P., Wright, V.P., 1992. Carbonate ramp depositional systems. Sediment. Geol. 79, 3–57. https://doi.org/10.1016/0037-0738(92)90003-A

Carlson, C.G., Anderson, S.B., 1965. Sedimentary and tectonic history of North Dakota part of Williston Basin. Bull. Am. Assoc. Pet. Geol. 49, 1833–1846.

Colby, N., Boardman, M., 1989. Depositional Evolution of a Windward, High-Energy Lagoon, Graham's Harbor, San Salvador, Bahamas. J. Sediment. Petrol. 59, 819–834.

Duke, W., 1990. Geostrophic Circulation or Shallow Marine Turbidity Currents? The Dilemma of Paleoflow Patterns in Storm-Influenced Prograding Shoreline Systems. J. Sediment. Petrol. 60, 870–883.

Egenhoff, S., 2017. The lost Devonian sequence - Sequence stratigraphy of the middle Bakken member, and the importance of clastic dykes in the lower Bakken member shale, North Dakota, USA. Mar. Pet. Geol. 81, 278–293. https://doi.org/10.1016/j.marpetgeo.2017.01.015

Egenhoff, S., Fishman, N., 2013. Traces In the Dark-Sedimentary Processes and Facies Gradients In the Upper Devonian-Lower Mississippian Upper Shale Member of the Bakken Formation, Williston Basin, North Dakota, U.S.A. J. Sediment. Res. 84, 839–841. https://doi.org/10.2110/jsr.2014.74

Egenhoff, S., Fishman, N.S., Ahlberg, P., Maletz, J., Jackson, A., Kolte, K., Lowers, H., Mackie, J., Newby, W., Petrowsky, M., 2015. Sedimentology of spice (Steptoean positive carbon isotope excursion): A high-resolution trace fossil and microfabric analysis of the middle to late Cambrian Alum Shale formation, southern Sweden. Spec. Pap. Geol. Soc. Am. 515, 87–102. https://doi.org/10.1130/2015.2515(05)

Ekdale, A.A., Mason, T.R., 1988. Characteristic trace-fossil associations in oxygen-poor sedimentary environments. Geology 16, 720–723. https://doi.org/10.1130/0091-7613(1988)016<0720:CTFAIO>2.3.CO;2

Gaswirth, S.B., Marra, K.R., 2015. U.S. Geological Survey 2013 assessment of undiscovered resources in the Bakken and Three Forks Formations of the U.S. Williston basin province. Am. Assoc. Pet. Geol. Bull. 99, 639–660. https://doi.org/10.1306/08131414051

Gaswirth, S.B., Lillis, P.G., Pollastro, R.M., Anna, L.O., 2013. Geologic Assessment of Undiscovered Oil and Gas in the Williston Basin Province, Montana, North Dakota, and South Dakota, in: US Geological Survey Williston Basin Province Assessment Team, Assessment of Undiscovered Oil and Gas Resources of the Williston Basin Province of North Dakota, Montana, and South Dakota. pp. 1–28.

Gerhard, L.C., Anderson, S.B., Fischer, D.W., 1990. Petroleum Geology of the Williston Basin, in: Interior Cratonic Basins. pp. 507–559.

Gerhard, L.C., Anderson, S.B., LeFever, J.A., Carlson, C.G., 1982. Geological Development, Origin, and Energy Mineral Resources of Williston Basin, North Dakota. Am. Assoc. Pet. Geol. Bull. V 66, 989–1020.

Grotzinger, J.P., 1989. Facies and evolution of precambrian carbonate depositional systems: emergence of the modern platform archetype. Control. carbonate Platf. basin Dev. based a Symp. 79–106.

Grover, P., 1996. Stratigraphy and Diagenesis of the Mississippian Bakken Shale-Lodgepole Limestone Sequence, Williston Basin, North Dakota. Texas A&M University.

Hallock, P., 1988. The role of nutrient availability in bioerosion: Consequences to carbonate buildups. Palaeogeogr. Palaeoclimatol. Palaeoecol. 63, 275–291. https://doi.org/10.1016/0031-0182(88)90100-9

Hansen, B., Long, G., 1991. Criteria for horizontal and vertical prospects in the Bakken Formation, Williston Basin, in: 1991 Guidebook to Geology and Horizontal Drilling of the Bakken Formation: Montana Geological Society, Billings, Montana. pp. 151–163.

Hart, M.B., 1991. The Late Cenomanian calcisphere global bioevent. Proc. Usher Soc. 7, 413–417.

Hogancamp, N.J., Pocknall, D.T., 2018. The biostratigraphy of the Bakken Formation: A review and new data. Stratigraphy 15, 197–224. https://doi.org/10.29041/strat.15.3.197-224

Holland Jr, F., Hayes, M., Thrasher, L., Huber, T., 1987. Summary of the biostratigraphy of the Bakken Formation (Devonian and Mississippian) in the Williston basin, North Dakota. Fifth Int. Willist. Basin Symp. 68–76.

Hubbard, D.K., Miller, A.I., David, A., Islands, U.S.V., 1990. Production and Cycling of Calcium Carbonate in a Shelf-Edge Reef System (St. Croix, U.S. Virgin Islands): Applications to the Nature of Reef Systems in the Fossil Record. J. Sediment. Petrol. 60, 335–360.

Kenter, J.A.M., Campbell, A.E., 1991. Sedimentation on a Lower Jurassic carbonate platform flank: geometry, sediment fabric and related depositional structures (Djebel Bou Dahar, High Atlas, Morocco). Sediment. Geol. 72, 1–34. https://doi.org/10.1016/0037-0738(91)90121-S

Kerr, D., 1988. Overview: Williston Basin Carbonate Reservoirs, in: Occurence and Petrophysical Properties of Carbonate Reservoirs in the Rocky Mountain Region. pp. 251–274.

Klostermann, L., Gischler, E., 2015. Holocene sedimentary evolution of a mid-ocean atoll lagoon, Maldives, Indian Ocean. Int. J. Earth Sci. 104, 289–307. https://doi.org/10.1007/s00531-014-1068-8

LeFever, J.A., 1990. History of Oil Production from the Bakken Formation, North Dakota, in: Geology and Horizontal Drilling of the Bakken Formation. pp. 3–18.

LeFever, J.A., Anderson, S.B., 1984. A little known carbonate reservoir within the lower Lodgepole Formation, northwestern North Dakota. Oil gas Saskatchewan 31–43.

LeFever, R., Crashell, J., 1991. Structural development of the Williston Basin in Southwestern North Dakota. Sixth Int. Willist. Basin Symp. 11, 222–233.

Li, Z., Schieber, J., 2018. Detailed facies analysis of the Upper Cretaceous Tununk Shale Member, Henry Mountains Region, Utah: Implications for mudstone depositional models in epicontinental seas. Sediment. Geol. 364, 141–159. https://doi.org/10.1016/j.sedgeo.2017.12.015

Loutit, T., Hardenbol, J., Vail, P., 1988. Condensed Sections: The Key to Age Determination and Correlation of Continental Margin Sequences, in Sea-Level Changes: An Integrated Approach. pp183-213

Mackie, J., 2013. Sedimentology and Diagenesis of the Lower Lodgepole Formation, Williston Basin, North Dakota. Colorado State University.

Macquaker, J.H.S., Bentley, S.J., Bohacs, K.M., 2010. Wave-enhanced sediment-gravity flows and mud dispersal across continental shelves: Reappraising sediment transport processes operating in ancient mudstone successions. Geology 38, 947–950. https://doi.org/10.1130/G31093.1

Macquaker, J. H. S., Keller, M.A., Davies, S.J., 2010. Algal Blooms and "Marine Snow": Mechanisms That Enhance Preservation of Organic Carbon in Ancient Fine-Grained Sediments. J. Sediment.

Res. 80, 934–942. https://doi.org/10.2110/jsr.2010.085

Martín, J.M., Braga, J.C., Betzler, C., Brachert, T., 1996. Sedimentary model and high-frequency cyclicity in a Mediterranean, shallow-shelf, temperate-carbonate environment (uppermost Miocene, Agua Amarga Basin, Southern Spain). Sedimentology 43, 263–277. https://doi.org/10.1046/j.1365-3091.1996.d01-4.x

Meissner, F., 1978. Petroleum Geology of the Bakken Formation Williston Basin, North Dakota and Montana, in: Geology and Horizontal Drilling of the Bakken Formation. pp. 19–42.

Merino-Tomé, O., Bahamonde, J.R., Samankassou, E., Villa, E., 2009. The influence of terrestrial run off on marine biotic communities: An example from a thrust-top carbonate ramp (Upper Pennsylvanian foreland basin, Picos de Europa, NW Spain). Palaeogeogr. Palaeoclimatol. Palaeoecol. 278, 1–23. https://doi.org/10.1016/j.palaeo.2009.04.002

Miller, K.B., Brett, C.E., Parsons, K.M., 1988. The Paleoecologic Significance of Storm-Generated Disturbance within a Middle Devonian. Palaios 3, 35–52.

Montgomery, S.L., 1996. Mississippian Lodgepole Play, Williston Basin: A review. Am. Assoc. Pet. Geol. Bull. 80, 795–810.

Nelson, C.S., Keane, S.L., Head, P.S., 1988. Non-tropical carbonate deposits on the modern New Zealand shelf. Sediment. Geol. 60, 71–94. https://doi.org/10.1016/0037-0738(88)90111-X

Novak, A., Egenhoff, S., 2019. Soft-sediment deformation structures as a tool to recognize synsedimentary tectonic activity in the middle member of the Bakken Formation, Williston Basin, North Dakota. Mar. Pet. Geol. 105, 124–140. https://doi.org/10.1016/j.marpetgeo.2019.04.012

Passey, Q.R., Bohacs, K.M., Esch, W.L., Klimentidis, R., Sinha, S., 2010. From oil-prone source rock to gas-producing shale reservoir - Geologic and petrophysical characterization of unconventional shale-gas reservoirs. SPE Middle East Oil Gas Show Conf. MEOS, Proc. 1, 6–34.

Peterhänsel, A., Pratt, B., 2001. Nutrient-triggered bioerosion on a giant carbonate platform masking the postextinction Famennian benthic community. Geology 29, 1079–1082. https://doi.org/10.1130/0091-7613(2001)029<1079:NTBOAG>2.0.CO;2

Pomar, L., 1991. Reef geometries, erosion surfaces and high-frequency sea-level changes, upper Miocene Reef Complex, Mallorca, Spain. Sedimentology 38, 243–269. https://doi.org/10.1111/j.1365-3091.1991.tb01259.x

Pomar, L., Brandano, M., Westphal, H., 2004. Environmental factors influencing skeletal grain sediment associations: A critical review of Miocene examples from the western Mediterranean. Sedimentology 51, 627–651. https://doi.org/10.1111/j.1365-3091.2004.00640.x

Purser, B., Seibold, E., 1973. The Principal Environmental Factors Influencing Holocene Sedimentation and Diagenesis in the Persian Gulf, in: The Persian Gulf Holocene Carbonate Sedimentation and Diagenesis in a Shallow Epicontinental Sea. pp. 1–10.

Randazzo, A., Baisley, K., 1995. Controls on carbonate facies distribution in a high energy lagoon, San Salvador Island, Bahamas, in: Terrestrial and Shallow Marine Geology of the Bahamas and Bermuda. pp. 157–175.

Rankey, E.C., 2004. On the Interpretation of Shallow Shelf Carbonate Facies and Habitats: How Much Does Water Depth Matter? J. Sediment. Res. 74, 2–6. https://doi.org/10.1306/071803740002

Reijmer, J.J.G., Ten Kate, W.G.H.Z., Sprenger, A., Schlager, W., 1991. Calciturbidite composition

related to exposure and flooding of a carbonate platform (Triassic, Eastern Alps). Sedimentology 38, 1059–1074. https://doi.org/10.1111/j.1365-3091.1991.tb00371.x

Ritter, A., Grammer, M., 2017. Utilizing sequence stratigraphy to develop a depositional model for Silurian (Niagaran) reefs in the Michigan Basin, in: Paleozoic Stratigraphy and Resources of the Michigan Basin: Geological Society of America Special Paper 531. pp. 81–104.

Savrda, C., Bottjer, D., 1987. The exaerobic zone, a new oxygen-deficient marine biofacies. Nature. 327, 54-56

Schieber, J., 2003. Simple Gifts and Buried Treasures- Implications of Finding Bioturbation and Erosion Surfaces in Black Shales. Sediment. Rec. 1, 4–8.

Schieber, J., 2009. Discovery of agglutinated benthic foraminifera in Devonian black shales and their relevance for the redox state of ancient seas. Palaeogeogr. Palaeoclimatol. Palaeoecol. 271, 292–300. https://doi.org/10.1016/j.palaeo.2008.10.027

Schieber, J., 2016. Mud re-distribution in epicontinental basins - Exploring likely processes. Mar. Pet. Geol. 71, 119–133. https://doi.org/10.1016/j.marpetgeo.2015.12.014

Schieber, J., Southard, J.B., 2009. Bedload transport of mud by floccule ripples - Direct observation of ripple migration processes and their implications. Geology 37, 483–486. https://doi.org/10.1130/G25319A.1

Schieber, J., Southard, J., Thaisen, K., 2007. Accretion of mudstone beds from migrating floccule ripples. Science. 318, 1760–1763. https://doi.org/10.1126/science.1147001

Schieber, J., Southard, J.B., Schimmelmann, A., 2010. Lenticular Shale Fabrics Resulting from Intermittent Erosion of Water-Rich Muds-Interpreting the Rock Record in the Light of Recent Flume Experiments. J. Sediment. Res. 80, 119–128. https://doi.org/10.2110/jsr.2010.005

Schieber, J., Southard, J.B., Kissling, P., Rossman, B., Ginsburg, R., 2013. Experimental Deposition of Carbonate Mud From Moving Suspensions: Importance of Flocculation and Implications For Modern and Ancient Carbonate Mud Deposition. J. Sediment. Res. 83, 1025–1031. https://doi.org/10.2110/jsr.2013.77

Schlager, W., 2003. Benthic carbonate factories of the Phanerozoic. Int. J. Earth Sci. 92, 445–464. https://doi.org/10.1007/s00531-003-0327-x

Scholle, P., Ulmer-Scholle, D., 2003. Other Micro- and Nannofossils in: A Color Guide to the Petrography of Carbonate Rocks: Grains, textures, porosity, diagenesis. AAPG Memoir 77. pp. 60-62

Scotese, C.R., 1994. Carboniferous paleocontinental reconstructions. U. S. Geol. Surv. Bull. 3–6.

Stroud, J., Sonnenberg, S.A., 2011. The Role of the Lower Lodgepole Formation in the Bakken Petroleum System, Billings Nose, North Dakota. Bakken-Three Forks Pet. Syst. Willist. Basin. Colorado School of Mines.

Vodrážková, S., Frýda, J., Suttner, T.J., Koptíková, L., Tonarová, P., 2013. Environmental changes close to the Lower-Middle Devonian boundary; the Basal Choteč Event in the Prague Basin (Czech Republic). Facies 59, 425–449. https://doi.org/10.1007/s10347-012-0300-x

Wilson, J.L., 1975. The Stratigraphy of Carbonate Deposits, in: Carbonate Facies in Geologic History. pp. 20–55. https://doi.org/10.1007/978-1-4612-6383-8_2

Wilson, R.D., Schieber, J., 2014. Muddy Prodeltaic Hyperpycnites In the Lower Genesee Group of

Central New York, USA: Implications For Mud Transport In Epicontinental Seas. J. Sediment. Res. 84, 866–874. https://doi.org/10.2110/jsr.2014.70

Zamagni, J., Mutti, M., Košir, A., 2008. Evolution of shallow benthic communities during the Late Paleocene-earliest Eocene transition in the Northern Tethys (SW Slovenia). Facies 54, 25–43. https://doi.org/10.1007/s10347-007-0123-3

Legend

Siliciclastic Facies

F2a/b= Not distinguishable in core

F1- Graded Argillaceous Mudstone

F2a- Massive Siliciclastic-Argillaceous Mudstone

F2b-Massive Calcareous-Argillaceous Mudstone

F3= Bioturbated Pyritized Bioclast-bearing Mudstone

F4=Lenticular Mudstone

F5-Bioclast-rich Wavy Mudstone

F6-Siliciclastic Siltstone

F7=Glauconitic Siltstone

F8=Calcareous Siltstone

Carbonate Facies

F9-Massive to Bioturbated Carbonate Mudstone

F10- Nodular Skeletal Wackestone

F10- Laminated Skeletal Packstone

Missing Core

Nature of Contact

Sharp, Planar

Sharp, Irregular

Erosional Contact

Gradational Contact

Special Features

Crinoids ★

Brachiopods

Concretion

Clastic Dike

Well: USA #1-24 (#8251) _____ County: Billings _____ State: ND _____

Company: Jerry Chambers _____ Stratigraphic iterval: Lower Lodgepole _____ Date: 5/2/18 & 3/5/19 _____

Depth	Sample/ Photo	Lithology	mudstone	wackestone	packstone	grainstone	breccia	Contact	Description	Interpretation
			clay	silt	fgs	mgs	cgs	gravel		
10,362										
10,363										
10,364										
10,365									Bluish grey carbonate MS that reacts vigorously with HCL	
10,366										
10,367										
10,368										
10,369	10,369.6								Black massive mudstone with rare bioclasts; Moderate effervescence	
10,370										
10,371										
10,372										
10,373										
10,374									Bioturbation evident	
10,375	10,375.1								Black massive mudstone; Does not effervesce.	
10,376									Bluish grey mudstone with pyritized bioclasts oriented parallel to bedding	
10,377	10,377								Black MS with trace bioclasts (<2 crinoids); Concretions near the top	
10,378									Bluish grey mudstone with grains oriented parallel to bedding; Bioclasts (~1-2%)	
10,379									Darker grey with laminae developed by grains; grains are randomly oriented.	
10,380									Greyish Blue WS; Decrease in grain size; Bioturbated; Increase in phosphate?; Decrease in grain size	
10,381										
10,382										
10,383										
10,384										
10,385									Brownish grey packstone; bioturbated	
10,386										
10387			Upper Bakken						Contact not exposed	

Well: Teddy 44-13 TFH (#18502)	County: Billings	State: ND
Company: Whiting Oil and Gas Co.	Stratigraphic iterval: Lower Lodgepole	Date: 5/3/18 & 3/8/19

Depth	Sample/ Photo	Lithology	mudstone — clay	wackestone — silt	packstone — fgs / mgs	grainstone — cgs	breccia — gravel	Contact	Description	Interpretation
10,491										
10,492										
10,493										
10,494										
10,495										
10,496									Laminae of bioclasts. Black mudstone with fine grained parallel, continuous, laminae	
10,497	10,496.7								Massice black mudstone with no bioclasts; moderate effervescence.	
10,498										
10,499									Massive brownish black mudstone with ~3-8% bioclasts (mostly pyritized); Moderate to high effervescence.	
10,500									Black mudstone with trace crinoids. Low effervescence.	
10,501	10,500.8								Black mudstone with brown concretions/burrows?	
10,502									Dark grey mudstone with ~5% crinoids and brachiopods	
10,503	10,502.1								Black mudstone with trace brachiopods; small brown blotches; low effervesce. Black pyrite? organics? Discontinuous shells (bioclasts and crinoids); Lamination? Black mudstone with bioclasts (~15%) brachiopods and crinoids. Greyish black mudstone with pyritized bioclasts. Laminated packstone with ~30% bioclasts (~0.1mm).	
10,504										
10,505									Bluish grey carbonate wackestone with ~10-15% bioclasts (Crinoids, gastropod), globular pyrite; bioturbated	
10,506										
10,507										
10,508									Light grey wackestone with ~15-20% bioclasts that are randomly oriented; discontinuous laminae; bioturbated	
10,509			Upper Bakken						Contact not exposed.	
10,510										

Depth	Sample/ Photo	Lithology	mudstone	wackestone	packstone	grainstone	breccia	Contact	Description	Interpretation
			clay	silt	fgs	mgs	cgs	gravel		

Well: Federal 12-1 (#9426/ E383)   County: Billings   State: ND

Company: Federal Exploration Co   Stratigraphic iterval: Lower Lodgepole   Date: 5/4/18

Depth	Sample/Photo	Description
10,778		
10,779		Grey massive carbonate mudstone with no bioclasts
10,780		
10,781	E383-10,781.3	Brown mudstone with pyritized bioclasts; High effervescence; Moderately bioturbated.
10,782	E383-10,782	
10,783	10,782.10 / 10,783.1	Black mudstone with thin mm thick laminations and a shell layer rich lamina at the base followed by faint dark and light lamina
10,784		
10,785	E383-10,785	
10,786	10,785.9	Dark brown to black mudstone with trace pyritized bioclasts and brown concretions and bioturbation
10,787	10,786.6	
10,788		
10,789	E383-10,789	
10,790		Bluish grey wackestone with some glauconite and phosphate?; Heavily bioturbated
10,791	E383-10,790.8	
10,792		
10,793	E383-10,793.2	
10,794		
10,795		
10,796		
10,797		
10,798		Greyish brown wackestone with ~15-25% bioclasts; crinoids (<0.5mm); silt laminae present throughout
10,799		
10,800	Upper Bakken	

67

Depth	Sample/Photo	Lithology	mudstone	wackestone	packstone	grainstone	breccia	Contact	Description	Interpretation
			clay	silt	fgs	mgs	cgs	gravel		

Depth	Description
10,496	
10,497	
10,498	
10,499	Massive bluish grey carbonate mudstone with <2% bioclasts and bioturbation?
10,500	
10,501	
10,502	
10,503	Dark blackish grey mudstone with 2-5% bioclasts
10,504	
10,505	
10,505.8 / 10,506	Massive bedded mudstone with no bioclasts; low to moderate effervescence
10,507	Dark blackish grey mudstone with ~2-5% bioclasts alligned parallel to bedding; Most bioclasts pyritized
10,508	
10,508.8	Dark black mudstone with rare bioclasts
10,509	Dark brown mudstone with bioclasts (~5%) parallel to bedding
10,509.7	Dark black mudstone with concretions and ~2% bioclasts
	Mudstone with bioclasts and phosphate intraclasts.
10,510	Dark grey massive mudstone with no clasts visible
10,511	Packstone with ~25% bioclasts, glauconite that decreases upsection
	Bluish grey wackestone
10,512	
10,513	
10,514	
10,515	
10,516	
10,517	Light grey wackestone with ~15% bioclasts and occasional silt rich laminae
10,518	
10,519	
10,520	
10,521	Upper Bakken

| Well: 3-17 TOC MEE USA (#7887/B659) | County: Billings | State: ND |
| Company: Tenneco Oil Co. | Stratigraphic iterval: Lower Lodgepole | Date: 4/3/18 |

Depth	Sample/ Photo	Lithology	mudstone	wackestone	packstone	grainstone	breccia	Contact	Description	Interpretation
			clay	silt	fgs	mgs	cgs	gravel		
									**Lots of missing core, so be cautious.	
10,758										
10,760										
10,762										
Scale Change 10,764									Grey massive bedded carbonate mudstone	
10,765										
10,766										
10,767										
10,768									Grey carbonate mudstone with bioturbation.	
10,769										
10,770									Black mudstone with up to 3% bioclasts and crinoids.	
10,771									Black mudstone with laminae identified by contrasting light brown and faint dark laminae.	
10,772										
10,773									Black mudstone with laminae identified by contrasting light brown and dark laminae. One lamina is composed of bioclasts.	
10,774									Dark grey mudstone with bioclasts and crinoids randomly distributed throughout and pyritized in places	
10,775	B659-10775								Black mudstone with calcareous concretion	
	B659-10775.6								Massive black mudstone with a bioclast	
10,776									Laminae with increase in both silt and bioclasts	
10,777	B659-10777									
10,778									Wackestone with increase in silt content	
10,779										
10,780									Decrease in grain size	
10,781										
10,782	B659-10782.3								Wackestone with bioclasts and crinoids (~10-15%) and trace amounts of pyrite	
10,783										
10,784										
10,785										
10,786										

Upper Bakken

| Well: Federal 11-4 (#10077/E385) | County: Billings | State: ND (Logged in ND & USGS) |

Company: Florida Exploration Co.   Stratigraphic iterval: Lower Lodgepole   Date: 5/4/18 & 3/8/19

Depth	Sample/Photo	Lithology	mudstone / clay	wackestone / silt	packstone / fgs	mgs	grainstone / cgs	breccia / gravel	Contact	Description	Interpretation
10,749											
10,750											
10,751										Massive bedded grey carbonate mudstone	
10,752											
10,753											
10,754											
10,755	E385-10754.5 E385-10755									Massive black shale	
10,756											
10,757											
10,758										Dark grey massive shale	
10,759	E385-10759.1								~~~~~	Dark shale with pyritized bioclasts	
10,760										Dark brown glauconite and shell laminae interbedded.	
10,761											
10,762											
10,763											
10,764											
10,765										Grey Wackestone (~10-15%) bioclasts, randomly oriented, cm thick laminae of shell rich layers.	
10,766											
10,767											
10,768		Upper Bakken									
10,769											

70

Well: AL Aguitaine 1-23BN (B832)	County: Billings	State: ND (Logged at USGS)
Company: Whiting Oil and Gas	Stratigraphic iterval: Lower Lodgepole	Date: 4/2/18

Depth	Sample/ Photo	Lithology	mudstone	wackestone	packstone	grainstone	breccia	Contact	Description	Interpretation
			clay	silt	fgs	mgs	cgs	gravel		

Depth	Description
10,328	
10,329	
10,330	
10,331	
10,332	
10,333	Massively bedded grey carbonate mudstone
10,334	
10,335	
10,336	
10,337	Calcareous mudstone with bioturbation
10,338	
10,339	Mudstone with pyritized bioclasts (~5-8%) oriented parallel to bedding
10,340	Massive dark mudstone
10,341	
10,342	Mudstone that contains pyritized bioclasts (~5-8%) elongated parallel to bedding. Becomes darker at 42'.
10,343	
10,344	Decrease in bioclast abundance with some pyrite throughout
10,345	
10,346	
10,347	
10,348	Wackestone with crinoids, some bioclasts (shells); grains randomly oriented; Cm-thick portions of the succession are clay rich laminae with an increase in shells (~20%); these laminae are irregularly thick and often pinchout
10,349	
10,350	
10,351	
10,352	
10353	Upper Bakken

Depth	Sample/Photo	Lithology	mudstone	wackestone	packstone	grainstone	breccia	Contact	Description	Interpretation
			clay	silt	fgs	mgs	cgs	gravel		

7,872

7,873

7,874

7,875 Massive calcareous mudstone with bioturbation in places

7,876

7,877

7,878 Large z-shaped calcareous dike in black mudstone
Thin laminations in a black shale

7,879 Thin discontinuous/continuous glauconite rich laminae intercalated with silt rich laminae; wavy bedding; phosphate clasts (<3cm)
Glauconite rich laminated packstone

7,880

7,881

7,882

7,883

7,884 Increase in grain abundance

7,885

7,886

7,887

7,888

7,889

7,890 Upper Bakken

Depth	Sample/ Photo	Lithology	mudstone		wackestone	packstone		grainstone	breccia	Contact	Description	Interpretation
			clay	silt		fgs	mgs	cgs	gravel			
9,151												
9,152											Nodular grey carbonate mudstone with some some wavy laminations	
9,153												
9,154												
9,155											Shell rich dark mudstone at the base that fines upward to a massive black mudstone. Grey carbonate mudstone that is heavily bioturbated with darker patches Dark glauconite rich bed with thin lighter colored laminations and burrows; No effervescence	
9,156												
9,157												
9,158												
9,159												
9,160												
9,161												
9,162												
9,163												
9,164												
9,165												
9,166		Upper Bakken										

Well: Grote 1-21H (#20648)   County: Burke   State: ND

Company: Continental Resources   Stratigraphic iterval: Lower Lodgepole   Date: 5/2/18 & 3/8/19

Well: Producer's 8-2H (#19773) _____ County: Burke _____ State: _ND _____

Company: Petro_Hunt LLC _____ Stratigraphic iterval:_ Lower Lodgepole _____ Date: 5/2/18 _____

Depth	Sample/ Photo	Lithology	mudstone		wackestone		packstone		grainstone		breccia	Contact	Description	Interpretation
			clay		silt		fgs	mgs	cgs		gravel			
													Core ends at 9,096ft, so likely additonal facies above	
9,096													Heavily bioturbated carbonate mudstone	
													Glauconite rich bed with laminations	
9,097													Bluish grey Wackestone with a decrease in bioclast abundance (~10%)	
9,098														
9,099													Grey Wackestone with ~15% bioclasts	
9,100														
9,101														
9,102														
9,103														
9,104														
9,105														
9,106														
9,107		Upper Bakken												

74

Well: Skarphol D#5 (#13167)	County: Divide	State: ND
Company: Conoco Inc.	Stratigraphic iterval: Lower Lodgepole	Date: 4/30/18 & 3/8/19

Depth	Sample/Photo	Lithology	mudstone — clay	wackestone — silt	packstone — fgs	— mgs	grainstone — cgs	breccia — gravel	Contact	Description	Interpretation
										Core ends at 8,905, so could be more shale units above. Also, core images online do not represent core seen at core center.	
8,905											
8,906										Nodular carbonate mudstone with laminae throughout and becomes darker in color upsection	
8,907											
8,908											
8,909											
										Glauconite rich(~25%) laminae	
8,910											
8,911											
8,912											
8,913										Grey wackestone with ~ 12-20% bioclasts and dicontinuous and continuous, irregular laminae with more bioclasts.	
8,914											
8,915											
8,916											
8,917											
8,918											
8,919											
8,920		Upper Bakken								Sharp contact	

75

Well: State ND 1-11H _____ County: Mountrail _____ State: _ND _____

Company: Amereda Hess Co. _____ Stratigraphic iterval: Lower Lodgepole _____ Date: 5/4/18 & 3/8/19 _____

Depth	Sample/Photo	Lithology	mudstone	wackestone	packstone	grainstone	breccia	Contact	Description	Interpretation
			clay	silt	fgs	mgs	cgs	gravel		
7,870										
7,871									Massive dark grey siltstone	
7,872										
7,873										
7,874										
7,875										
7,876										
7,877										
7,878										
7,879										
7,880										
7,881										
7,882										
7,883										
7,884										
7,885										
7,886										
7,887										
7,888									Grey siltstone-becomes more grey and effervesces slighlty more	
7,889										
7,890										

Well: Blooming Prairie (#17396)	County: Divide	State: ND
Company: Samson Resources Co.	Stratigraphic iterval: Lower Lodgepole	Date: 3/6/19

Depth	Sample/Photo	Lithology	mudstone — clay	wackestone — silt	packstone — fgs	— mgs	grainstone — cgs	breccia — gravel	Contact	Description	Interpretation
7,890											
7,891											
7,892											
7,893											
7,894											
7,895											
7,896											
7,897											
7,898											
7,899											
7,900										Thin <1mm shell layer laterally discontinuous	
7,901											
7,902											
7,903											
7,904										Laminations with a basal lamination composed of phosphatic clasts ~1mm thick	
7,905	7,904.8										
7,906											
7,907											
7,908											
7,909											
7,910										Faint laminations that are laterally continuous; alternate between black and slighlty grey; ~1-3mm	
7,911											
7,912											
7,913											
7,914										Black siltstone	
7,915											

Well: Blooming Prairie (#17396) Continued (2)_____ County: Divide_____ State: _ND_____

Company: Samson Resources Co._____ Stratigraphic iterval: Lower Lodgepole_____ Date: 3/6/19_____

Depth	Sample/ Photo	Lithology	mudstone	wackestone	packstone	grainstone	breccia	Contact	Description	Interpretation
			clay	silt	fgs	mgs	cgs	gravel		
7,915										
7,916	7,915.8								Slightly inclined and wavy contact with burrows from overlying mudstone	
7,917										
7,918									Lighter brown siltstone	
7,919										
7,920										
7,921										
7,922									Appears to be oil stained in places	
7,923										
7,924										
7,925										
7,926										
7,927										
7,928										
7,929										
7,930										
7,931										
7,932										
7,933										
7,934										
7,935										
7,936									~10 brachiopods and 1 crinoid on left side of core; each ~1mm and no preferential orientation	
7,937										
7,938									Massive black to dark brown siltstone with rare bioclasts (~1%) randomly throughout. Parallel to subparallel wavy fractures. Faint laminations in places	
7,939										
7,940										

78

Depth	Sample/Photo	Lithology	mudstone	wackestone	packstone	grainstone	breccia	Contact	Description	Interpretation
			clay	silt	fgs	mgs	cgs	gravel		
7,940										
7,941									Dark brownish black siltstone with moderate effervescence; Mostly massive with some faint laminae in places. Fractures and phosphate sparsely throughout	
7,942	7,942.1									
7,943									Phosphatic grains? form a laterally discontinuous lamina	
									Becomes darker due to more siliciclastic input	
7,944										
7,945										
									Hard ground	
7,946										
7,947										
7,948										
7,949										
7,950										
7,951										
7,952										
7,953										
7,954										
7,955										
7,956										
7,957										
7,958										
7,959										
7,960										
7,961										
7,962										
7,963										
7,964										
7,965										

Well: Rosenvold 1-30H (#19709)	County: Divide	State: ND
Company: Continental Resources	Stratigraphic iterval: Lower Lodgepole	Date: 4/30/18

Depth	Sample/Photo	Lithology	mudstone		wackestone	packstone	grainstone	breccia	Contact	Description	Interpretation
			clay	silt	fgs	mgs	cgs	gravel			
9,248										Carbonate mudstone with <10% bioclasts; nodular; some irregular laminae	
9,249											
9,250										Siliciclastic mudstone with ~15-20% bioclasts that are parially alligned parallel to bedding	
	9,250.3									Massive black mudstone	
9,251	9,251									Bioturbated carbonate mudstone	
										Laminated glauconite rich and poor beds with low effervescence	
9,252											
9,253										Wackestone with bioclasts (~10%); irregular laminae (0.1-1mm) that are continuous and discontinuous	
9,254											
9,255											
9,256											
9,257											
9,258											
9,259											
9,260											
9,261			Upper Bakken								

Well: Carus Fee #21-19 (#12785)		County: Dunn		State: ND
Company: Maxus Exp Co.		Stratigraphic iterval: Lower Lodgepole		Date: 5/4/18 & 3/5/19

Depth	Sample/Photo	Lithology	mudstone / clay	wackestone / silt	packstone / fgs	mgs	grainstone / cgs	breccia / gravel	Contact	Description	Interpretation
11,265											
11,266											
11,267											
11,268											
11,269										Grey Nodular Carbonate Mudstone	
11,270											
11,271										Bioturbated Carbonate Mudstone	
11,272											
11,273											
11,274	11,273.6										
11,275	11,274.6 / 11,275									Pyritized bioclasts randomly distributed throughout.	
11,276	11,276									Black to dark blue mudstone with rare brachiopod shells (~5mm); Low effervescence; Faint dark laminations when looking critically.	
11,277										Black mudstone with low to mod effervescence; Irregular brown blotches (<1mm) in a black matrix. Lag deposit with dark black matrix and bioclasts and phosphate intraclasts (up to 5mm).	
11,278	11,277.10									Laminated packstone with bioclasts and phosphate intraclasts; Dark grey. Grey carbonate mudstone with ~5% bioclasts (mostly crinoids)	
11,279	11,278.3										
11,280											
11,281											
11,282											
11,283										Nodular; Darker blue grey color; increase in silt laminae; bioclasts randomly oriented	
11,284											
11,285											
11,286										Grayish colored; Crinoids ~0.1mm on average and randomly oriented; heavily bioturbated; irregular continuous and discontinuous laminae.	
11,287											
11,289										Contact with Upper Bakken not exposed.	

Well: Angus Kennedy F32-24D (#607)		County: Dunn		State: ND
Company: Soconov-Vacuum Oil Co.		Stratigraphic iterval: Lower Lodgepole		Date: 3/30/18 & 3/8/19

Depth	Sample/ Photo	Lithology	mudstone	wackestone	packstone	grainstone	breccia	Contact	Description	Interpretation
			clay	silt	fgs	mgs	cgs	gravel		
10,483										
10,484										
			F1-F4?						Massive black mudstone with rare bioclasts; low effervescence	
10,485										
10,486			F1-F4?						Massive black mudstone with rare bioclasts; Low effervescence	
10,487	10,487								Massive black mudstone with rare brachiopod shells parallel to bedding; Low effervescence	
10,488									Black mudstone with pyritized bioclasts; low effervescence	
10,489										
10,490										
10,491									Grey nodular carbonate wackestone/mudstone	
10,492										
10,493										
10,494			F1-F4?						Black shale with thin brown parallel laminae faintly distinguishable (F4)?; 1 pyritized shell; No effervescence.	
10,495									Grey carbonate wackestone/mudstone (~10% bioclasts); irregular discontinuous laminae	
10,496										
10,497										
10,498										
10,499										
10,500										
10,501										
10,502										
10,503										
10,504									Grey wackestone with ~15% bioclasts randomly oriented	
10,505										
10,506										
10,507										
10508									Contact at 10508.8; Not exposed	

Upper Bakken

82

Depth	Sample/ Photo	Lithology	mudstone	wackestone	packstone	grainstone	breccia	Contact	Description	Interpretation
			clay	silt	fgs	mgs	cgs / gravel			
9,874										
9,875	9,875.6									
9,876										
9,877									Light grey carbonate mudstone with parallel laminations?; Dark grains (Phosphate?Glauconite?) alligned parallel to bedding	
9,878										
9,879	9,879 / 9,879.2								Dark black mudstone with laterally discontinuous brown blotches; low to moderate effervescence.; Similar to F5	
9,880									Darker mudstone/carbonate with phosphate clasts, bioclasts, crinoids, rip up clasts. Bioclasts not evenly distributed throughout with bioturbation from above.	
									Heavily bioturbated grey carbonate mudstone	
9,881									Bioturbated black mudstone with pyritized bioclasts	
9,882									Darker matrix with increase in mud content and pyrite lenses. Dark grey laminated packstone	
9,883									Wackestone with >10% bioclasts and carbonate nodules and irregular silt laminae that increase in abundance and thickness.	
9,884										
9,885										
9,886										
9,887										
9,888									Wackestone to mudstone with ~6-12% bioclasts and decrease in storm laminae	
9,889										
9,890										
9,891										
9,892										
9,893										
9,894									Wackestone with ~15% bioclasts, mostly crinoids; Irregular discontinuous silt laminae	
9,895										
9,896										
9,897										
9,898			Upper Bakken						Conformable contact with burrows present that are filled with Lodgepole	

Depth	Sample/Photo	Lithology	mudstone	wackestone	packstone	grainstone	breccia	Contact	Description	Interpretation
			clay	silt	fgs	mgs	cgs	gravel		

Depth	Sample/Photo	Description
10,245		
10,246		
10,247		Heavily bioturbated grey carbonate mudstone
10,248		
10,249		Dark mudstone with up to 2% bioclasts and moderate to high effervescence. Possibly horizontal burrows
10,250		Dark gray mudstone with up to 7% bioclats and bioturbation
10,251		
	10,251.6	Light brown mudstone with some bioclasts parallel to bedding
10,252		Dark mudstone with ~10-13% bioclasts
10,253		Carbonate mudstone that is bioturbated and lacks bioclasts
10,254		
	10,254.7	Laminations that are discontinuous; glauconite and bioclasts; Bioturbated
10,255		
10,256		
10,257		Gradual decrease in bioclast abundance to about 12%; rugose coral
10,258		
10,259		
10,260		
10,261		
10,262		
10,263		Wackestone with bioclasts (15%), crinoids, and a few gastropods
10,264		Upper Bakken

Depth	Sample/ Photo	Lithology	mudstone	wackestone	packstone	grainstone	breccia	Contact	Description	Interpretation
			clay	silt	fgs	mgs	cgs	gravel		
10,353									Middle Lodgepole	
10,354										
10,355										
10,356										
10,357									Thin discontinuous crinoid lag?	
10,358	10,358								Dark blue to black massive mudstone	
10,359										
10,360										
10,361										
10,362										
10,363										
10,364										
10,365										
10,366										

Depth	Sample/ Photo	Lithology	mudstone	wackestone	packstone	grainstone	breccia	Contact	Description	Interpretation
			clay	silt	fgs	mgs	cgs	gravel			
10,366											
10,367											
10,368											
10,369											
10,370	10369.9									Mudstone with black and brown laminations; with black laminae being thicker; Moderate effervescence	
10,371											
10,372											
10,373											
10,374											
10,375											
10,376											
10,377											
10,378											
10,379											
10,380											
10,381										Massive grey mudstone	
10,382											
10,383											
10,384										Glauconitized grains	
10,385										Carbonate mudstone that appears to have planar, continuous laminae?	
10,386											
10,387											
10,388											
10,389											
10,390											
10,391			Three Forks								

Well: Maus 23-22 (#19917)_____ County: Golden Valley_____ State: _ND_____

Company: Whiting Oil and Gas Co._____ Stratigraphic interval Lower Lodgepole_____ Date: 3/6/19_____

Depth	Sample/ Photo	Lithology	mudstone		wackestone	packstone		grainstone	breccia	Contact	Description	Interpretation
			clay	silt		fgs	mgs	cgs	gravel			
10,525												
10,526												
10,527												
10,528												
10,529												
10,530												
10,531											Massive grey carbonate mudstone	
10,532												
10,533											Contains ~2% pyritized bioclasts oriendted parallel to bedding	
10,534	10,533.8										Contains blotchy greyish brown blotches	
	10,534.4										Laminated mudstone with thin brown lamina <1mm that are straight and continuous lamina and some shell lamina	
10,535	10,534.7										Massive dark blue mudstone with moderate effervescence and rare bioclasts. F3?	
10,536												
10,537												
10,538												
10,539												
10,540												
10,541												
10,542												
10,543			Three Forks									

Well: Mariana Trust 12X-20G2 (#24123) Continued _____ County: McKenzie _____ State: _ND_____

Company: XTO Energy Inc._____ Stratigraphic iterval:_Lower Lodgepole_____ Date: 4/30/18 & 3/8/19_____

Depth	Sample/ Photo	Lithology	mudstone		wackestone		packstone		grainstone		breccia	Contact	Description	Interpretation
			clay		silt		fgs	mgs	cgs		gravel			
11,006														
11,007														
11,008														
11,009														
11,010														
11,011														
11,012														
11,013														
11,014														
11,015														
11,016														

Well: Mariana Trust 12X-20G2 (#24123) _____ County: McKenzie _____ State: _ND _____

Company: XTO Energy Inc _____ Stratigraphic iterval: Lower Lodgepole _____ Date: 4/30/18 & 3/8/19 _____

Depth	Sample/ Photo	Lithology	mudstone	wackestone	packstone	grainstone	breccia	Contact	Description	Interpretation
			clay	silt	fgs	mgs	cgs	gravel			
11,016											
11,017											
11,018											
11,019											
11,020											
11,021											
11,022											
11,023											
11,024											
11,025											
11,026											
11,027											
11,028											
11,029											
11,030											
11,031											
11,032											
11,033											
11,034											
11,035											
11,036											
11,037											
11,038											
11,039											
11,040											
11,041											

Depth	Sample/Photo	Lithology	mudstone	wackestone	packstone	grainstone	breccia	Contact	Description	Interpretation
			clay	silt	fgs	mgs	cgs	gravel		
11,220										
11,221										
11,222										
11,223										
11,224										
11,225										
11,226									Nodular light grey carbonate mudstone with trace amounts of pyrite shells	
11,227										
11,228										
11,229									Thin black mudstone that is shell rich (mostly brachiopod shells)	
									Dark mudstone with up to 5% pyritized bioclasts	
11,230	F1-F4?								Massive black mudstone with rare brachiopod shells parallel to bedding; Low effervescence	
11,231										
11,232										
11,233									Decrease in bioclasts (~10%)	
11,234										
11,235										
11,236									Contact distinguished by hard surface with borings	
11,237									Wackestone with up to 20% bioclasts (mostly crinoids); dicontinuous shell-rich laminae; carbonate nodeules; bioturbation	
11,238										
11,239										
11,240										
11,241									Conformable contact with burrows and liquefaction indicating soft sediment	
11,242		Upper Bakken								

Depth	Sample/Photo	Lithology	mudstone / clay	wackestone / silt	packstone / fgs	mgs	grainstone / cgs	breccia / gravel	Contact	Description	Interpretation

10,700

10,701

10,702 Nodular grey carbonate mudstone with bioturbation

10,703

Bioturbated mudstone

10,704 Massive black mudstone with moderate effervescence

Dark grey mudstone with ~5-8% bioclasts

10,705 Black mudstone with ~5% bioclasts and calcareous concretions

Black mudstone with rare bioclasts and possibly faint laminations

Lag deposit with phosphate clasts and bioclasts (crinoids & brachiopods)

10,706 Dark blue massive mudstone with rare bioclasts; moderate to high effervescence

10,707

10,708

10,709

10,710

10,711

10,712

10,713

10,714

10,715

10,716

Upper Bakken

10,717

91

Well: Fairbanks 1-20H (#21966) _____ County: Williams _____ State: _ND _____

Company: Continental Resources _____ Stratigraphic iterval: _Lower Lodgepole _____ Date: 3/7/19 _____

Depth	Sample/Photo	Lithology	mudstone		wackestone	packstone		grainstone	breccia	Contact	Description	Interpretation
			clay		silt	fgs	mgs	cgs	gravel			
10,539												
10,540												
10,541												
10,542												
10,543												
10,544												
10,545											Dark grey mudstone with ~5-10% bioclasts (<1mm) alligned parallel to bedding. Possibly F3? Dark blue massive mudstone with moderate to high effervescence	
10,546											Dark grey mudstone with concretions that effervesce. Black shells/clasts? in a black matrix	
10,547												
10,548												
10,549												
10,550												
10,551												
10,552												
10,553												
10,554												
10,555												
10,556												
10,557			Upper Bakken										

92

Depth	Sample/Photo	Lithology	mudstone		packstone	grainstone	breccia	Contact	Description	Interpretation
			clay	silt	fgs	mgs	cgs	gravel		

Depth markers:
9,415
9,416
9,417
9,418
9,419 — Slighlty more carbonate rich than usual
9,420
9,421 — Massive grey biouturbated carbonate mudstone
9,422 — Massive grey biouturbated carbonate mudstone
9,423
9,424 — Dark grey mudstone with large concretions within a matrix of pyritized bioclasts
9,425
9,426
9,427
9,428 — Greyish blue wackestone with an increase in silt rich laminae
9,429
9,430
9,431
9,432 — White wackestone with ~10% bioclasts and occasional pyrite nodules. Rare silt rich discontinuous laminae
9,433
9,434
9,435
9,436
9,437
9,438
9,439
9,440

Well: State ND 1-11H _____ County: Mountrail _____ State: _ND_____

Company: Amereda Hess Co._____ Stratigraphic iterval: Lower Lodgepole _____ Date: 5/4/18 & 3/8/19 _____

Depth	Sample/ Photo	Lithology	mudstone		wackestone	packstone		grainstone	breccia	Contact	Description	Interpretation
			clay		silt	fgs	mgs	cgs	gravel			
9,403												
9,404												
9,405												
9,406												
9,407											Nodular Carbonate MS	
9,408												
9,409											Heavily Bioturbated Carbonate MS	
											Dark MS with pyrite stringers	
9,410											Dark black MS with effervescent brown blotches	
											Nodular Carbonate MS	
9,411												
											Heavily Bioturbated Carbonate MS	
9,412												
											Laminated glauconite bed with silt laminae that effervesce little.	
9,413											Darker grey carbonate PS with bioclasts, glauconite, and phosphate?; Laminations	
9,414												
9,415												
9,416												
9,417											Slight decrease in bioclast	
9,418												
9,419												
9,420												
9,421	9420.5											
9,422												
9,423											Grey nodular carbonate WS; bioclast randomly oriented.	
9,424												
9,425			Upper Bakken								Conformable contact with Upper Bakken	

94

Well: Wayzetta 46-11M (#26661) Continued	County: Mountrail	State: ND
Company: EOG Resources	Stratigraphic iterval: Lower Lodgepole	Date: 3/7/19

Depth	Sample/Photo	Lithology	mudstone		packstone	grainstone	breccia	Contact	Description	Interpretation
				wackestone						
			clay	silt	fgs	mgs	cgs	gravel		
9,311										
9,312										
9,313									Nodular bioturbated carbonate mudstone	
9,314										
9,315										
9,316									Thin shell layer at the base overlain by thin black massive mudstone	
9,317										
9,318										
9,319										
9,320									Bioturbated nodular carbonate mudstone	
9,321										
9,322										
9,323										

95

Well: Wayzetta 46-11M (#26661) _____ County: Mountrail _____ State: _ND _____

Company: EOG Resources _____ Stratigraphic iterval: _Lower Lodgepole _____ Date: 3/7/19 _____

Depth	Sample/Photo	Lithology	mudstone	wackestone	packstone	grainstone	breccia	Contact	Description	Interpretation
			clay	silt	fgs	mgs	cgs	gravel		
9,323										
9,324									Heavily bioturbated carbonate mudstone	
9,325										
9,326										
9,327	9,327.2								Bioturbated from above	
									Appears to have parallel laminations with thin lighter layer; maybe lithoclasts?	
9,328									Dark grey mudstone with up to 8% bioclasts	
9,329										
9,330										
9,331									Dark grey carbonate mudstone with up to 8% bioclasts	
									Heavily bioturbated or clastic dike?	
9,332									Black mudstone with ~5-8% bioclasts not pyritized	
9,333										
9,334										
9,335										
9,336										
9,337										
9,338										
9,339										
9,340										
9,341										
9,342										
9,343										
9,344										
9,345										
9,346										
9,347										
9,348			Upper Bakken							

Depth	Sample/Photo	Lithology	mudstone		wackestone	packstone	grainstone	breccia	Contact	Description	Interpretation
			clay	silt		fgs	mgs	cgs	gravel		
9,690										Massive bioturbated nodular carbonate mudstone	
9,691											
9,692										Mudstone with laterally continuous laminae (<2mm thick). Lamina identified by variation between black and browns. Grey more carbonate rich mudstone with ~8% bioclasts	
9,693											
9,694										Nodular bioturbated carbonate mudstone	
9,695											
9,696											
9,697											
9,698											

| Well: Ness 41-21-2XH (#28036) | | | | | | | | County: Mountrail | | State: ND | |
| Company: Whiting Oil and Gas Co. | | | | | | | | Stratigraphic iterval: Lower Lodgepole | | Date: 3/8/19 | |

Depth	Sample/ Photo	Lithology	mudstone	wackestone	packstone	grainstone	breccia	Contact	Description	Interpretation
			clay	silt	fgs	mgs	cgs	gravel			

Depth	Sample/Photo	Lithology	mudstone clay	wackestone silt	packstone fgs	grainstone mgs	breccia cgs gravel	Contact	Description	Interpretation
9,698	9,698.4								Black mudstone with concretions and bioturbation	
9,699									Laminated mudstone with a thin layer of pyritized shells at base	
									Black mudstone with little effervescence and rare bioclasts	
9,700										
9,701									Black mudstone with light grey carbonate concretions and bioturbation	
									Low effervescence in mudstone. Concretions get larger upsection.	
9,702									Lag deposit with scour surface. Clay clasts present (<5mm)	
									Heavily bioturbated carbonate mudstone	
9,703										
9,704										
9,705										
9,706										
9,707										
9,708										
9,709										
9,710										
9,711										
9,712										
9,713										
9,714										
9,715										
9,716										
9,717										
9,718										
9,719										
9,720										
9,721										
9,722										
9,723			Upper Bakken								

98

Depth	Sample/ Photo	Lithology	mudstone clay	wackestone silt	packstone fgs	grainstone mgs	breccia cgs	gravel	Contact	Description	Interpretation
10,433											
10,434											
10,435											
10,436											
10,437											
10,438										Nodular carbonate mudstone	
10,439											
10,440										Black mudstone with bioclasts	
10,441										Laminated packstone with bioclasts in a dark matric	
10,442										Nodular grey carbonate mudstone with a few silt-rich laminae	
10,443											
10,444										Brown carbonate mudstone with bioturbation	
										Black massive mudstone	
10,445										Black mudstone with pyritized bioclasts	
10,446										Increase in grain size (~0.5mm)	
10,447											
10,448											
10,449											
10,450											
10,451											
10,452										Grey wackestone with bioclasts (15-20%) ~0.2-0.3mm	
10,453											
10,454											
10,455											
10,456			Upper Bakken							Contact not exposed	

Depth	Sample/Photo	Lithology	mudstone		packstone	grainstone	breccia	Contact	Description	Interpretation
			clay	silt	fgs	mgs	cgs	gravel		

Well: J. Horst 1-11H (#15986)   County: Mountrail   State: ND

Company: Amereda Hess Co.   Stratigraphic iterval: Lower Lodgepole   Date: 5/1/18

Depth values (top to bottom): 10,491 — 10,510

Sample/Photo: 10,494.1 ; 10,494.5

Descriptions:
- Nodular carbonate mudstone
- Black mudstone with ~2% pyritized bioclasts alligned parallel to bedding.
- Black mudstone with up to 2% bioclasts and grey concretions
- Bioturbated carbonate mudstone
- Laminated packstone with bioclasts. Increase in silt content
- Wackestone with up to 20% bioclasts (~0.2mm and up to 1mm) Irregular laminae throughout
- Dark grey nodular wackestone with bioclasts and crinoids (~0.1mm) and ammonite?

Upper Bakken

Well: A Trout 6H 2-14 (#19472)	County: Renville	State: ND
Company: Renegade Petroleum	Stratigraphic iterval: Lower Lodgepole	Date: 5/2/18 & 3/8/19

Depth	Sample/ Photo	Lithology	mudstone / clay	wackestone / silt	packstone / fgs	/ mgs	grainstone / cgs	breccia / gravel	Contact	Description	Interpretation
5,408											
5,409											
5,410											

Depth	Sample/Photo	Lithology	mudstone	wackestone	packstone	grainstone	breccia	Contact	Description	Interpretation
			clay	silt	fgs	mgs	cgs	gravel			

Well: A Trout 6H 2-14 (#19472)   County: Renville   State: ND

Company: Renegade Petroleum   Stratigraphic iterval: Lower Lodgepole   Date: 5/2/18 & 3/8/19

Well: Praus 21-28TFH (#20002)_____ County: Stark_____ State:_ND_____

Company: Whiting Oil and Gas Co._____ Stratigraphic iterval:_Lower Lodgepole_____ Date:_5/2/18_____

Depth	Sample/ Photo	Lithology	mudstone	wackestone	packstone	grainstone	breccia	Contact	Description	Interpretation
			clay	silt	fgs	mgs	cgs	gravel		

Depth									Description	Interpretation
10,026										
10,027										
10,028										
10,029									Grey carbonate mudstone	
10,030										
10,031										
10,032										
10,033										
10,034										
10,035										
10,036										
10,037										
10,038										
10,039									Dark mudstone that increases in pyritized bioclasts	
10,040									Dark grey massive mudstone	
10,041									Dark mudstone with ~ 15% bioclasts / Laminated packstone with glauconite and bioclasts	
10,042										
10,043									Decrease in bioclasts and increase in glauconite; globular pyrite	
10,044										
10,045									Lighter gray wackestaone with ~15% bioclasts	
10,046										
10,047										
10,048	10,047.8 Upper Bakken								Contact is wavy with shells in the upper 1 cm of the Bakken. Possible flame structures and load casts indicating the shale was still soft when carbonate was deposited on top.	

Well: IM Shorty 0805 (#17272) _ _ _ _ _ _ _ _ _ _ _ _ _ _ _ _ _ County: Ward _ _ _ _ _ _ _ _ _ _ _ _ _ _ _ _ _ _ _ State: _ND _ _ _ _ _ _ _ _ _ _ _ _ _ _ _

Company: Hess Corporation _ _ _ _ _ _ _ _ _ _ _ _ _ _ _ _ Stratigraphic iterval: Lower Lodgepole _ _ _ _ _ _ _ Date: 5/2/18 _ _ _ _ _ _ _ _ _ _ _

Depth	Sample/Photo	Lithology	mudstone	wackestone	packstone	grainstone	breccia	Contact	Description	Interpretation
			clay	silt	fgs	mgs	cgs / gravel			
7,540									Bioturbated carbonate mudstone	
7,541										
7,542									Black mudstone with possible laminations	
									Dark Laminated packstone that is still rich in silt	
7,543									Bioturbated carbonate mudstone	
									Very heavily bioturbated from overling facies	
7,544									Dark grey mudstone that effervesces	
7,545									Wavy Laminated packstone with crinoids, glauconite, and phosphate.	
7,546										
7,547										
7,548										
7,549										
7,550										
7,551									Grey Wackestone with ~12% bioclasts and carbonate nodules; Irregular silt laminae	
7,552										
7,553										
7,554										
7,555										
7,556										
7,557										
7,558			Upper Bakken							

104

Well: Loren 5303 14-12T (#27216)	County: Williams	State: ND
Company: Oasis Petroleum	Stratigraphic iterval: Lower Lodgepole	Date: 3/7/19

Depth	Sample/ Photo	Lithology	mudstone	wackestone	packstone	grainstone	breccia	Contact	Description	Interpretation
			clay	silt	fgs	mgs	cgs	gravel		
10,675										
10,676										
10,677									Black mudstone with light grey concretions and a pyritized ostracod shell?	
10,678									Black massive mudstone with up to 3% bioclasts	
10,679									Heavily bioturbated carbonate mudstone	
10,680									Black mudstone with light grey concretions	
10,681									Increase in black grains (Glauconite/Pyrite?)	
10,682										
10,683										
10,684										
10,685										
10,686										
10,687										
10,688										
10,689										
10,690		Upper Bakken								

105

Facies 2a

#12886-10505.8 (Facies 2a): This thin section is composed entirely of massively bedded facies 2a. It contains silt-sized detrital quartz, calcite, and mica distributed throughout a dark brown matrix. No biogenes or bioclasts >0.05mm are present within this thin section. *Phycosiphon* isp. fecal strings can be seen throughout this facies. For grain sizes and modal abundances see Tables 2 and 3.
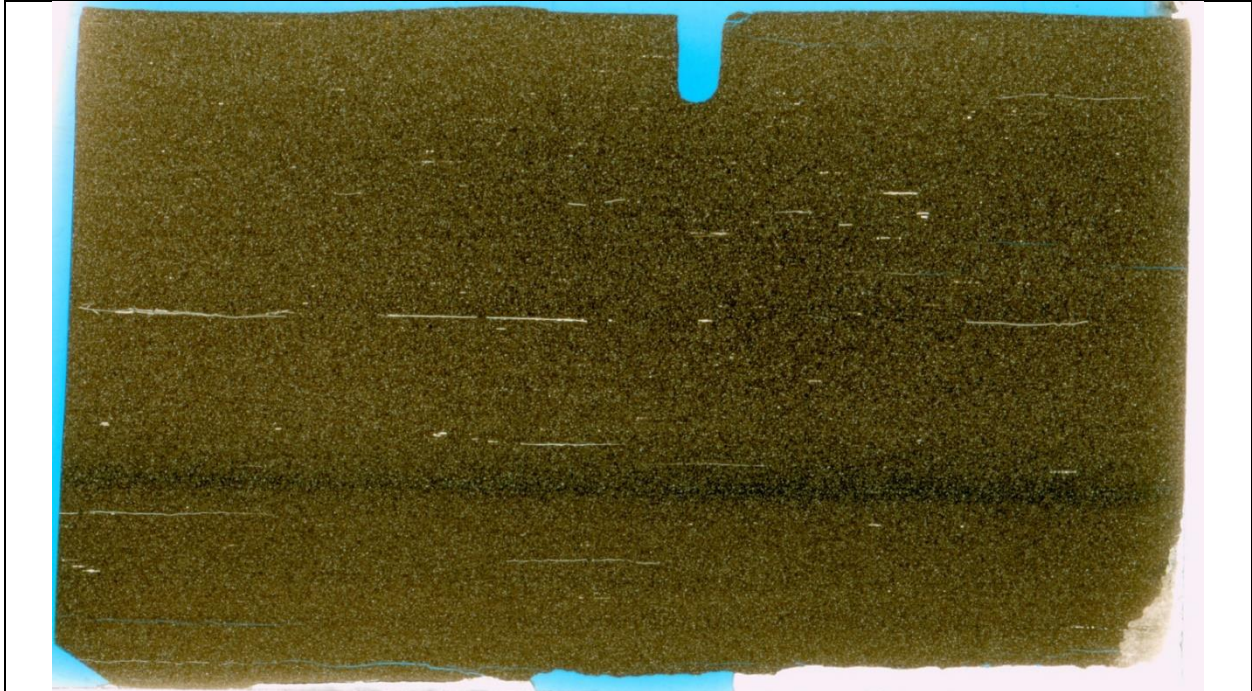
#12785-11273.6 (Facies 2a): This thin section is massively bedded with silt grains distributed evenly throughout. These silt grains are mostly detrital quartz with some calcite in a dark brown to black matrix. Bioclasts are rare and often oriented parallel to bedding. In places, *Phycosiphon* isp. fecal strings can be seen bisecting the matrix. For grain sizes and modal abundances see Tables 2 and 3.

#9426-10782.1 (Facies 2a): This thin section is comprised of massively bedded facies 2a with detrital silt distributed evenly throughout a dark brown to black matrix. The silt grains are mostly composed of quartz with some calcite present. Bioclasts are oriented parallel to bedding but are rare throughout this thin section. For grain sizes and modal abundances see Tables 2 and 3.

B832-10337.5 (USGS; Facies 2a): Silt grains account for about 15% of this thin section with detrital quartz (~10%) and calcite (~3%) making up the majority of the silt grains in addition to rare micas. These silt grains are distributed evenly throughout a dark brown to black matrix. Faint laminations of facies 2a are present within this thin section. No biogenes or bioclasts are present within this thin section.
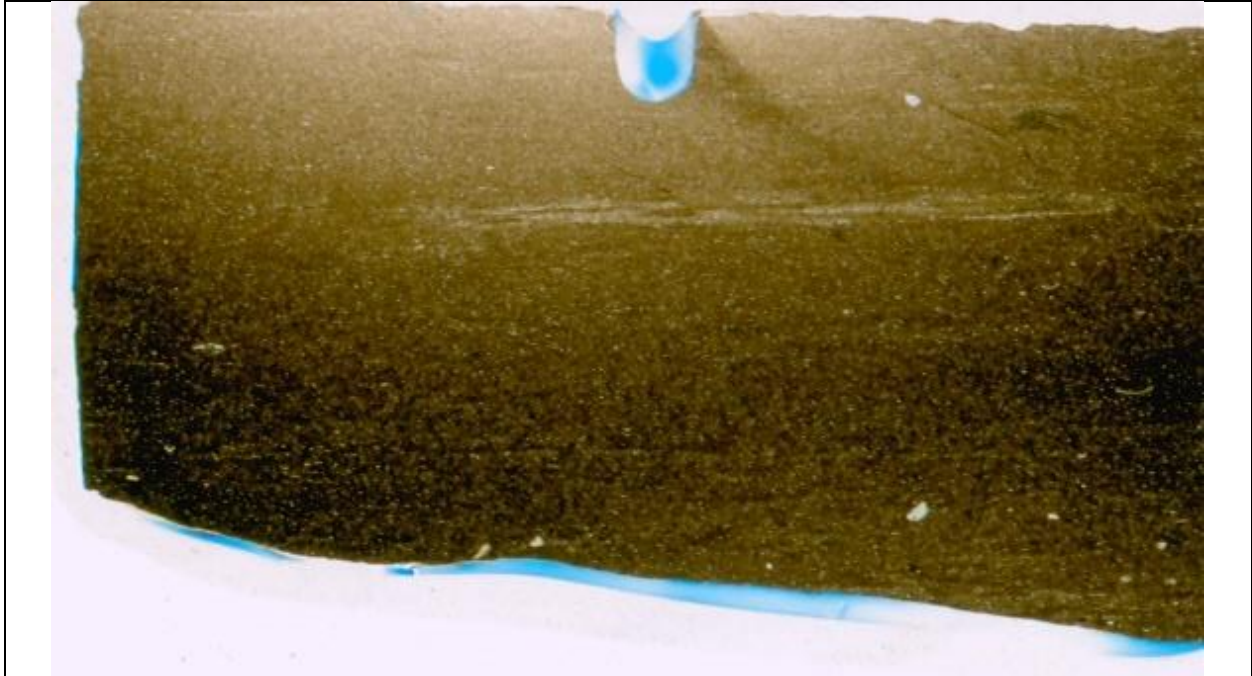
E385-10755 (USGS; Facies 2a): This thin section is comprised of silt grains (~15%) distributed within a dark brown matrix. Detrital quartz makes up the majority of the silt sized fraction in addition to some calcite. Furthermore, bioclasts are present in places although rare.

Facies 2b
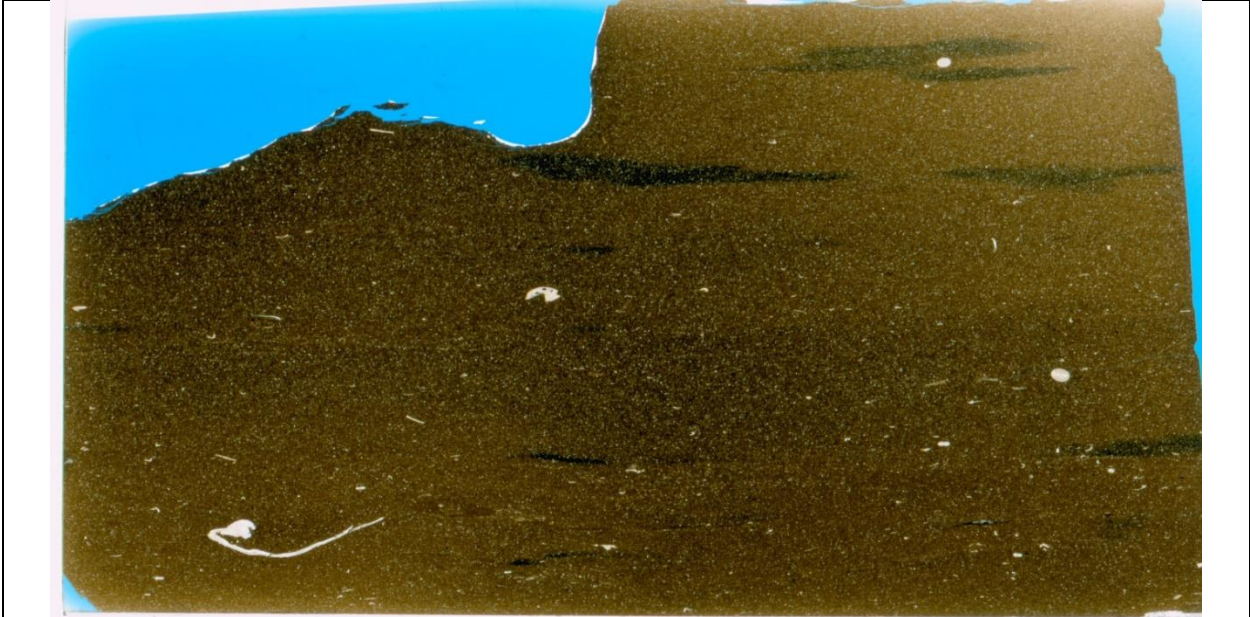
#15986-10494.1 (Facies 2b): This facies is massive and comprised of calcite, quartz, and mica silt distributed evenly throughout a mostly dark brown matrix. In addition, large brachiopod shell fragments and some echinoderms can be seen distributed evenly throughout. Sub-millimeter size roundish grains consisting of pyrite occur throughout and in places the matrix is darker in color due to a high abundance of pyrite. *Phycosiphon* isp. fecal strings bisect this thin section. For grain sizes and modal abundances see Tables 3 and 4.

#8251-10369.6 (Facies 2b): This thin section is composed of massively bedded facies 2b. Silt grains consist of calcite, quartz, and mica that are randomly distributed in a dark brown matrix. Brachiopod

shell fragments occur in places with the long axis parallel to bedding. In places, *Phycosiphon* isp. fecal strings bisect this facies. For modal abundances see Table 3 and for SEM data see Appendix 3.
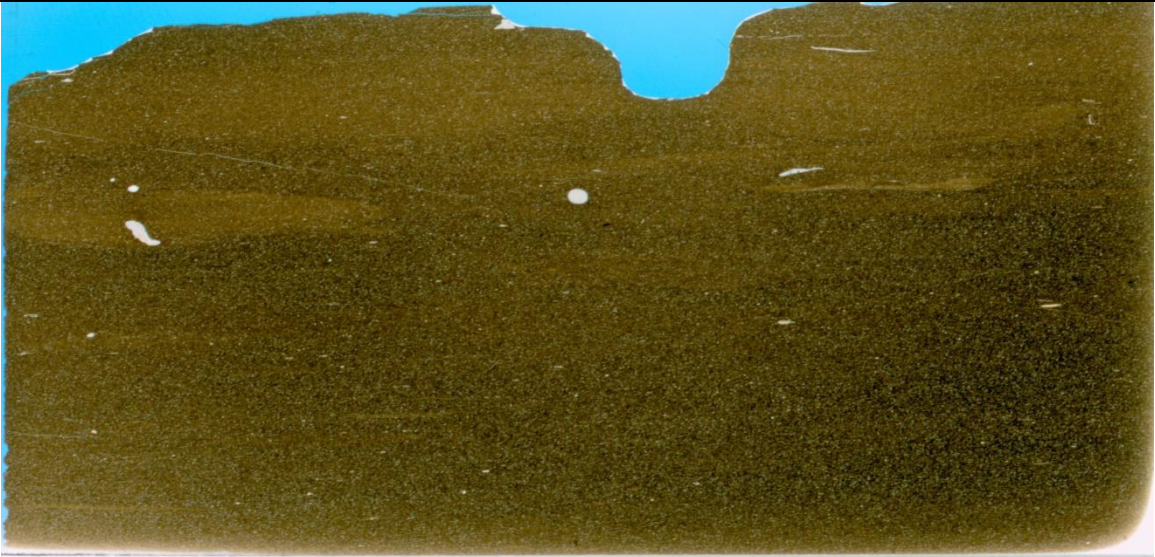
#8251-10375.1 (Facies 2b): Massive bedding is evident in this thin section which has a silt fraction composed of mostly calcite with some quartz. In addition, brachiopods and echinoderms are rare and occur within a dark brown matrix. In the upper portion of the thin section, a light brown concretion is evident. For grain sizes and modal abundances see Tables 3 and 4.
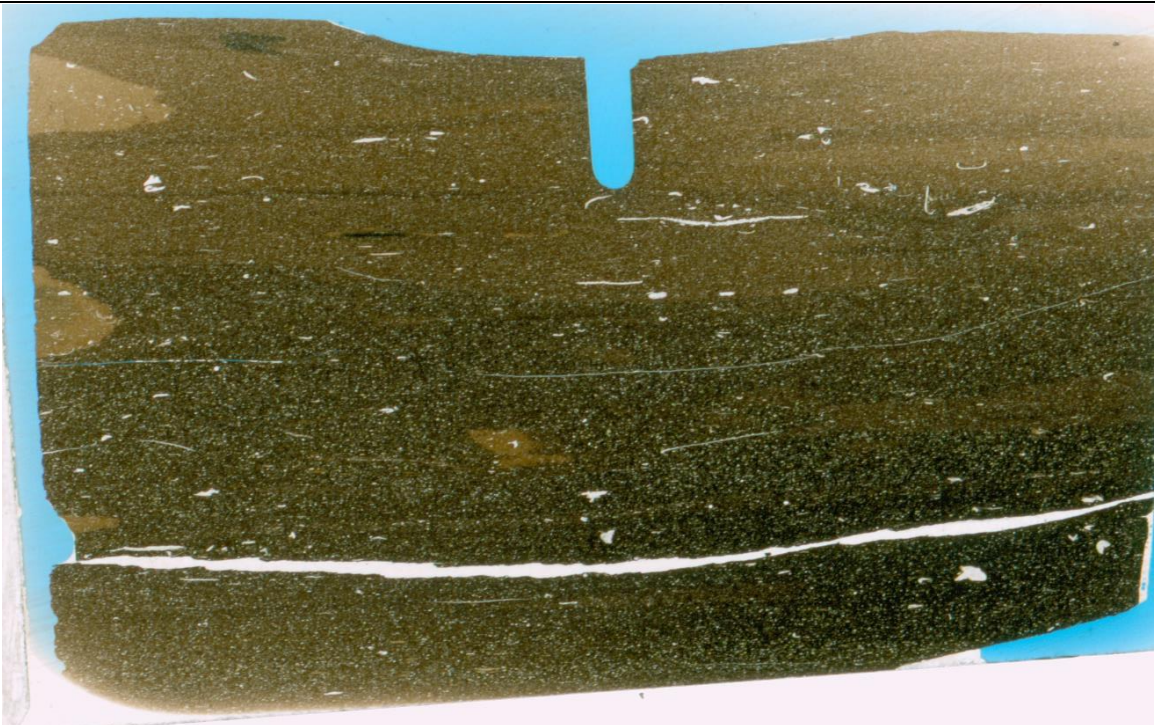
#8251-10377 (Facies 2b): Calcite and quartz silt grains occur throughout this thin section within a dark brown to black matrix. Brachiopods and bioclastic material are present throughout this facies. Two

concretions can be seen along the edge of the upper half of the thin section and are light brown in color. For grain sizes and modal abundances see Tables 3 and 4.
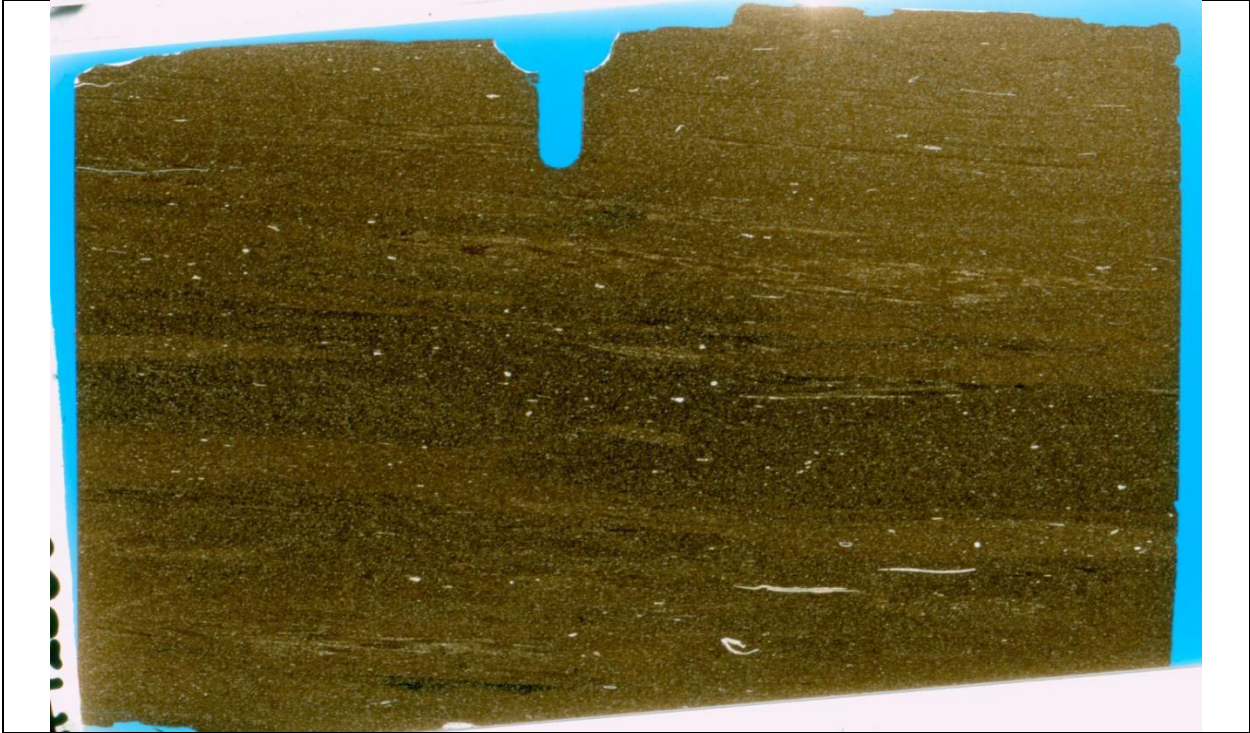
#12886-10508.8 (Facies 2b): This facies is comprised of silt grains consisting of calcite, quartz, and mica that are distributed evenly throughout a brown matrix. Brachiopods and agglutinated foraminifera can be seen within this thin section, however, both are rare. *Planolites* isp. burrows are present within this thin section and have little silt within them. For grain sizes and modal abundances see Tables 3 and 4 and for SEM data see Appendix 3.
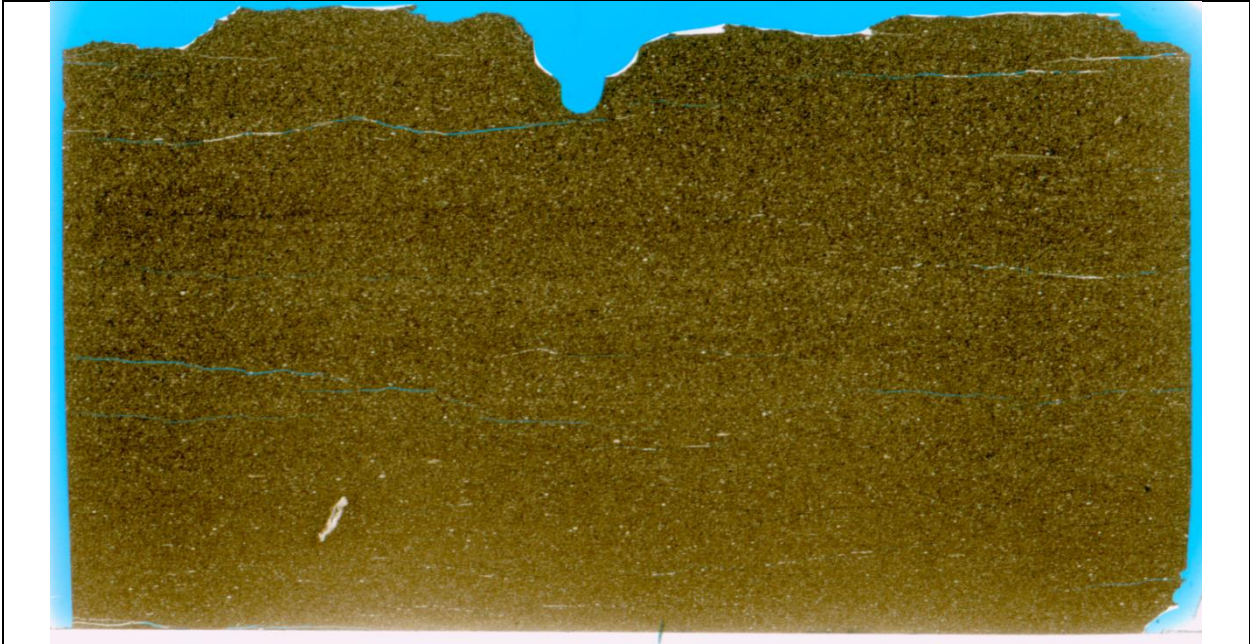
#18502-10496.7 (Facies 2b): This thin section has an abundance of calcite silt with some quartz grains intermixed in a dark brown matrix that is massively bedded. Rare large bioclasts are present, however, coarse silt grains appear to be the remains of broken bioclasts. Calcispheres make up a small portion of the silt-sized fraction. For grain sizes and modal abundances see Tables 3 and 4.
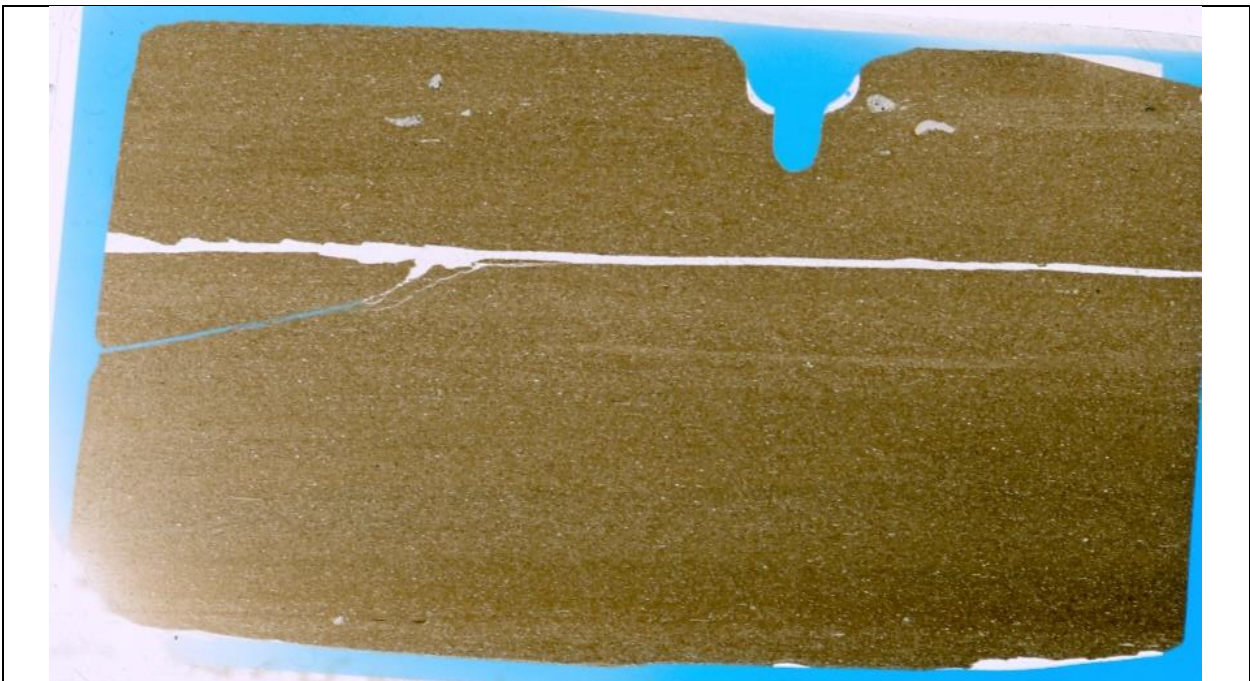
#19917-10534.7 (Facies 2b): This thin section is composed of laminae of facies 2b that have about 20% silt grains distributed throughout a brown matrix. Calcite accounts for about 15% of these silt grains in addition to about 5% quartz. In the upper portion of the thin section, several large bioclasts are present, however, broken bioclasts make up a portion of the silt sized fraction. *Planolites* isp.

occur throughout this facies and are light brown in color. *Phycosiphon* isp. also occur within this facies.
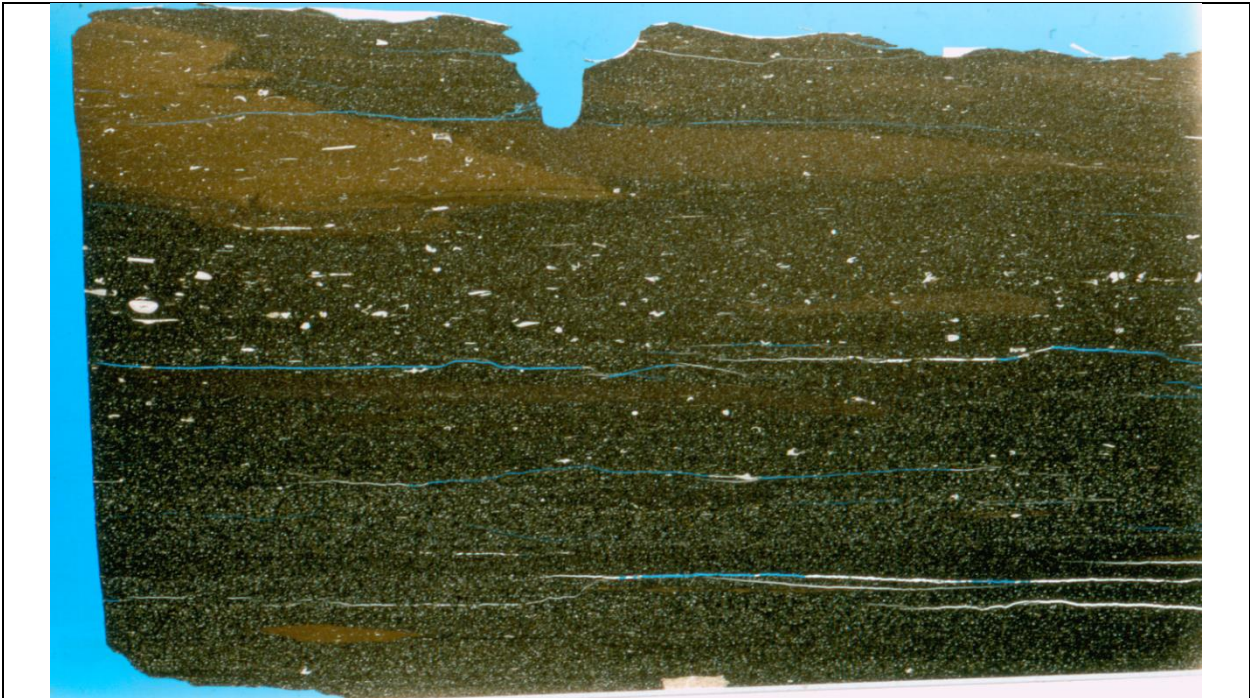
#18502-10502.1 (Facies 2b): This thin section has calcite and quartz silt present within a dark brown to black matrix. Bioclasts are present throughout, however, occur in higher concentrations in the upper half of the thin section. Echinoderms and agglutinated foraminifera can be identified but are rare in the thin section. In the upper left-hand portion of the thin section a light brown concretion is present with a similar concentration of silt and bioclasts as the surrounding matrix. For grain sizes and modal abundances see Tables 3 and 4.
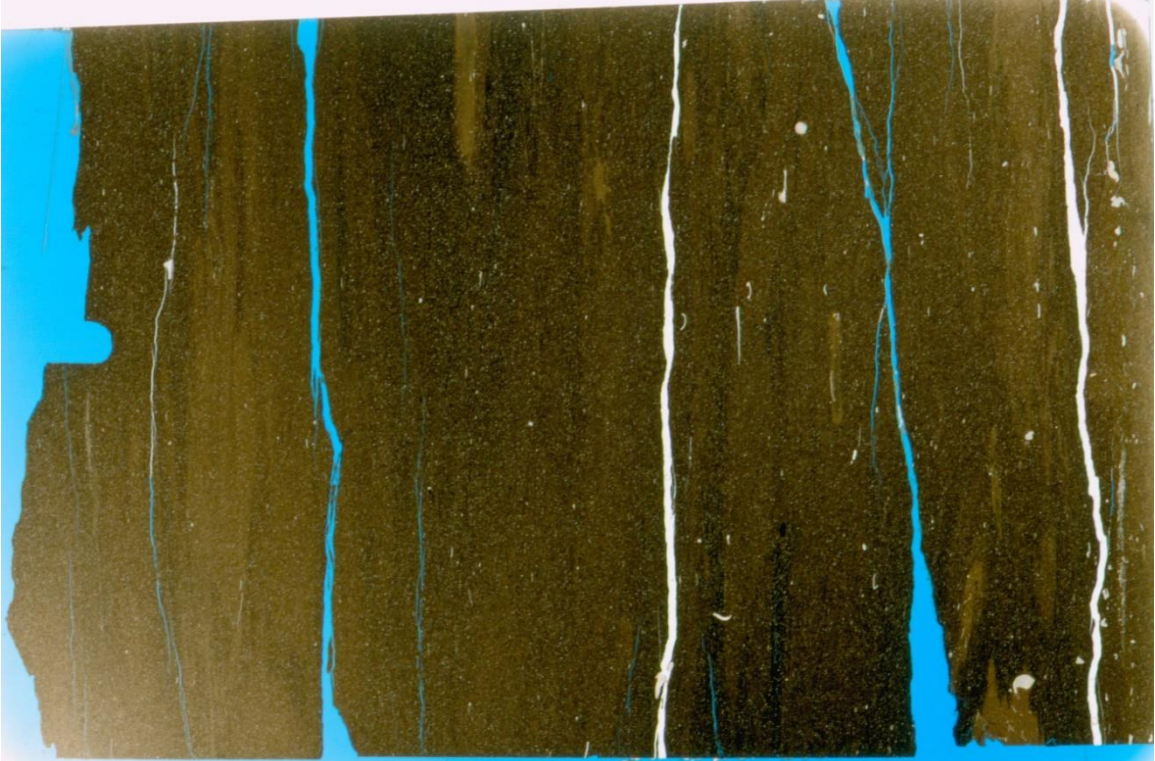
#18502-10500.8 (Facies 2b): This thin section is massively bedded and comprised entirely of facies 2b with a silt-sized fraction that has more detrital calcite that quartz silt. Although not abundant, bioclasts are present throughout this facies. Light brown concretions are present and often irregularly shaped with sharp edges. *Planolites* isp. burrows are present within this thin section although not common. For grain sizes and modal abundances see Tables 3 and 4.

#12785-11276 (Facies 2b): Silt grains are distributed throughout this thin section and mostly composed of calcite. This thin section has two massive beds of this facies with light brown concretions extending several centimeters across the thin section that appear to grow from burrows. Bioclasts are present in low concentrations throughout this facies and are slightly more abundant within the concretions. For grain sizes and modal abundances see Tables 3 and 4.

#12785-11274.6 (Facies 2b): This thin section has a matrix that varies in color from brown to black in places. Calcite silt is present throughout in addition to some quartz and micas. Brachiopods and agglutinated foraminifera can be identified within this thin section but mostly bioclasts are present. Sub-millimeter-sized components consisting of pyrite are distributed throughout and occur more often where the matrix is black and are less abundant when it is brown. For grain sizes and modal abundances see Tables 3 and 4.

#9426-10785.9 (Facies 2b): This thin section is composed of silt grains with more calcite than quartz silt in a light to dark brown matrix. Light brown concretions are present throughout and comprised of the same abundance of silt grains as the surrounding dark brown matrix, but the concretions have slightly more bioclasts. For grain sizes and modal abundances see Tables 3 and 4.
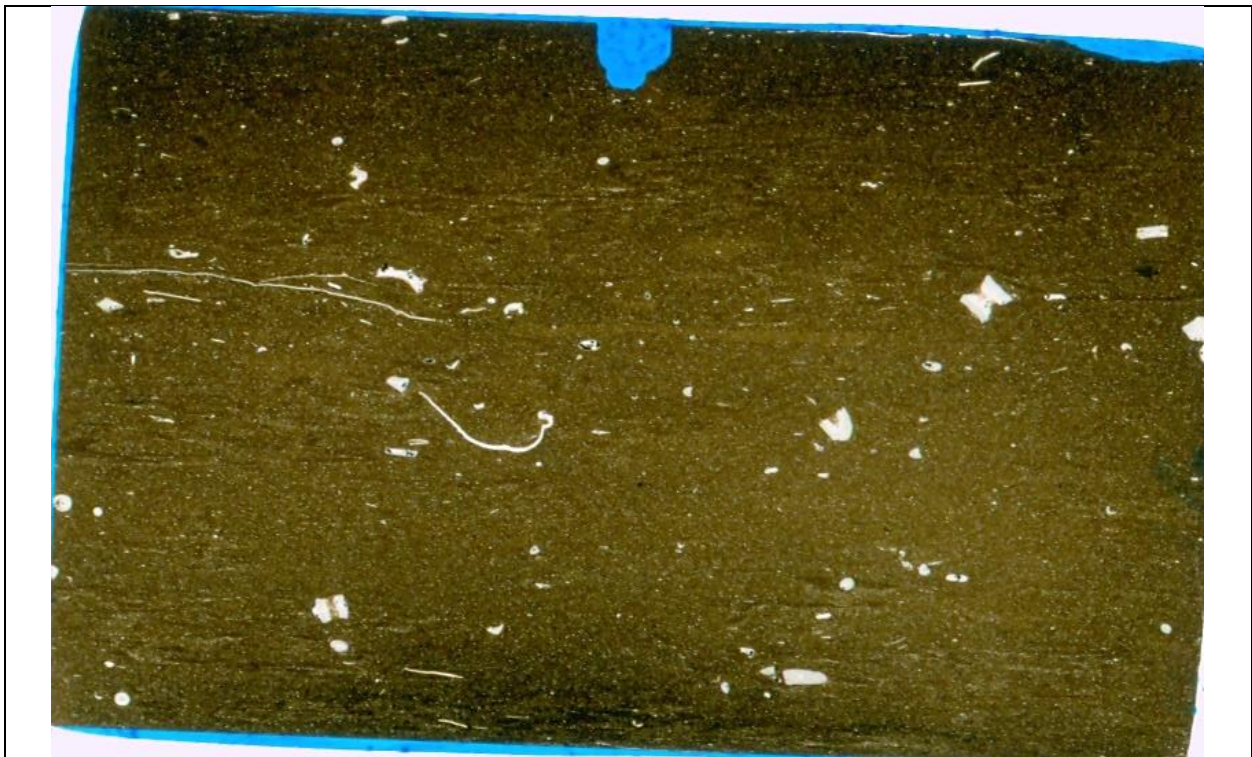
E383-10782 (USGS; Facies 2b): This facies is massively bedded with more calcite (~10%) than quartz silt (~4%). In addition, both brachiopod and echinoderms are distributed throughout this facies in a brown matrix. *Planolites* isp. burrows can be identified in places as they are lighter in color than the surrounding matrix.
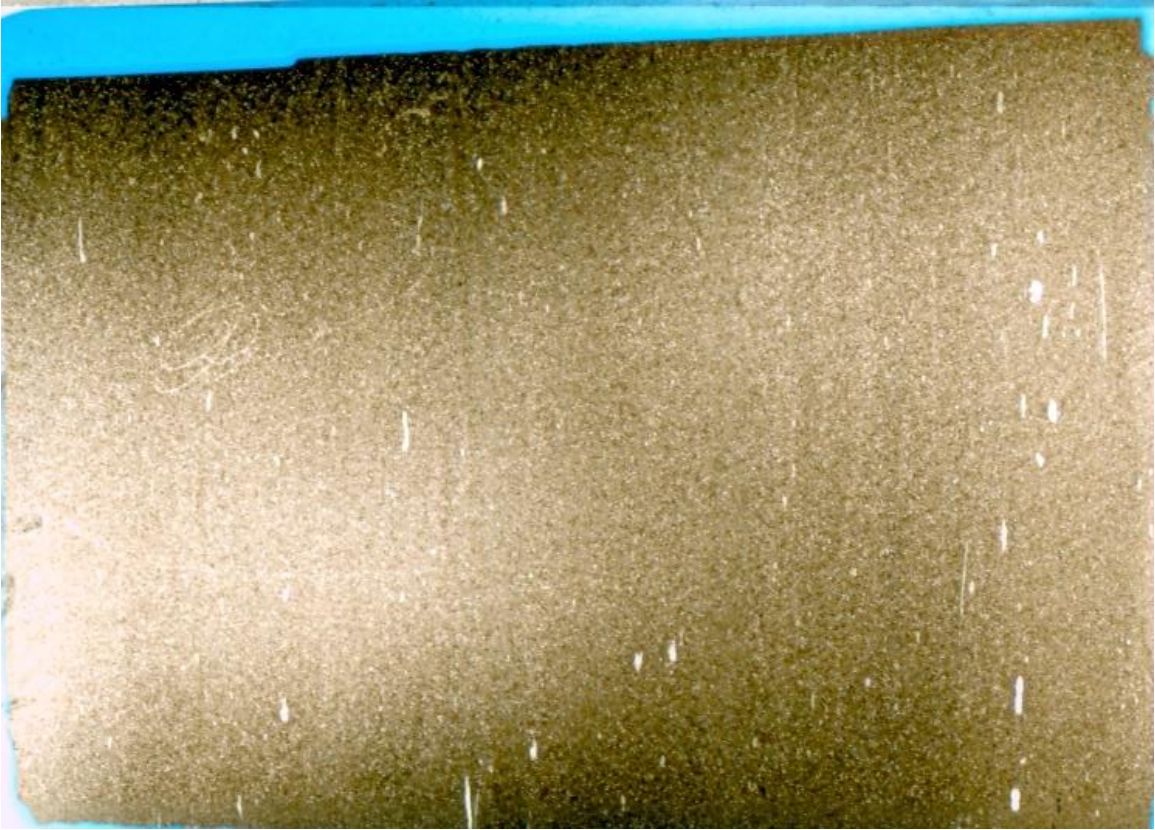
B659-10775 (USGS; Facies 2b): This thin section is comprised of several laminae with detrital silt grains distributed throughout evenly. Silt grains (~25%) are composed of detrital calcite (~18%), some quartz (~6%), and rare micas. In addition, bioclasts are present in places and are generally oriented parallel to bedding. These grains occur within a brown matrix.

Facies 3
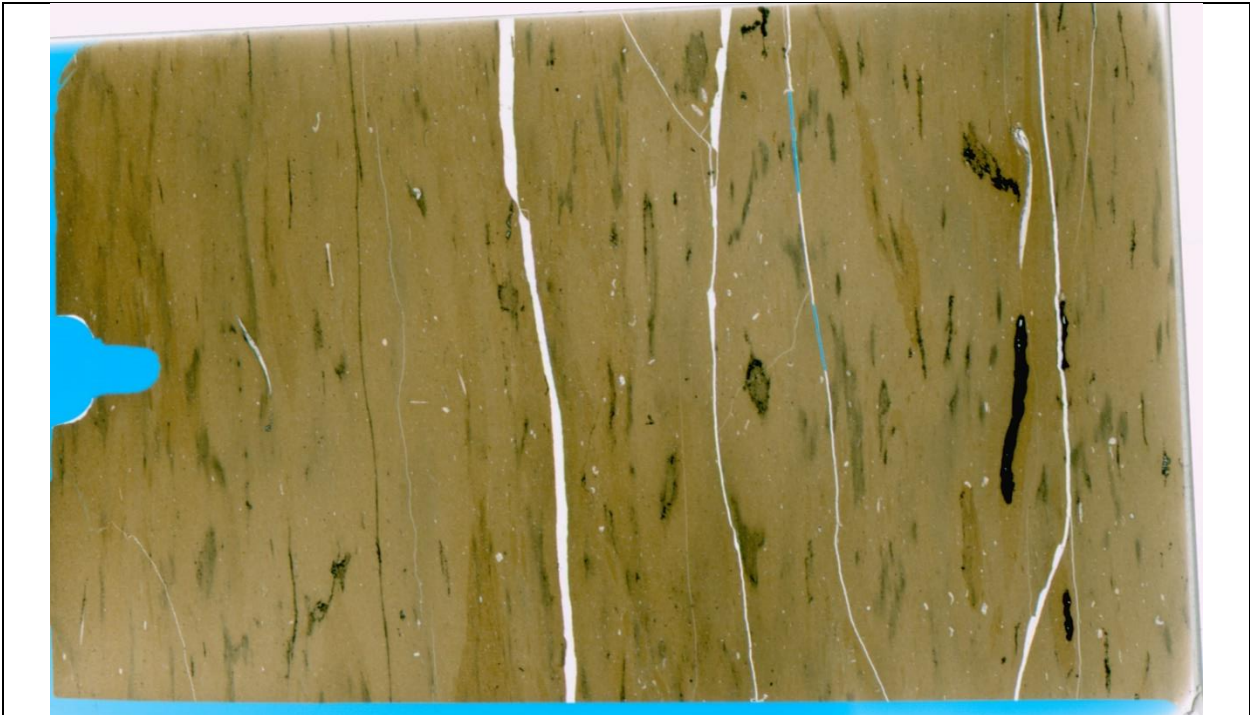
#20453-10251.6 (Facies 3): This thin section is comprised of a massive bed of facies 3 containing some brachiopod debris, however, most bioclasts have been pyritized. Although not in great concentrations, detrital calcite and quartz silt are distributed evenly throughout the light brown matrix that has more calcite than quartz within it. *Chondrite*s isp. burrows occur parallel to bedding. For grain sizes and modal abundances see Tables 3 and 4.
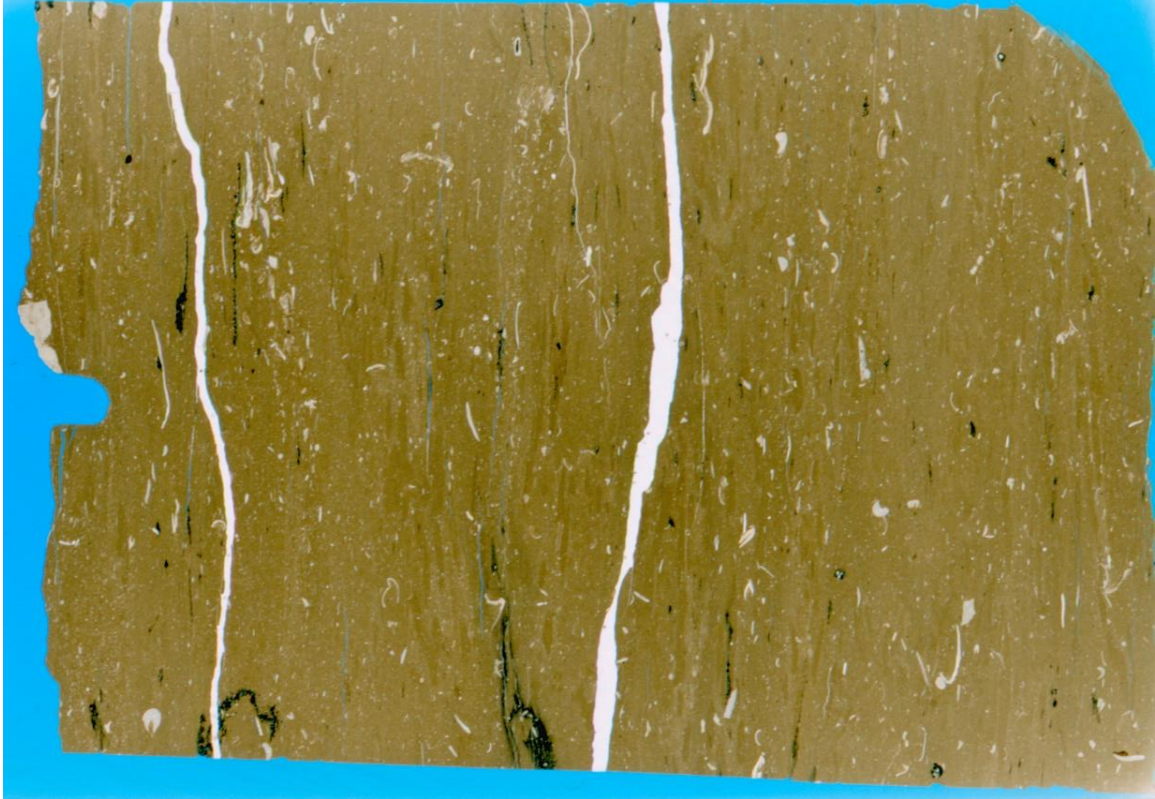
#12886-10509 (Facies 3): This thin section is composed of bioclasts that are evenly distributed throughout a light brown matrix. Most biogenes can be identified as echinoderms and brachiopods composed of calcite, however, some are replaced by pyrite. In addition, silt is present and comprised mostly of calcite with minor amounts of quartz. *Chondrite*s isp. burrows occur parallel to bedding and often in close proximity to one another. For grain sizes and modal abundances see Tables 3 and 4.
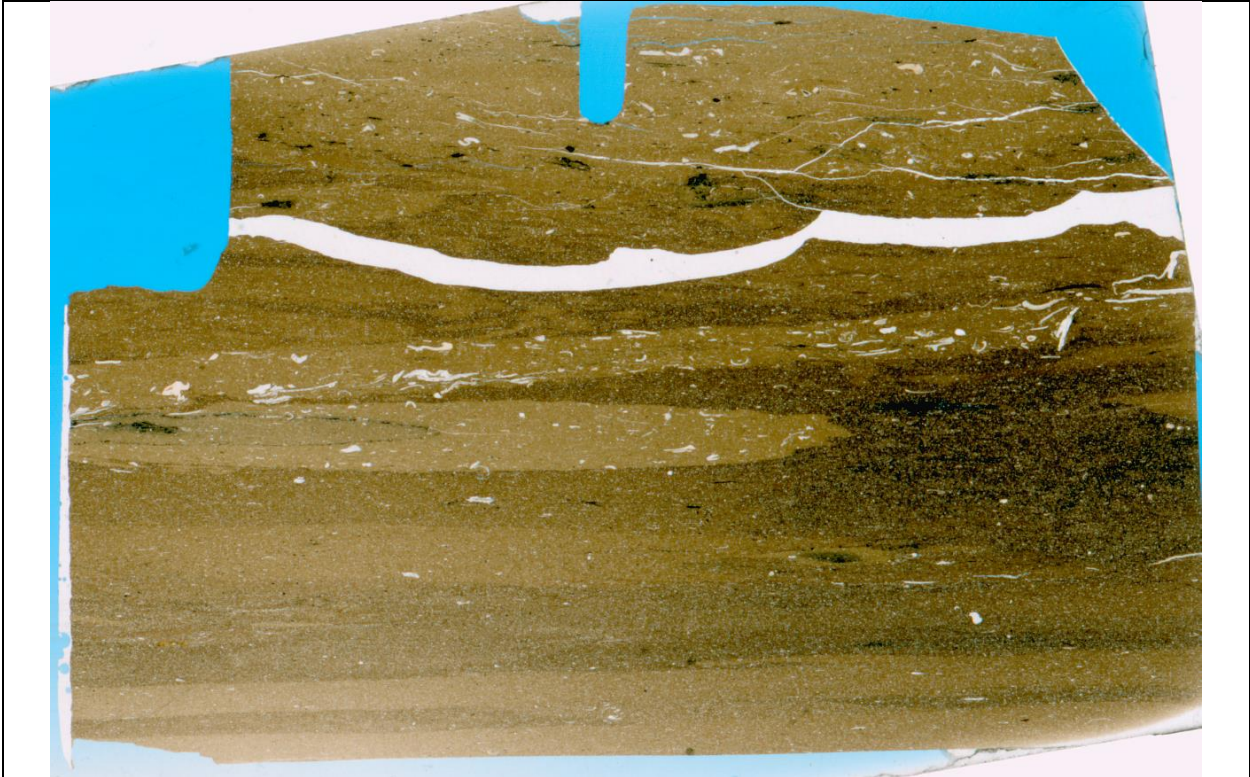
#12886-10509.7 (Facies 3): Bioclasts are present in most of this thin section with some of them being pyritized. In addition, calcite silt is distributed throughout with some quartz silt. Light brown concretions occur within this thin section and have a slightly higher concentration of bioclasts when compared to the surrounding rock. *Chondrite*s isp. burrows are present and elongated parallel to bedding; they often occur in close proximity to one another. For grain sizes and modal abundances see Tables 3 and 4.
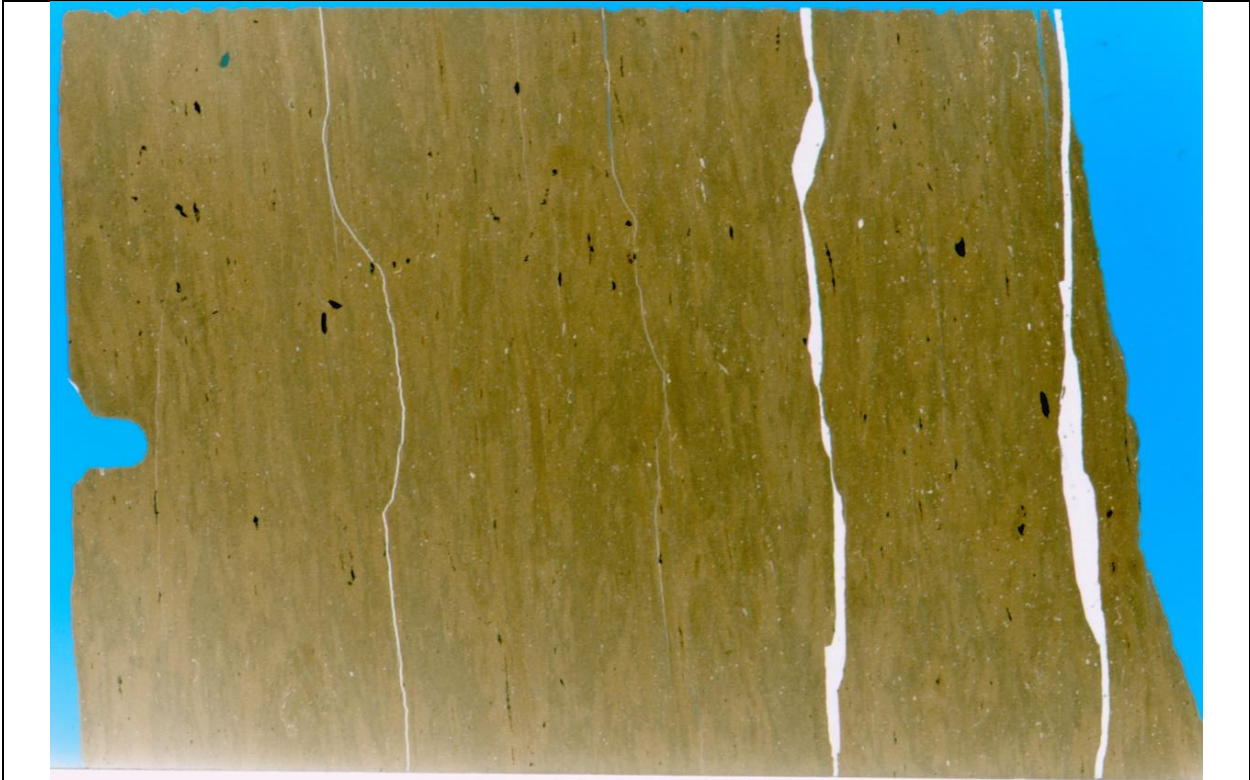
#12785-11277.10 (Facies 3): This thin section is dominated by a light grey to brown matrix with some silt grains throughout in low modal abundances. The silt-sized fraction is composed mostly of calcite with some quartz grains. Pyritized bioclasts are present throughout this thin section in addition to calcareous bioclasts that are randomly oriented. This thin section has a high abundance of *Chondrite*s isp. burrows bisecting through the matrix. For grain sizes and modal abundances see Tables 3 and 4.

#21734-10358 (Facies 3): Facies 3 makes up this thin section and is bisected by *Chondrites* isp. burrows. In addition, bioclastic material (~3%) is distributed throughout the entire thin section with a slightly higher concentration near the top. Calcispheres and agglutinated foraminifera are present but rare within this thin section. Silt grains account for about 15% of this facies and are comprised of detrital calcite with rare quartz grains. The silt and bioclast grains occur within a light brown matrix that likely has more calcite than quartz.
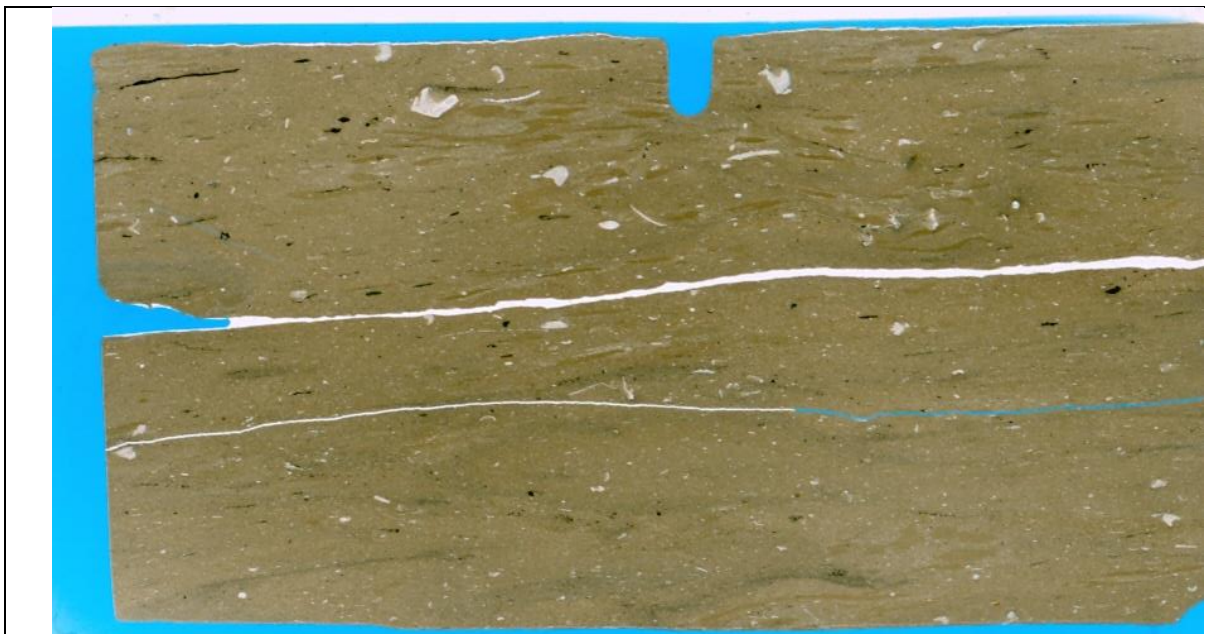
#19917-10533.8 (Facies 3): This thin section has bioclasts distributed throughout with some of the bioclasts being pyritized. This thin section has about 10% silt grains with detrital calcite accounting for 9% of the silt in addition to 1% quartz. These grains are distributed throughout a light brown matrix. *Chondrites* isp. burrows occur in clusters in various places throughout this thin section.
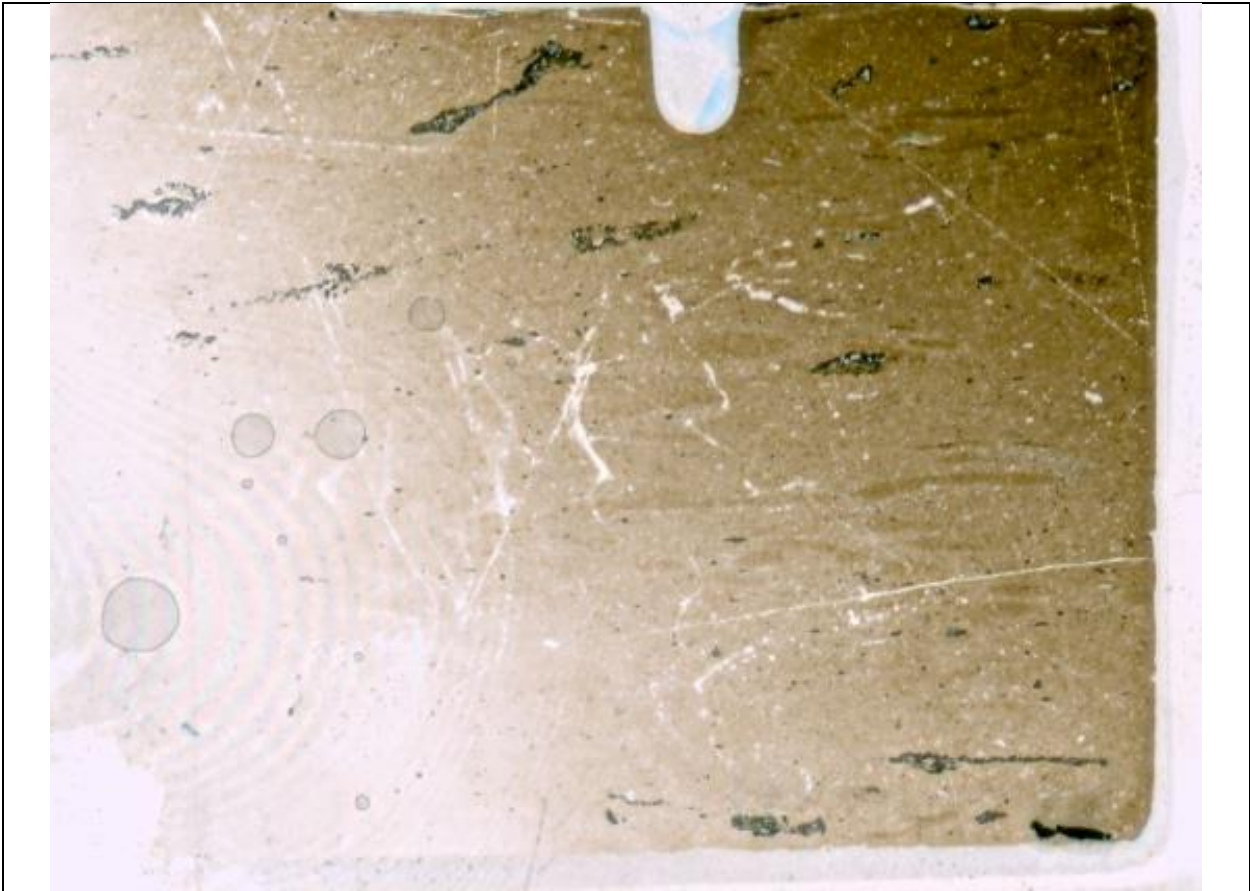
B832-10338.9 (USGS; Facies 3): This thin section contains detrital calcite (~10%) and some quartz (~5%) silt in a light brown matrix. Large pyritized bioclasts are present in addition to brachiopods. *Chondrite*s isp. burrows occur parallel to bedding within this thin section.
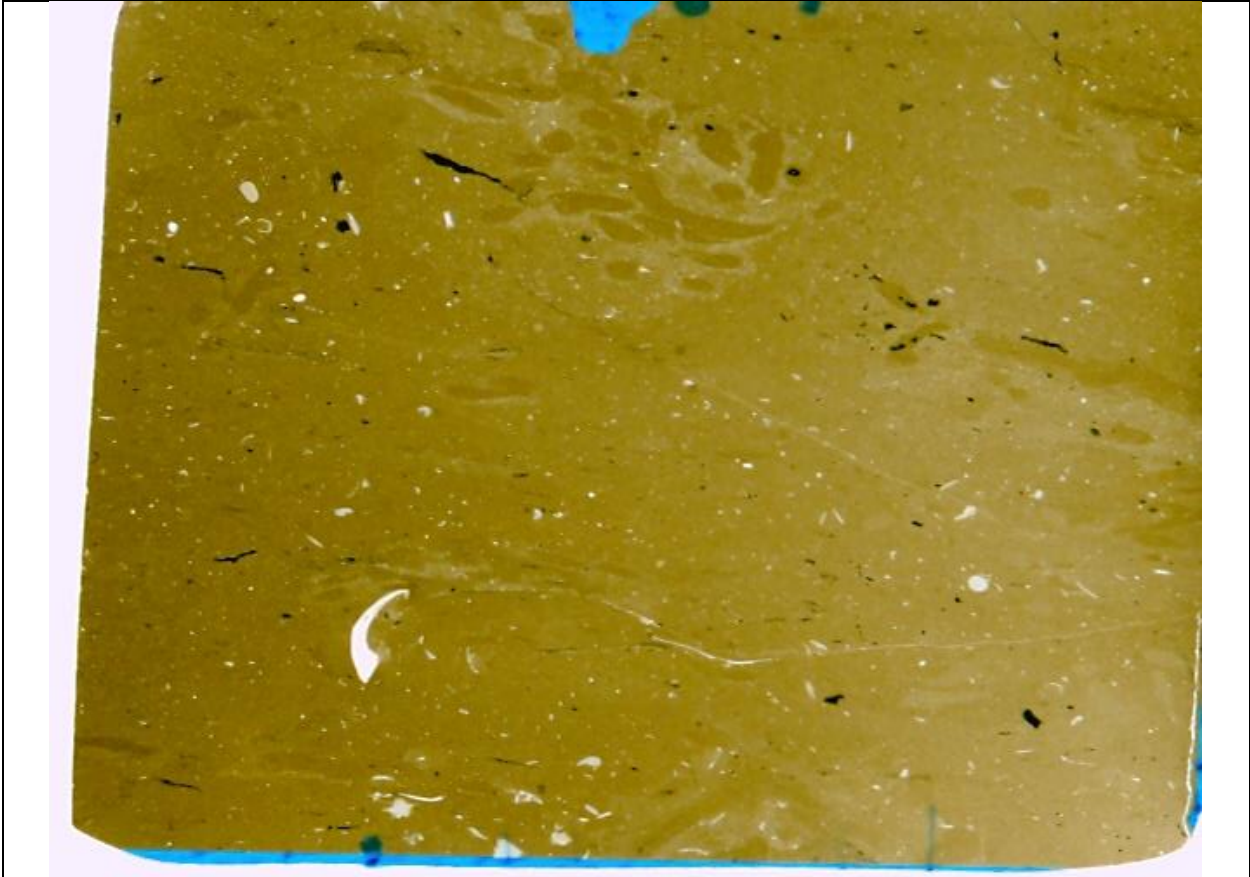
E383-10781.3 (USGS; Facies 3): This thin section is massively bedded and composed entirely of facies 3. Both brachiopods and echinoderms can be identified, however, other bioclasts are pyritized. Bioclasts are often oriented at random angles to bedding. In addition, detrital calcite (~12%) and quartz (~3%) silt are distributed throughout this facies. *Chondrites* isp. burrows are abundant and occur in clusters.
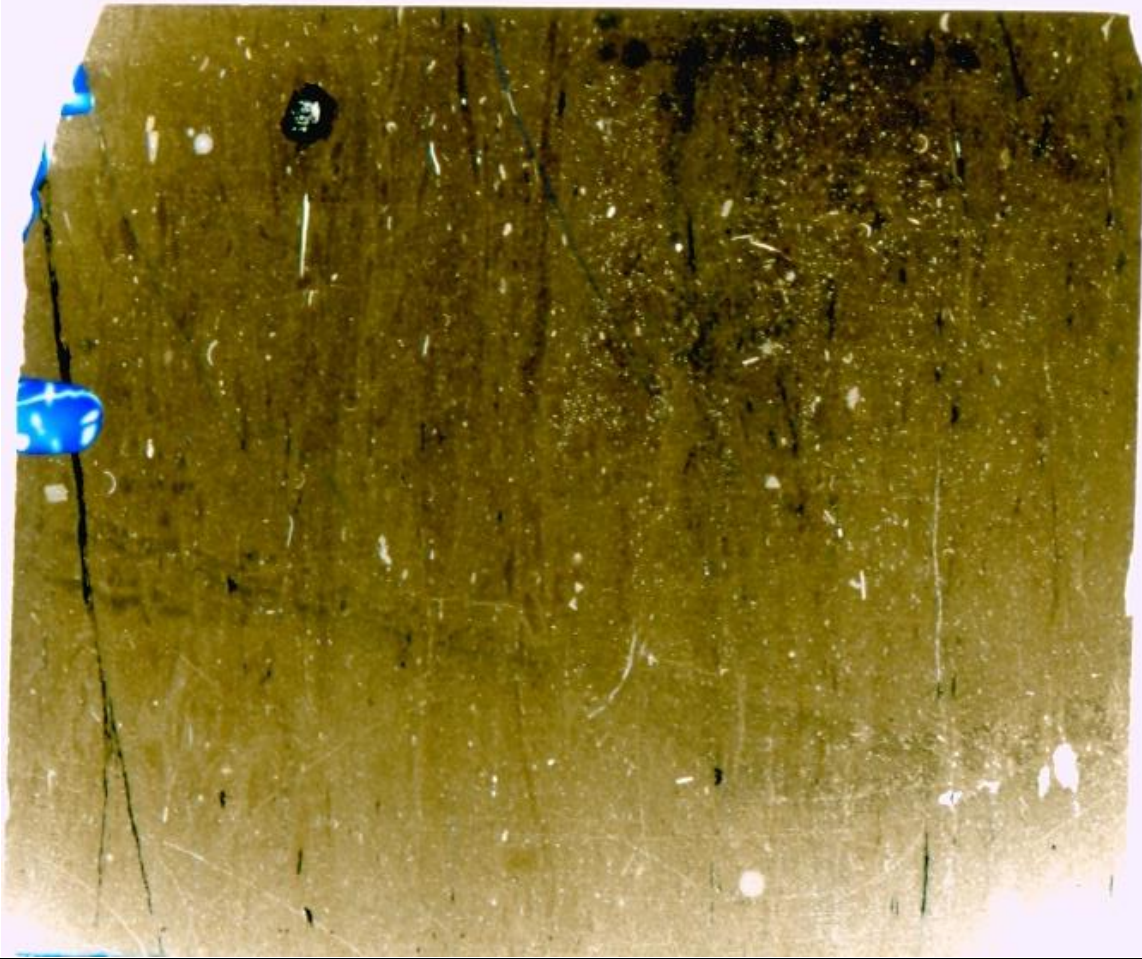
B659-10772.7 (USGS; Facies 3): This thin section is comprised of both bioclasts (~2%) and silt (~18%) that occur within a brown massive matrix. Echinoderms can be identified but most grains are disarticulated bioclasts or have been pyritized. The silt grains are mostly composed of detrital calcite (~12%) in addition to some quartz (~3%). *Chondrites* isp. burrows are present in various areas of this thin section.
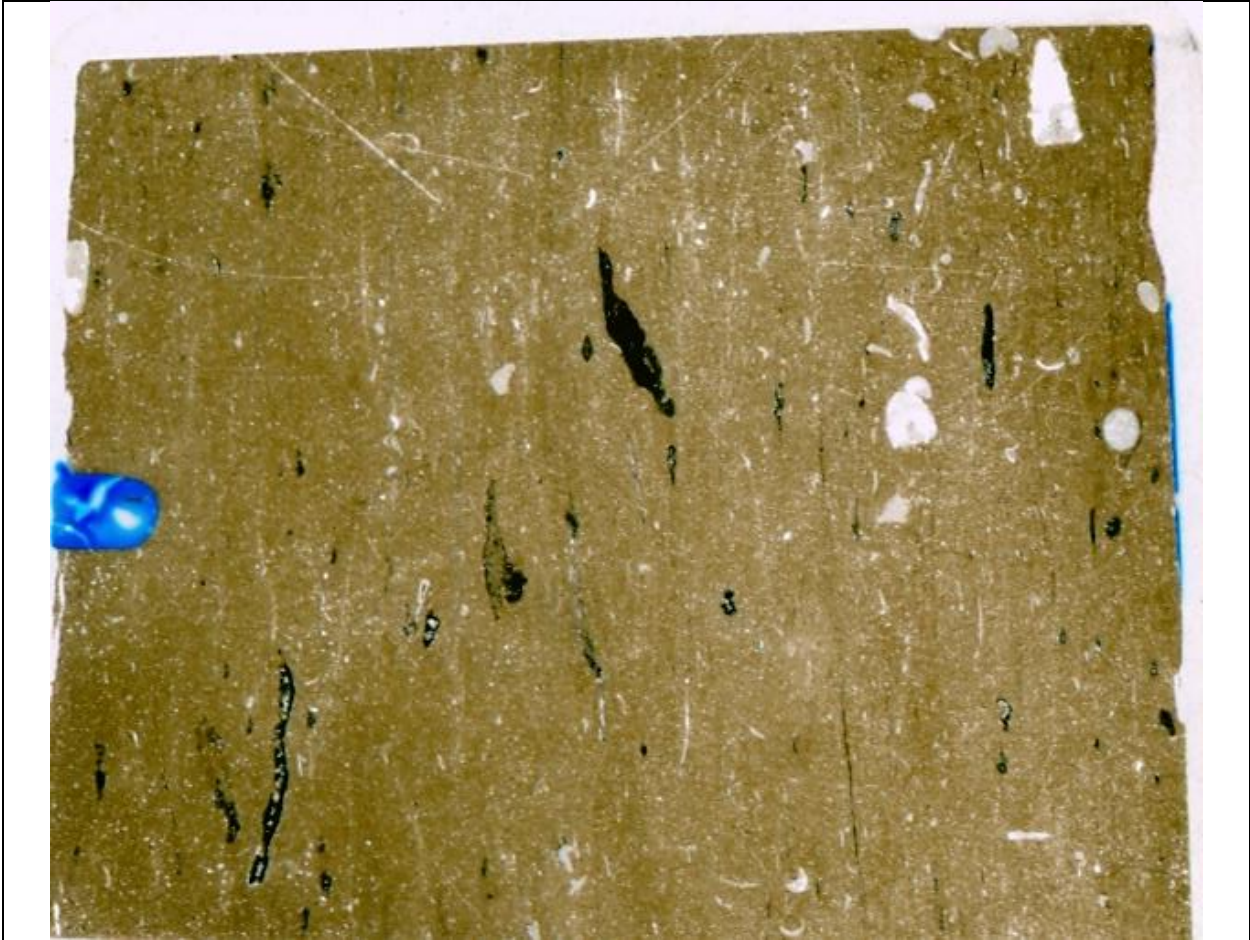
B659- 10775.6 (USGS; Facies 3): This thin section is massive and comprised of bioclasts (~6%) and calcite (~15%) silt distributed throughout a light brown matrix. Echinoderms can be identified; however, most grains are bioclasts with some having been pyritized. Silt grains do make up a portion of this thin section and are mostly comprised of detrital calcite (~15%) with some quartz (~3%) silt.
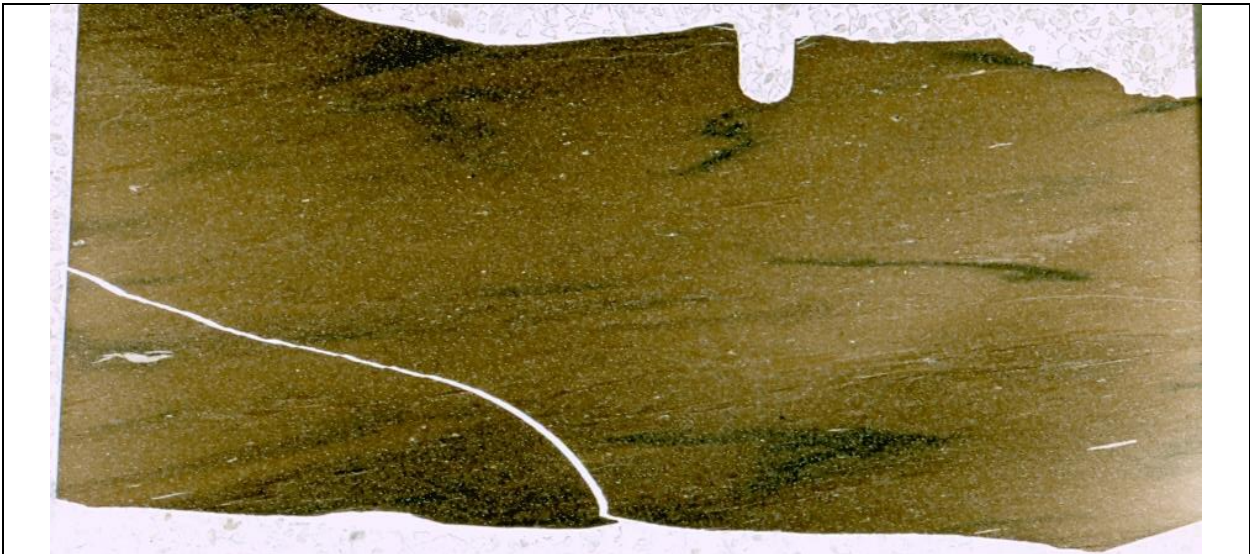
E383-10785 (USGS; Facies 3): This thin section has calcite (~8%) and quartz (2%) silt within a mostly light brown matrix; however, in places the matrix is a darker black color because of an increase in pyrite. Bioclasts are rare and can be pyritized although pyritization is not common.

E385-10754.5 (USGS; Facies 3): This thin section is massively bedded with up to ~2% bioclasts present with some being pyritized. In addition, calcite (~8%) silt is distributed evenly throughout with some quartz (3%) silt as well. Bioclasts are often randomly oriented relative to bedding. *Chondrites* isp. are present throughout this thin section.

Facies 4
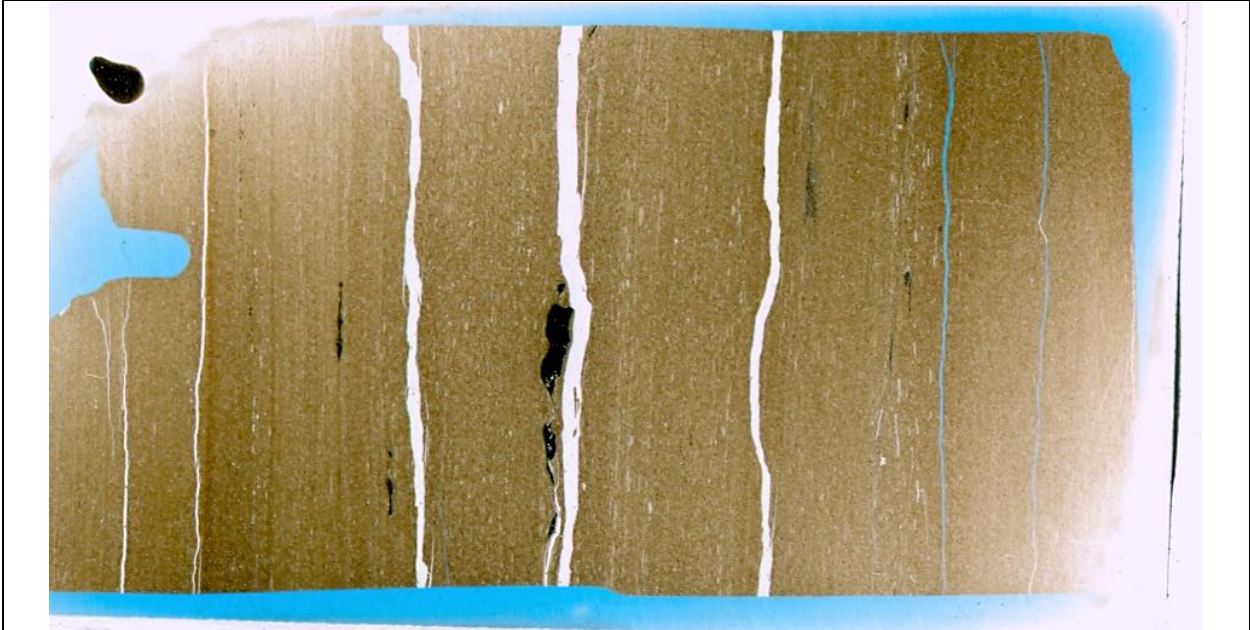
#28036-9698.4 (Facies 4): This thin section is composed of multiple laminae up to a centimeter thick that extend across the entire thin section. These laminae are comprised of silt grains that vary in abundance from ~20 to 30% in addition to ~60-75% clay clasts oriented parallel to bedding. These clay clasts are comprised of calcite, quartz, and feldspars and are often outlined by brown organic matter. In places, bioclasts may be present and oriented parallel to bedding. See table 4 for grain size data.
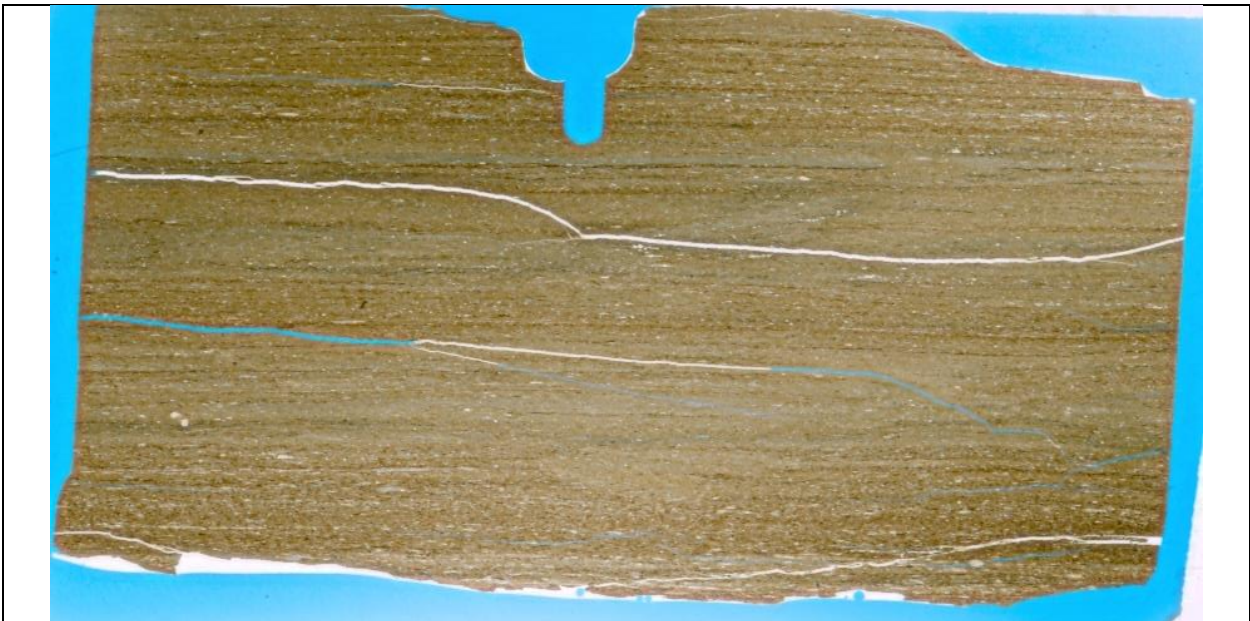
#26661-9327.3 (Facies 4): This thin section is comprised of multiple laminae with clay clasts throughout. These clay clasts account for about 60 to 70% of these laminae in addition to silt grains and organic matter. These laminae often have sharp contacts with one another. See Appendix 3 for SEM data.
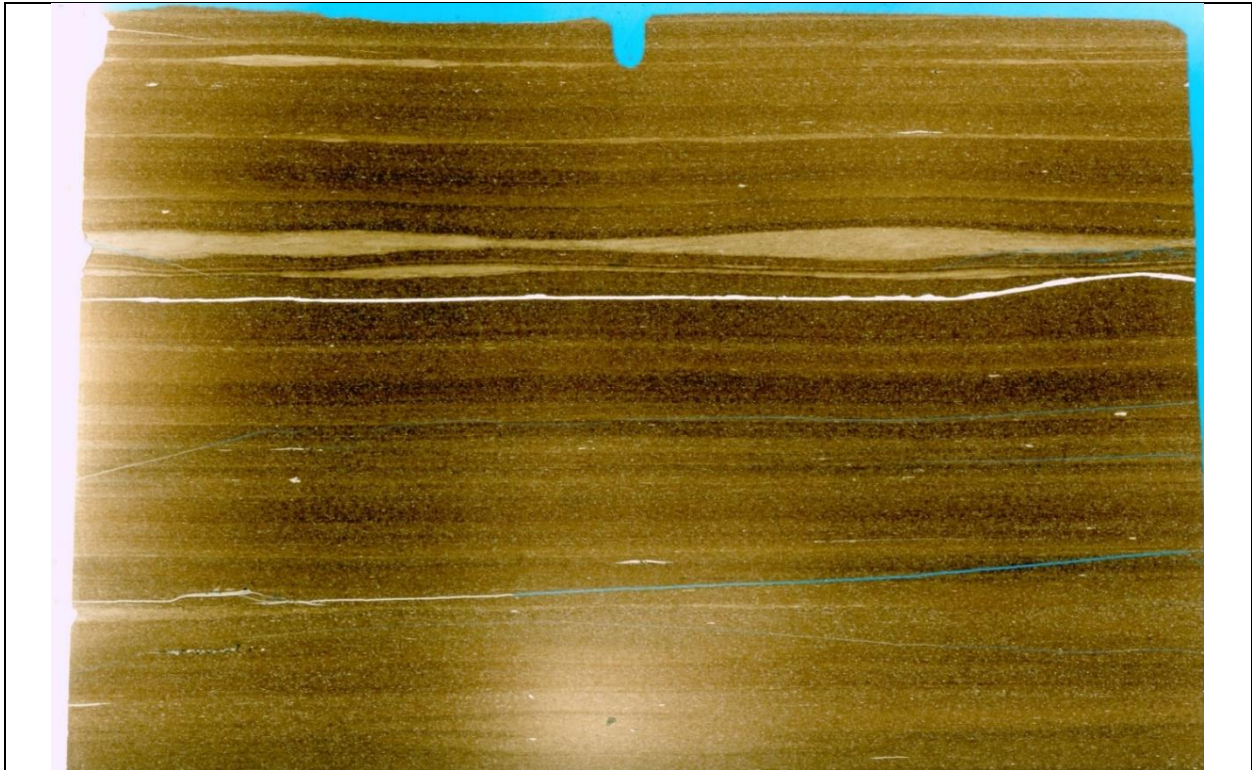
#21734-10369.9 (Facies 4): This thin section is made up of multiple laminae of facies 4 containinf varying abundances of clay clasts. Light laminae that thicken and thin laterally are comprised almost entirely of clay clasts (90-100%) with little silt. These clay clasts are made up of calcite, quartz, and feldspars and have organic matter occurring around the clay clasts. However, other laminae are also present that have silt grains (~20-40%) intermixed with clay clasts (60-80%). These clay clasts are oriented parallel to bedding in laminae with high amounts of silt, however, they also may be inclined to bedding forming foresets within laminae dominated by clay clasts.
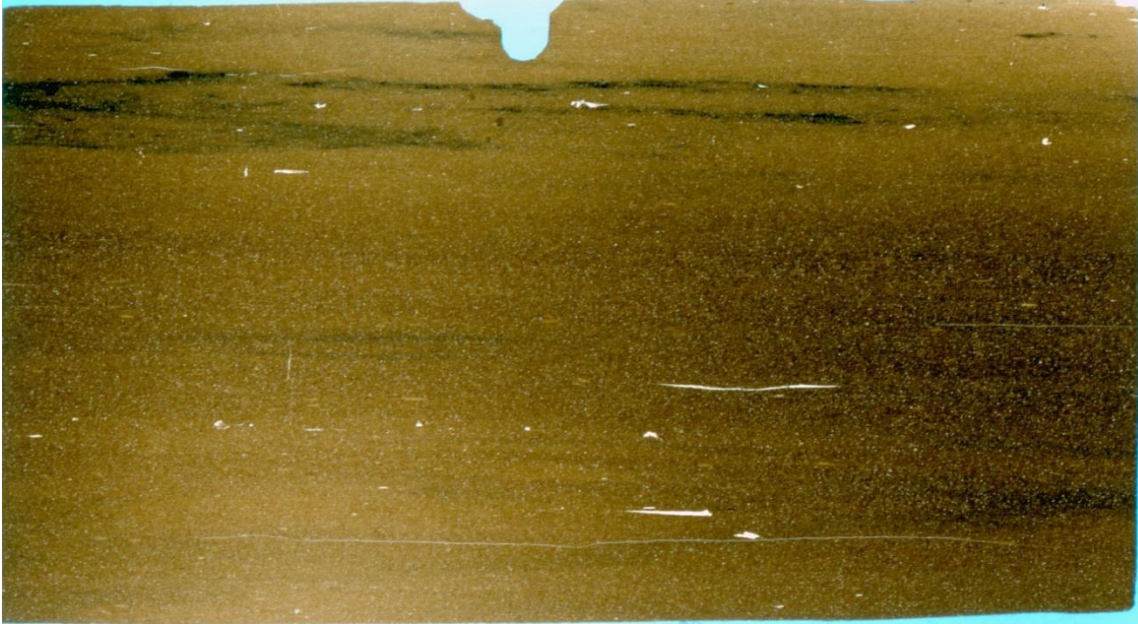
#607-10487 (Facies 4): This thin section consists entirely of facies 4 laminae that extend across the entire thin section and have sharp contacts with one another. Laminae are up to 5mm thick and composed of clay clasts (~60%), quartz (~10%), and calcite (5%) silt. Elongate brachiopod shell fragments occur within these laminae and are aligned parallel to bedding. In places, there are laminae that extend laterally for several centimeters that have a dark matrix with sub-millimeter rounded pyrite grains.
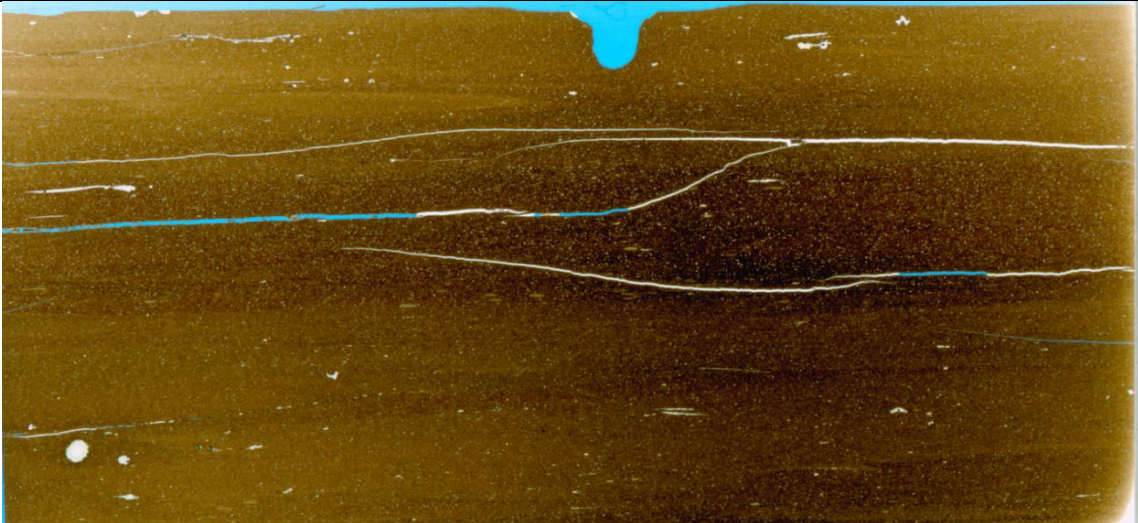
#22092-9879 (Facies 4): This thin section is made up of several laminae of facies 4 that extend across the entire thin section and have sharp contacts with one another. These laminae have clay clasts (~70%) oriented parallel to bedding intermixed with quartz (~10%) and calcite (~5%) silt. In addition, dark organic matter, elongate brachiopods, and echinoderms occur in these laminae. For SEM data see Appendix 3.

Facies 5
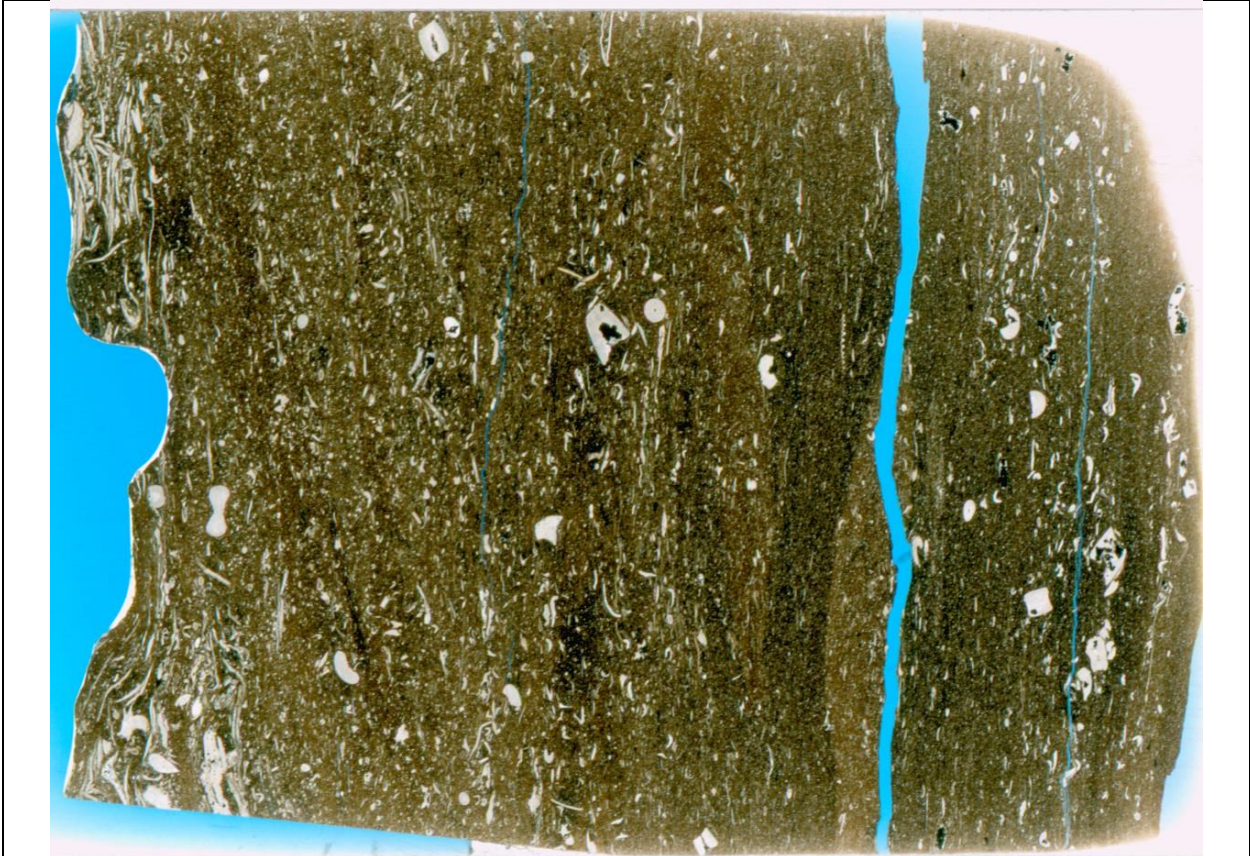
#19709-9250.3 (Facies 5): This entire thin section has biogenes and bioclasts distributed throughout. In places, concentrations of bioclasts are more abundant along bedding planes. Biogenes such as echinoderms and brachiopods can be distinguished; however, most grains have been broken and are no longer identifiable. All grains occur within a dark brown matrix. For grain sizes and modal abundances see Tables 3 and 4 and see Appendix 3 for SEM data.

E383-10784.7B (USGS; Facies 5): The top half of this thin section is comprised of bioclasts within a brown matrix. Some biogenes such as brachiopods and echinoderms are present. In addition, phosphate grains occur but are rare within this thin section.

Facies 6
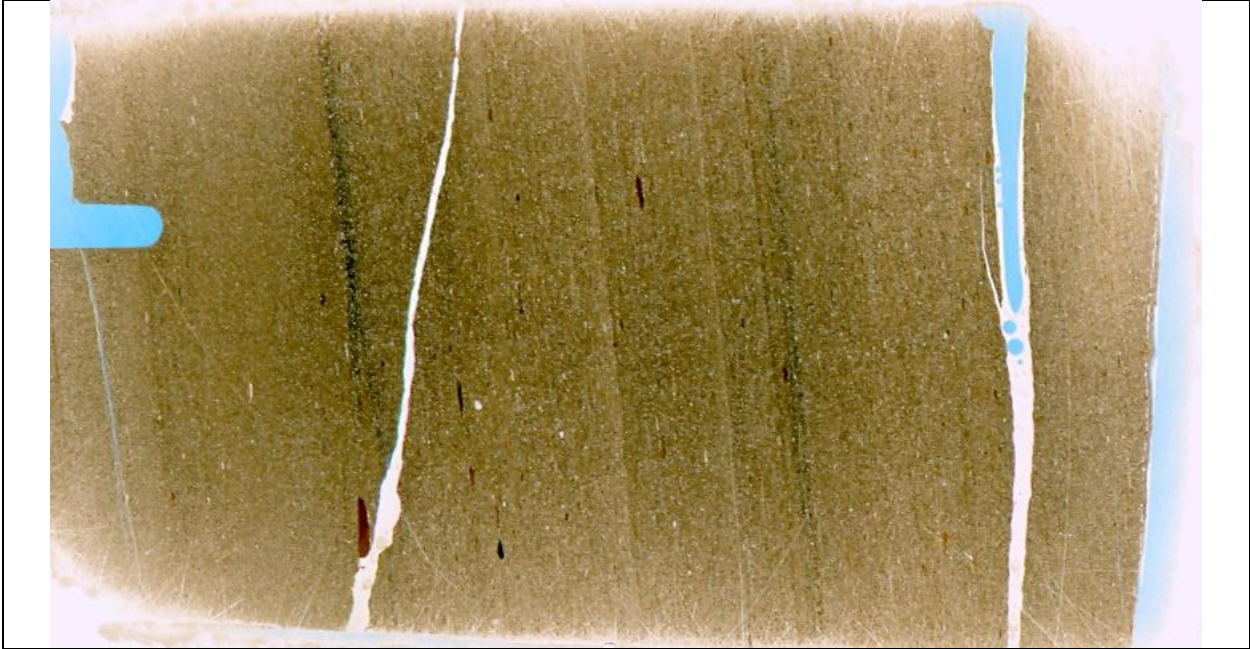
#17396-7942.1 (Facies 6): This thin section is composed of several laminae that range in thickness from 1 to 4cm. These laminae have about 55% silt grains with quartz silt (~30%) and calcite silt (~25%) being distributed evenly throughout. In addition, phosphate grains, brown in color, are present in places and oriented parallel to bedding. Conodonts are rare. Contacts between laminae are sharp and planar across the entire thin section. See table 4 for grain size data and see Appendix 3 for SEM data.

Facies 8
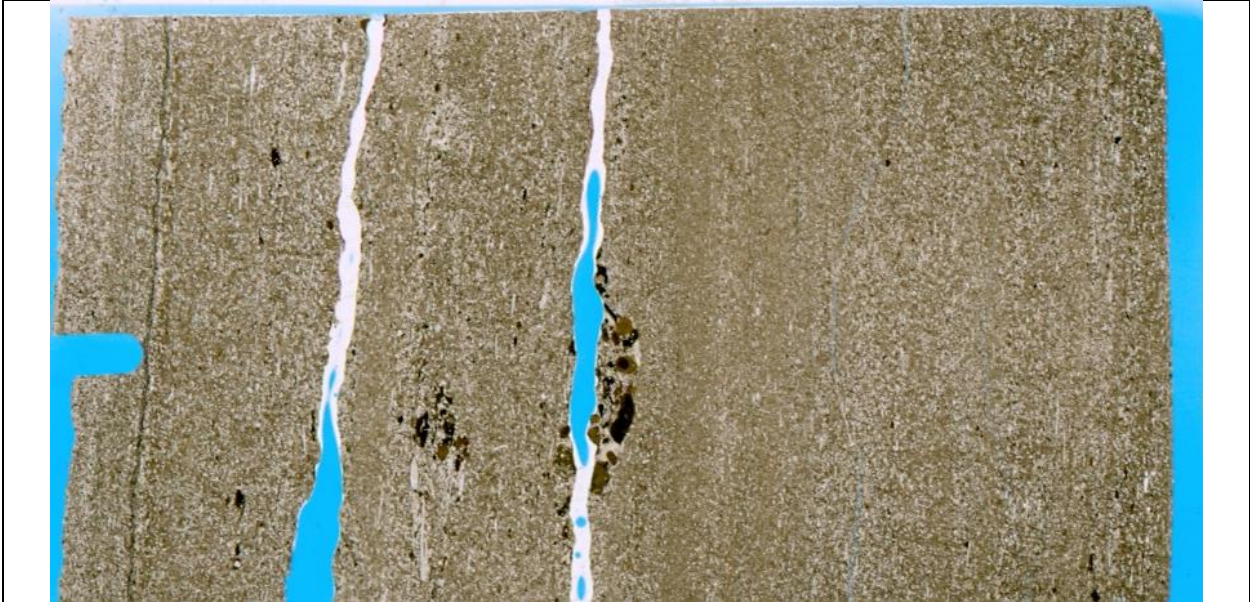
#17396-7904.8 (Facies 8): This thin section is comprised of several calcareous siltstone laminae that extend across the entire thin section and are up to several centimeters thick. Silt grains account for about 50 to 60% of this thin section with calcispheres accounting for about 35% of this thin section in addition to bioclast fragments (~15%) and quartz (~15%). Phosphate grains occur in places and are associated with coarse grained bioclasts in places. *Planolites* isp. are present in places and lighter in color than the surrounding matrix. See table 4 for grain size data.

Facies 9
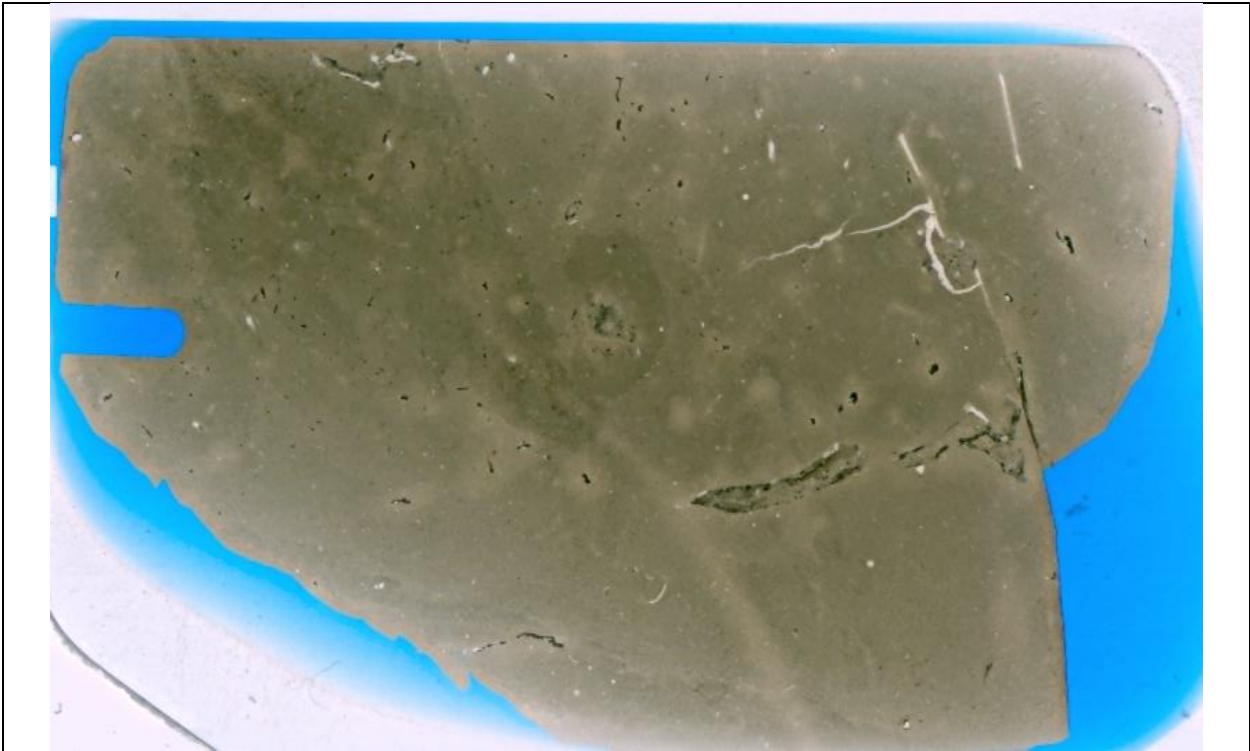
#12785-11271.5 (Facies 9): This thin section consists of massively bedded carbonate mudstone. Carbonate mud accounts for 98% of this thin section. Calcispheres and quartz silt are rare accounting for less than 2% of this facies and are often around 0.05mm in diameter. In addition, several bioclasts are present within the silt sized fraction.

Facies 10
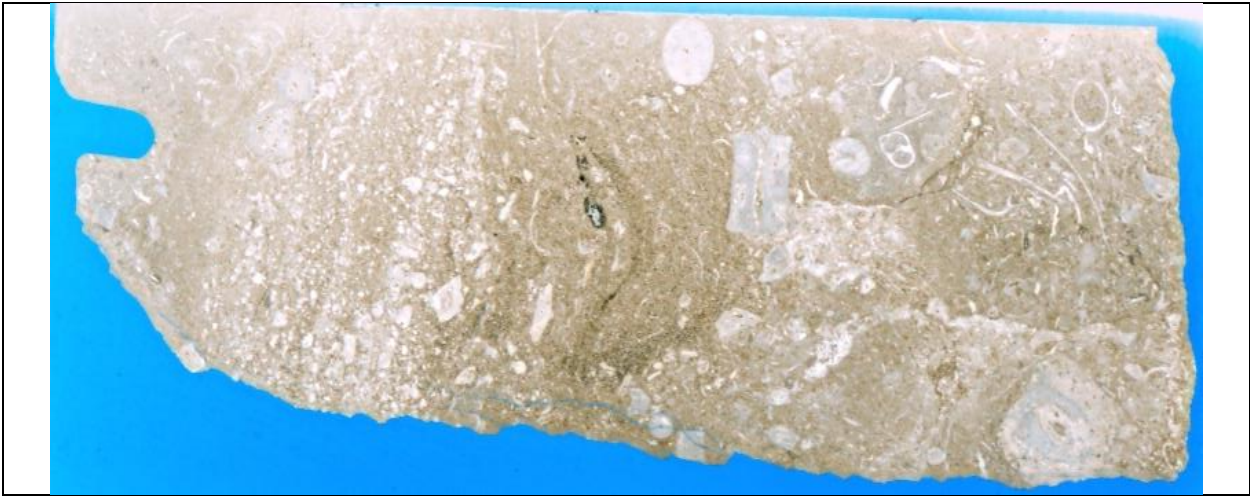
#16160-9420.5 (Facies 10): This thin section is comprised of about 25-30% bioclasts distributed throughout a carbonate mud matrix. Biogenes such as echinoderms, brachiopods, ostracods, trilobites, and gastropods can be identified within this thin section. Calcite silt is also present throughout the matrix and accounts for ~10% of this thin section. In places, the abundance of bioclasts is more dense or coarser grained in comparison to other places.
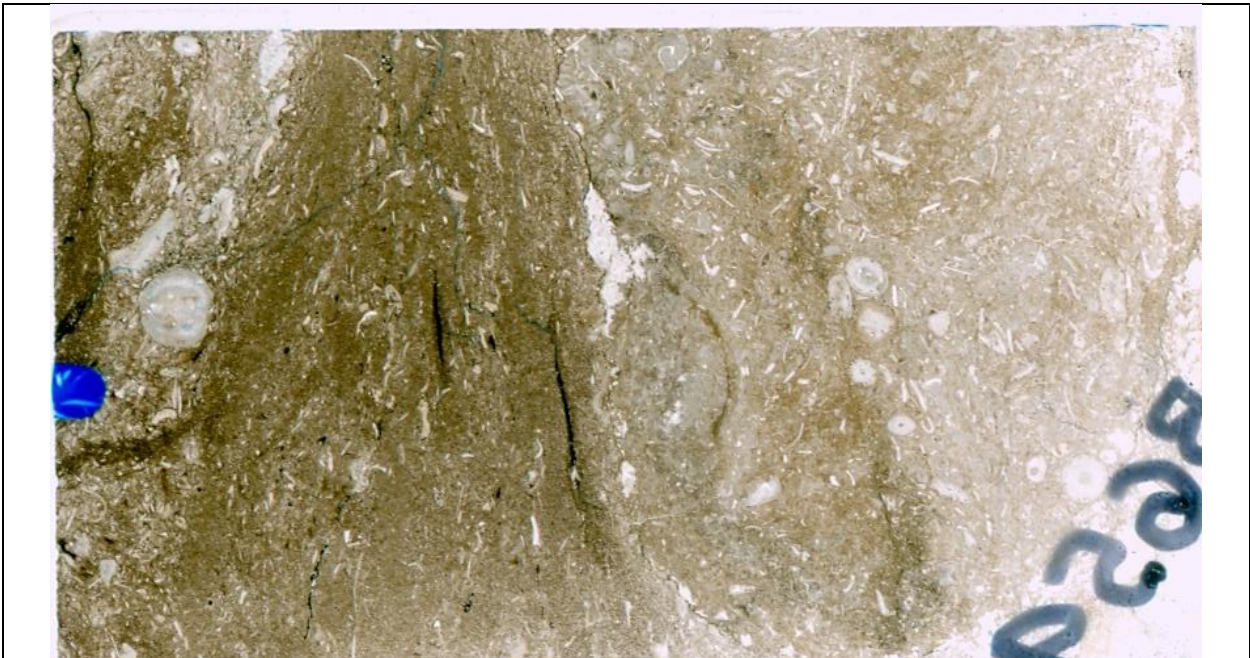
B659-10782.3 (USGS; Facies 10): This thin section has bioclasts present throughout that vary in abundance from 20 to 30% and are present within a carbonate mud matrix. These bioclasts are randomly oriented relative to bedding. Echinoderms and brachiopods can be identified within this thin section in addition to trilobites and some ostracods.

Facies 11
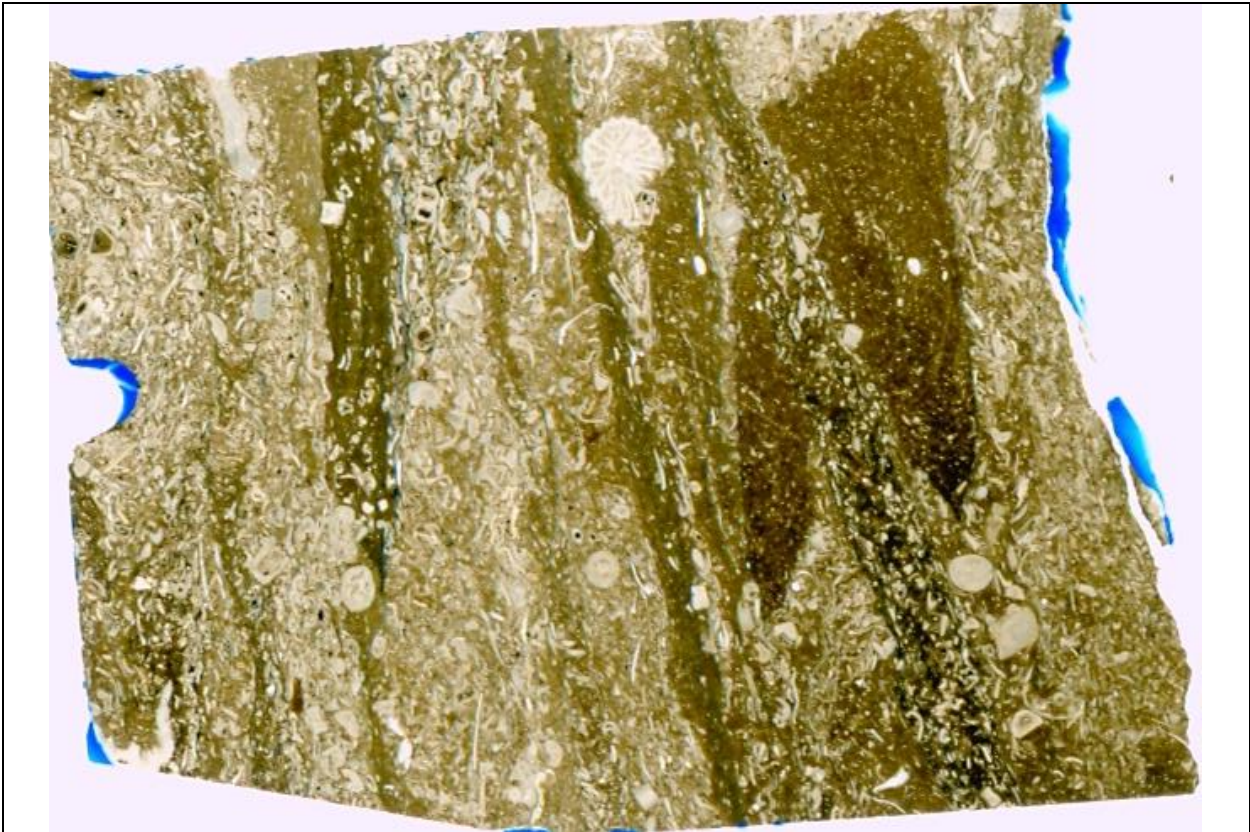
B659-10777 (USGS; Facies 11): Several laminae that are comprised of about 50 to 60% bioclasts are present within this thin section. Biogenes such echinoderms, brachiopods, rugose corals, and trilobites can be identified when not disarticulated. These bioclasts occur within a light grey to brown carbonate mud matrix. In addition, irregular dark brown clay lenses with silt grains are also present within this thin section.
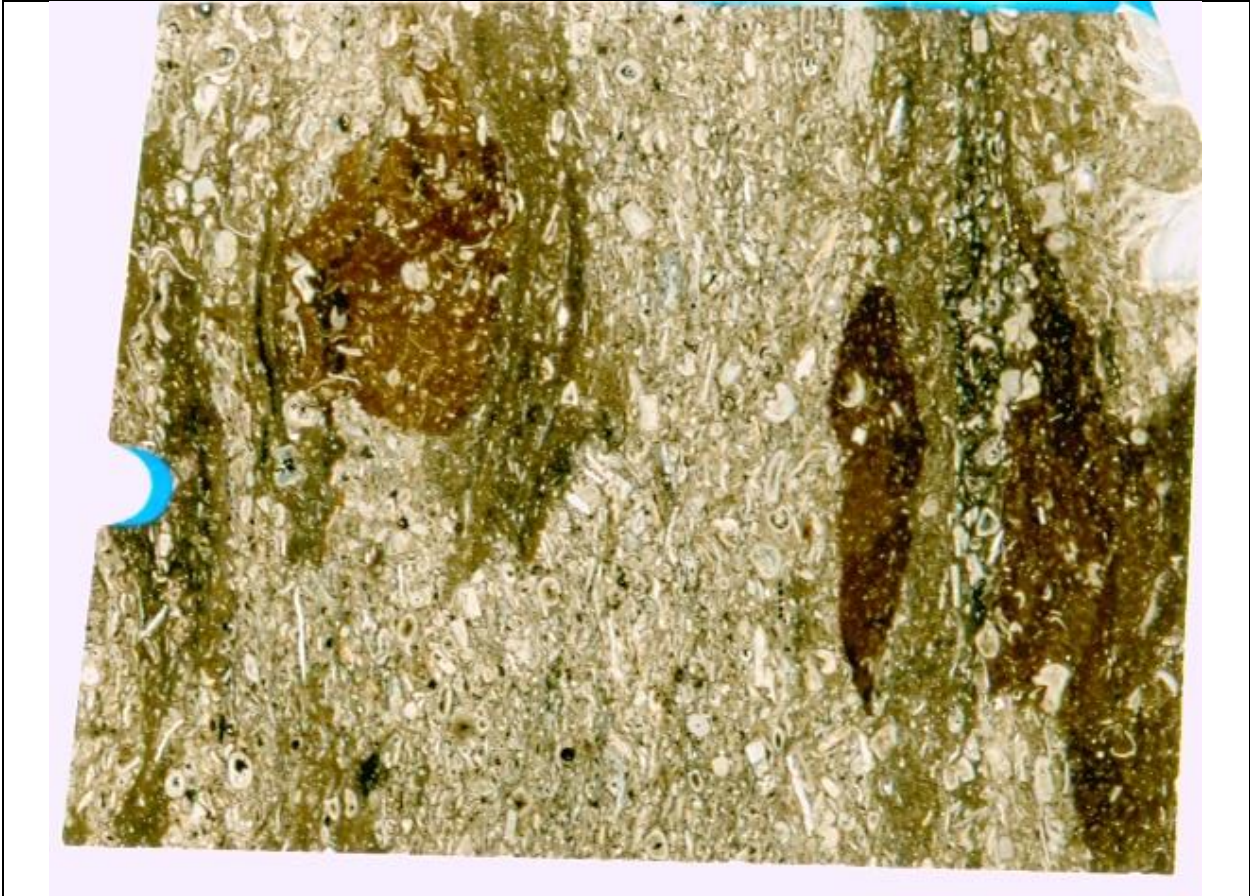
E385-10759.1 (USGS; Facies 11): This thin section has a high abundance of bioclasts (<60%) that are distributed throughout. In places, irregular dark brown clay lenses are present and have only a few bioclasts within them. Biogenes are identifiable and are mostly echinoderms.
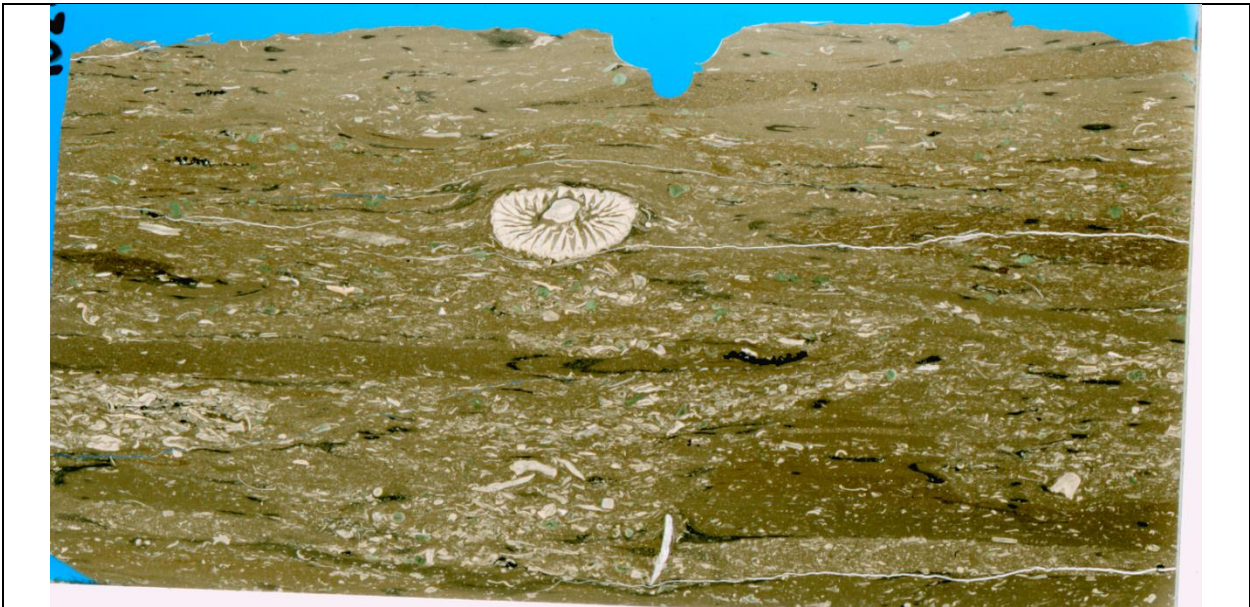
#20453-10254.7 (Facies 11): This thin section is dominated by bioclast-rich laminae that extend across the entire thin section and have a sharp wavy basal contact. Echinoderms, brachiopods, and rugose corals can be identified in addition to an abundance of bioclasts with biogenes and bioclasts accounting for ~50% of this thin section. In certain laminae, there are areas with a high density of bioclasts compared to other portions of the same laminae. Thin laminae that are not continuous are also present and have only few bioclasts present. Rare glauconite grains occur in this facies.

Multiple facies in one thin section
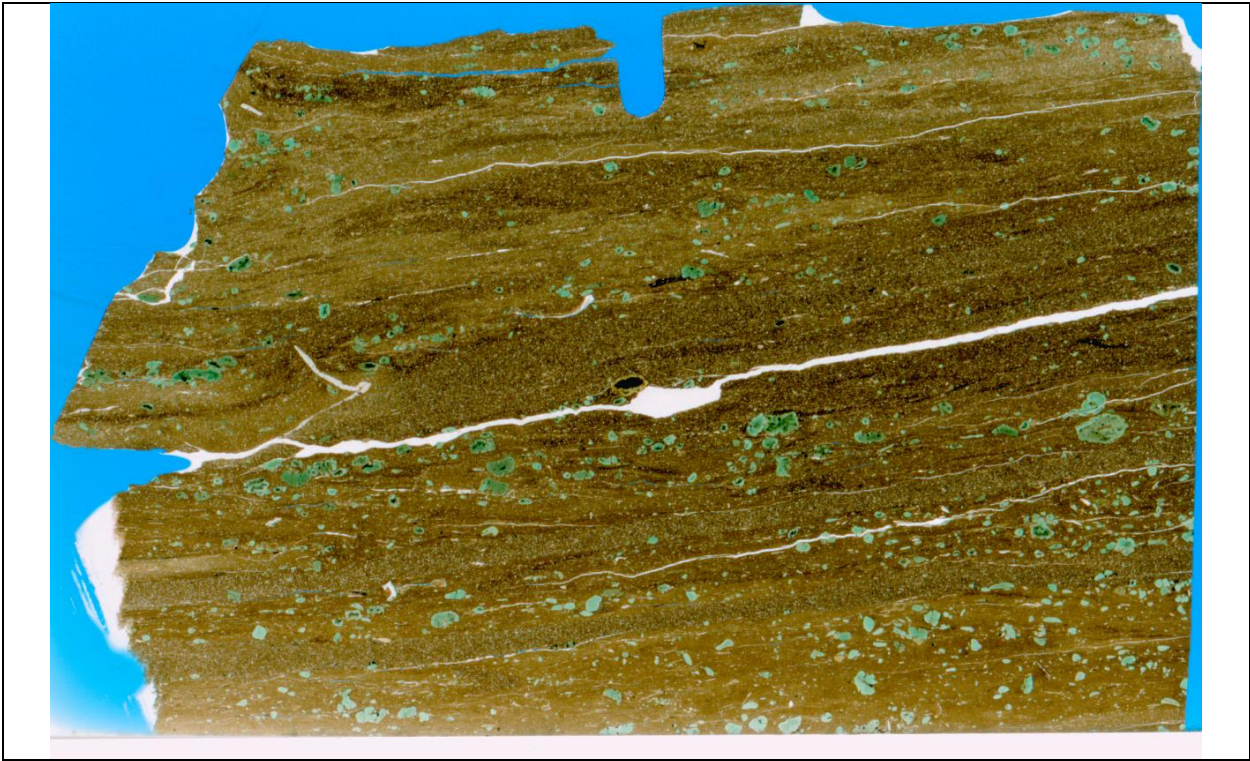
#19709-9251 (Facies 6): Laminae extend across this thin section and have both a sharp, wavy upper and basal contact with facies 7. Facies 6 laminae are comprised of mostly quartz silt (~30%) and calcite silt (~20%) distributed evenly throughout a brown matrix.

#19709-9251 (Facies 7): Facies 7 laminae extend across this thin section and have both a sharp, wavy upper and basal contact with facies 6. These laminae can be easily distinguished by the abundance of glauconite grains (~15-20%). In addition, quartz silt is present in concentrations of up to 25% and occurs within a light brown matrix. For point counts on grain sizes see Table 4.

#12785-11275: (Facies 2a): This facies comprises 98% of this thin section and is easily distinguished by the dark brown to black matrix with mostly quartz silt distributed throughout in addition to some calcite and micas. Bioclasts are very rare and only present near the very top of the thin section. *Phycosiphon* isp. fecal strings are easily identified throughout this thin section. For grain sizes and modal abundances see Tables and 4.

#12785-11275: (Facies 1): This facies only occurs as two thin laminae (<2mm) that extend across the entire thin section. These laminae have a distinctly smaller silt-size fraction compared to the underlying and overlying facies 2a, but are still comprised of mostly quartz with some calcite and micas. These fine-grained laminae show a faint fining-upwards; however, in places this fining upwards is difficult to distinguish because *Phycosiphon* isp. fecal strings bisect through the entire lamina in places. For point counts on grain sizes see Table 4.

See Appendix 3 for SEM images and data.
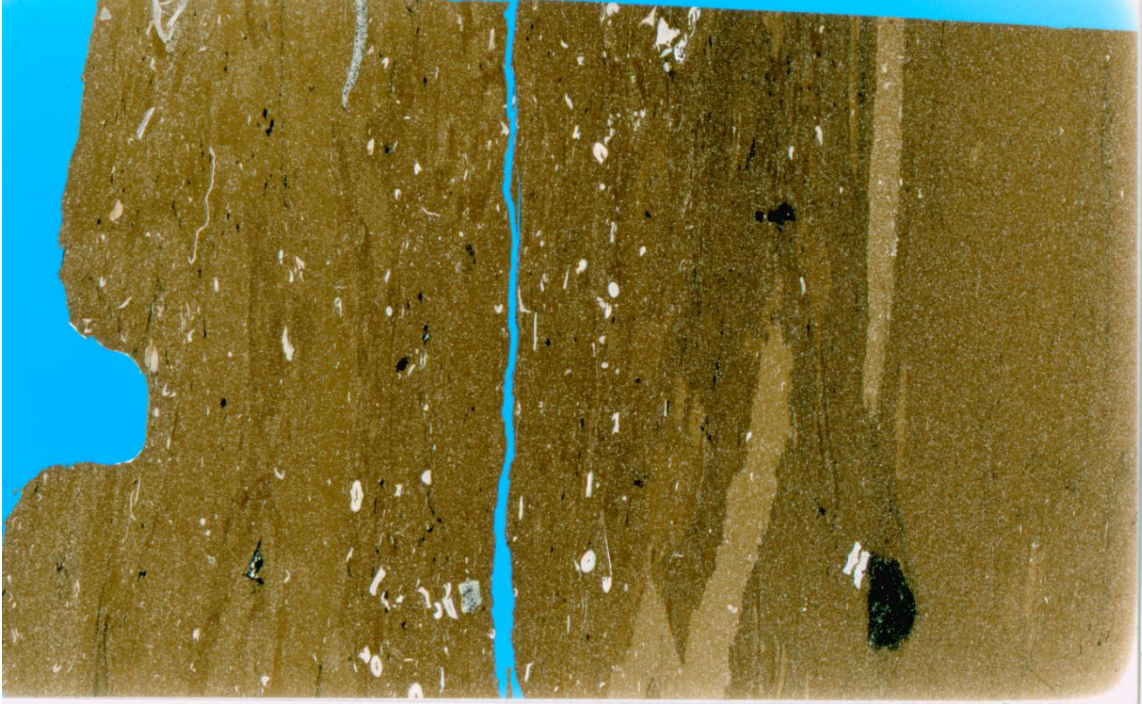
#15986-10494.5: (Facies 3) This thin section has bioclasts distributed throughout with some being pyritized. In addition, detrital calcite and quartz silt also occur throughout this thin section. In places, *Chondrite*s isp. burrows occur parallel to bedding. For grain sizes and modal abundances see Tables 3 and 4.

(Facies 2b) The lower half of this thin section is comprised of a massive bed with mostly calcite silt and some bioclasts within a brown matrix. Irregular Z-shaped concretions can be seen in places and are lighter in color than the surrounding matrix.

#9426-10786.6: (Facies 3) The lower quarter of this thin section is comprised of a bed that is light brown in color with few pyritized and calcareous bioclasts. In addition, the silt grains are mostly detrital calcite with rare quartz. *Chondrites* isp. are common throughout this bed and often slightly darker in color than the surrounding matrix.

#9426-10786.6: (Facies 5) The upper three fourths of this thin section has a bed up to several centimeters thick with an abundance of bioclasts within a brown matrix. Biogenes such as echinoderms, brachiopods, and agglutinated foraminifera can be identified. A large phosphate intraclast that is brown in color occurs in the upper center of the thin section. In addition to the sand-sized grains, both detrital calcite and quartz are intermixed throughout this bed. The basal contact with the underlying facies 4 bed is sharp and wavy. For grain sizes and modal abundances see Tables 3 and 4.
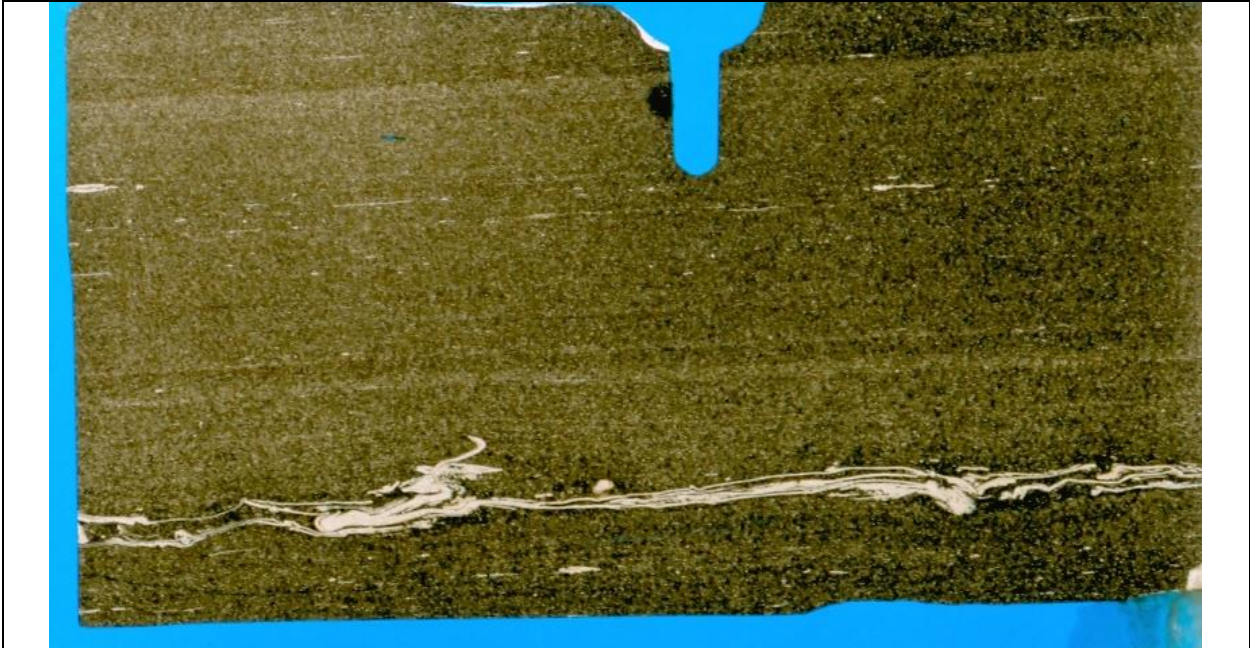
#9426-10783.1: (Facies 2b) Laminae from 1 to 3cm thick make up the majority of this thin section. These laminae have sharp planar contacts with one another and extend across the entire thin section. Silt grains are present throughout all laminae and comprised of about 15% calcite and 5 to 10% quartz. More elongate calcite silt is oriented parallel to bedding. These grains occur within a brown matrix.
(Facies 5) In the lower half of this thin section, there is one lamina that extends across the entire thin section and is composed of brachiopod fragments within a dark brown matrix.

E383-10786 (USGS): (Facies 5) The top half of this thin section is composed of mostly bioclasts. Brachiopod and echinoderms can be identified. In addition, two large (~2cm) phosphate intraclasts are present within this thin section. Rip-up clasts composed of calcite and quartz silt in a brown matrix are also present but have little to no bioclasts.

(Facies 3) The lower half of the thin section is a massive bed of facies 3 that has mostly calcite silt in a light brown matrix. A few bioclasts are present and have been pyritized. *Chondrites* isp. are present in places.
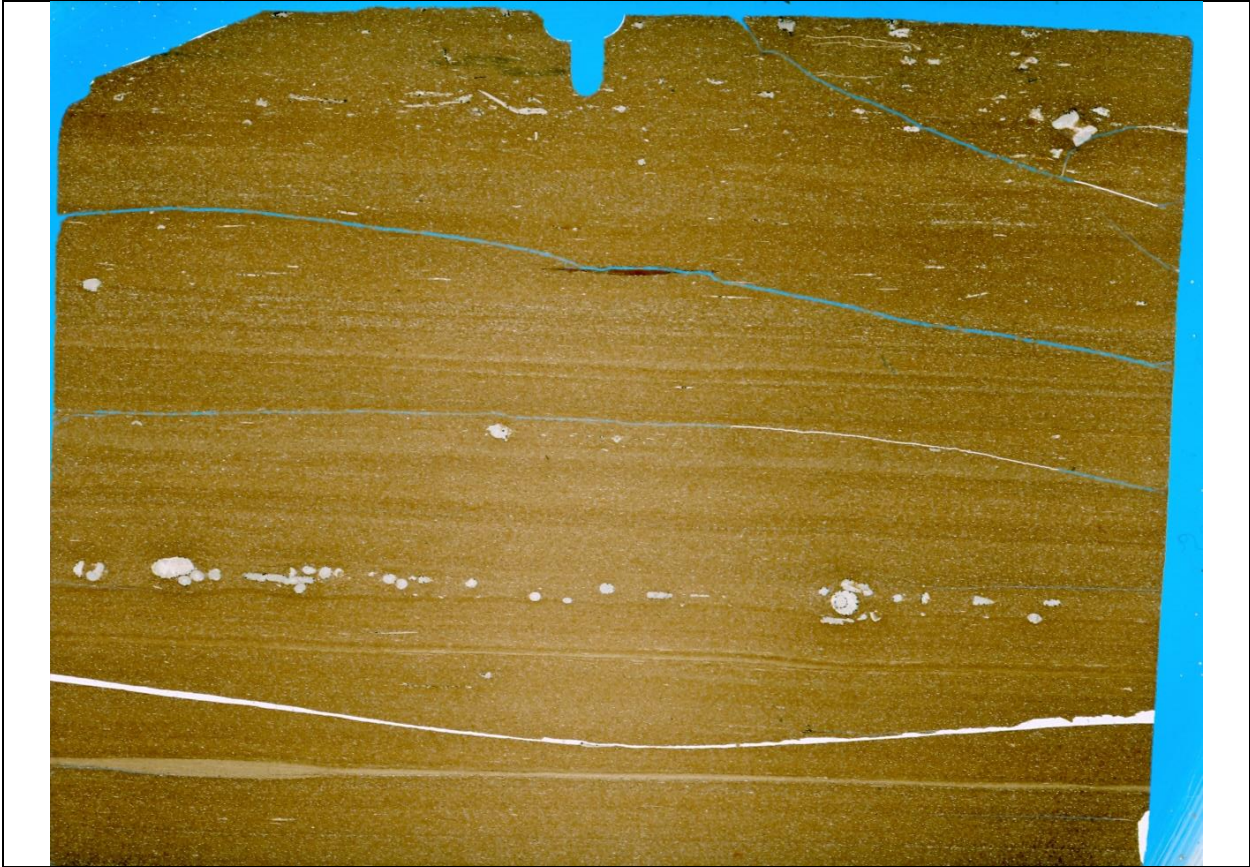
#19917-10534.5: (Facies 4) Several laminae of facies 4 are present within this thin section. In the lower part of the thin section a light lamina of this facies is present. This lamina thickens and thins laterally and is composed of 95% clay clasts in addition to some silt grains and organic matter. Other laminae of this facies are up to 2mm thick with ~30% quartz and calcite silt intermixed with clay clasts (~60%).

(Facies 5) In the center of the thin section a lamina with a sharp wavy basal contact shows an abundance of echinoderms present within it in addition to detrital calcite and quartz silt grains in a brown matrix.
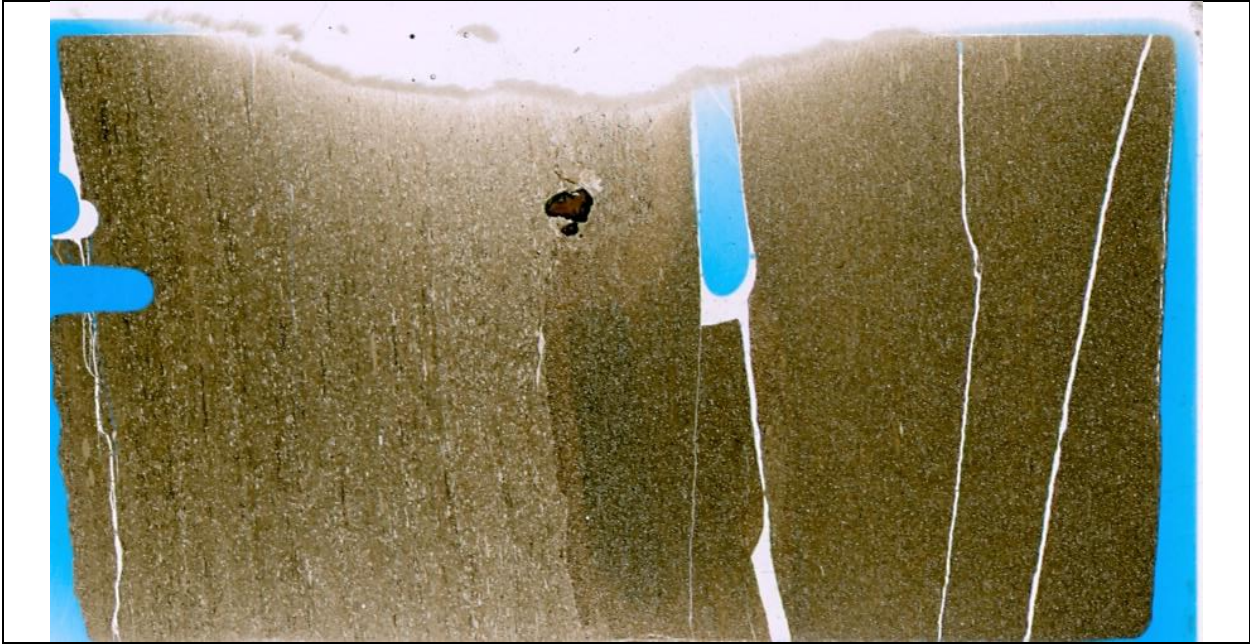
#17396-7915.8: (Facies 6): The lower half of this thin section is comprised of a massive bed of this facies which has about 55% silt that is dominated by quartz silt (35%) and detrital calcite silt (20%) in a dark brown matrix. Rip up clasts composed of silt grains in a light brown matrix are present within the thin section and often oriented parallel to bedding. *Planolites* isp. burrows occur throughout.
(Facies 8): The upper half of this thin section is dominated by calcispheres (~35%) with some quartz (~20%) silt distributed throughout a light brown matrix. In addition, a phosphate intraclast several millimeters in diameter is present at the base of this facies. Several laminae comprise the upper half of this thin section. *Planolites* isp. burrows are present throughout this portion of the thin section.

#12785-11278.3 (USGS): (Facies 10) The lower two-thirds of this thin section is comprised of a massive bed of facies 10. Bioclasts are distributed evenly throughout and randomly oriented. Bioclasts account for about 20 to 25% of this bed and are distributed throughout a carbonate mud matrix. In places, echinoderms, brachiopods, and gastropods can be identified, however, most grains are disarticulated and not identifiable. In addition, detrital calcite accounts for about 8% of this facies. (Facies 11) This facies occurs as several laminae in the upper portion of this thin section and contains up to 60% bioclasts in places. Echinoderms are most common with brachiopods also being present. These bioclast-rich laminae have irregular clay laminae that can extend across a single thin section but often do not. The basal contact with facies 10 is sharp and wavy.

Facies 1

Electron Image 1

Spectrum 1
+

Spectrum 2
+

Spectrum 3
+

Spectrum 4
+

100μm

#12785-11275-(F1) Fine grained lamina at bottom half of thin section left of pyrite.

Pt1	Calcite
Pt2	Quartz
Pt3	Sphalerite
Pt4	Pyrite

Electron Image 2

50μm
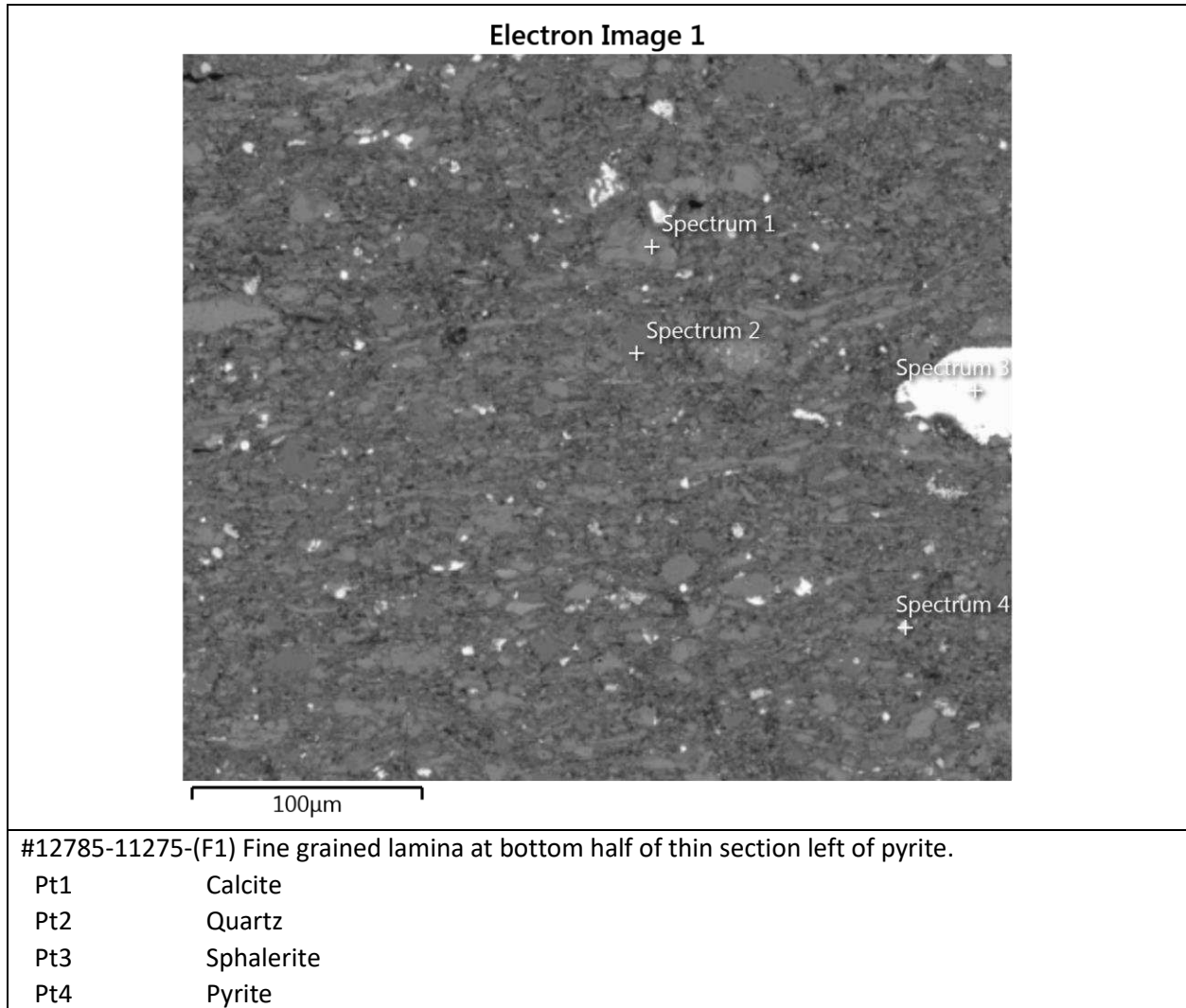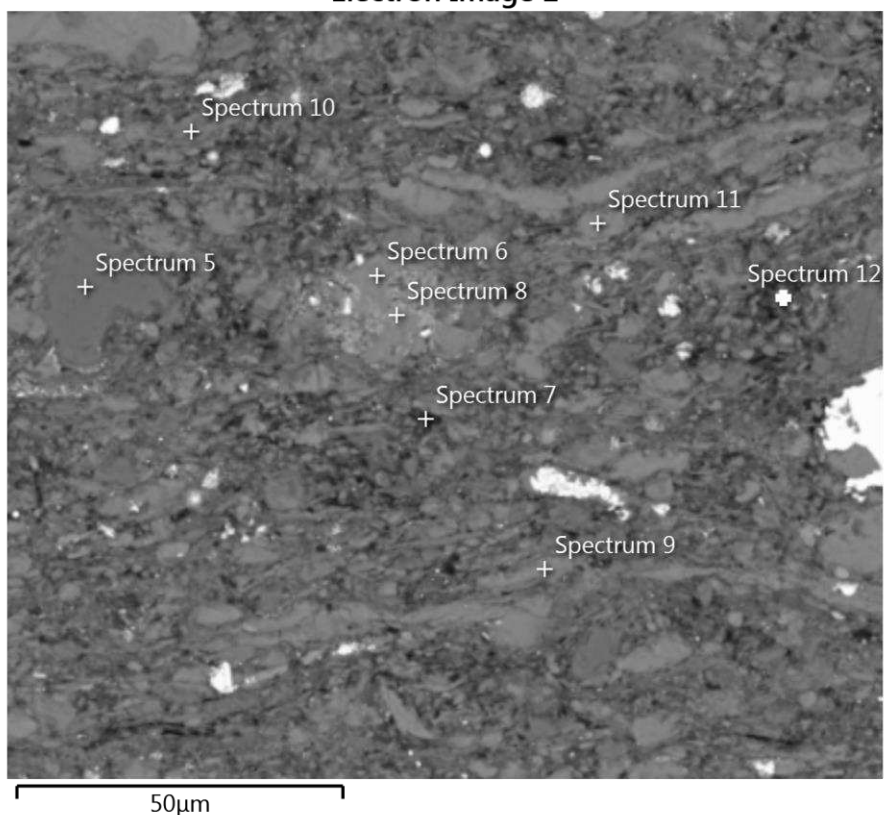
#12785-11275-Zoomed in image of same lamina (F1).

Pt5   Quartz
Pt6   Calcite
Pt7   Carbon (Likely epoxy)
Pt8   Apatite Replacing Calcite
Pt9   Calcite
Pt10   Muscovite
Pt11   Calcite
Pt12   Pyrite

Electron Image 3

5μm
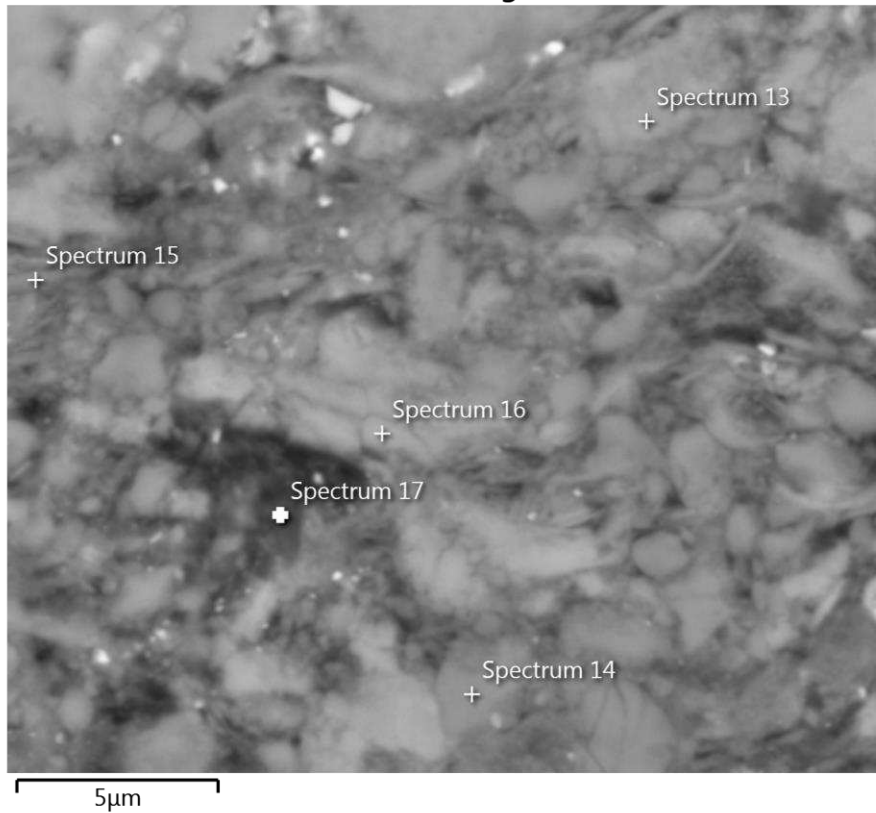
#12785-11275-Matrix of lamina (F1)

Pt13   Calcite
Pt14   Quartz
Pt15   Illite
Pt16   Kspar
Pt17   Everything and OM

Facies 2a

Electron Image 4

100μm
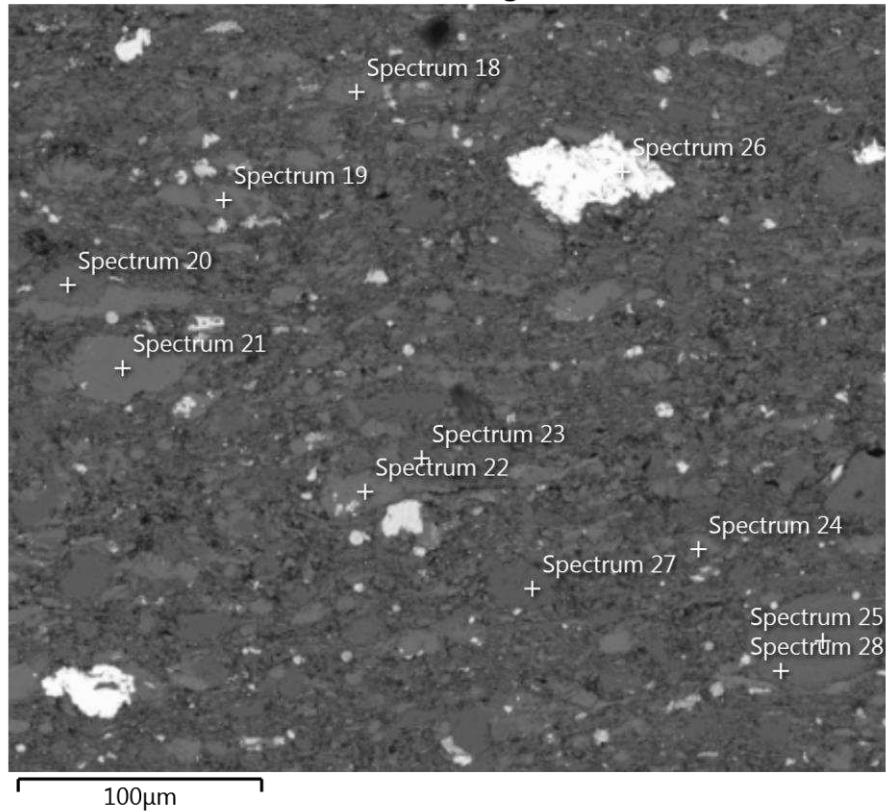
#12785-11275: Facies 2a coarse grains

Pt18   Calcite
Pt19   Calcite
Pt20   Biotite
Pt21   Kspar
Pt22   Calcite
Pt23   Quartz
Pt24   Calcite
Pt25   Biotite
Pt26   Sphalerite
Pt27   Quartz
Pt28   Biotite-Likely Metamorphic because Chlorite comes in

Electron Image 5
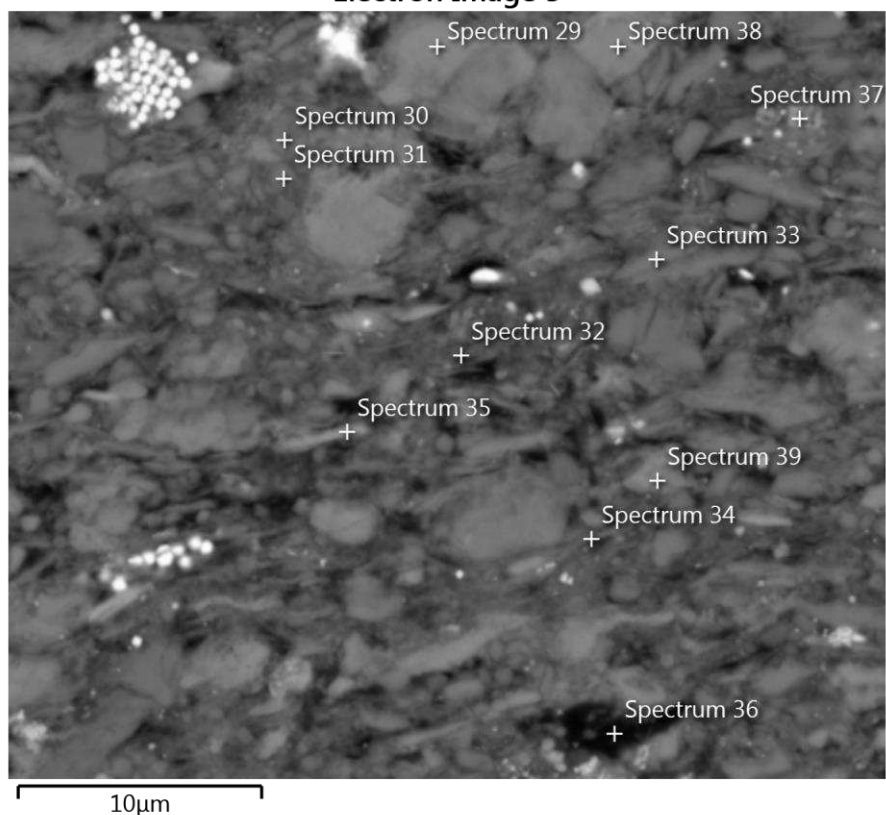
#12785-11275: Matrix within Facies 2a

pt29   Calcite
pt30   Quartz
pt31   Quartz
pt32   MixtureIllite-like clay
pt33   MixtureIllite-like clay
pt34   Calcite and Clay
pt35   Biotite   Fe oxide in clay-Biotite on its way to chlorite
pt36   Illite and OM
pt37   Apatite
pt38   Calcite
pt39   Calcite

Electron Image 6

10μm
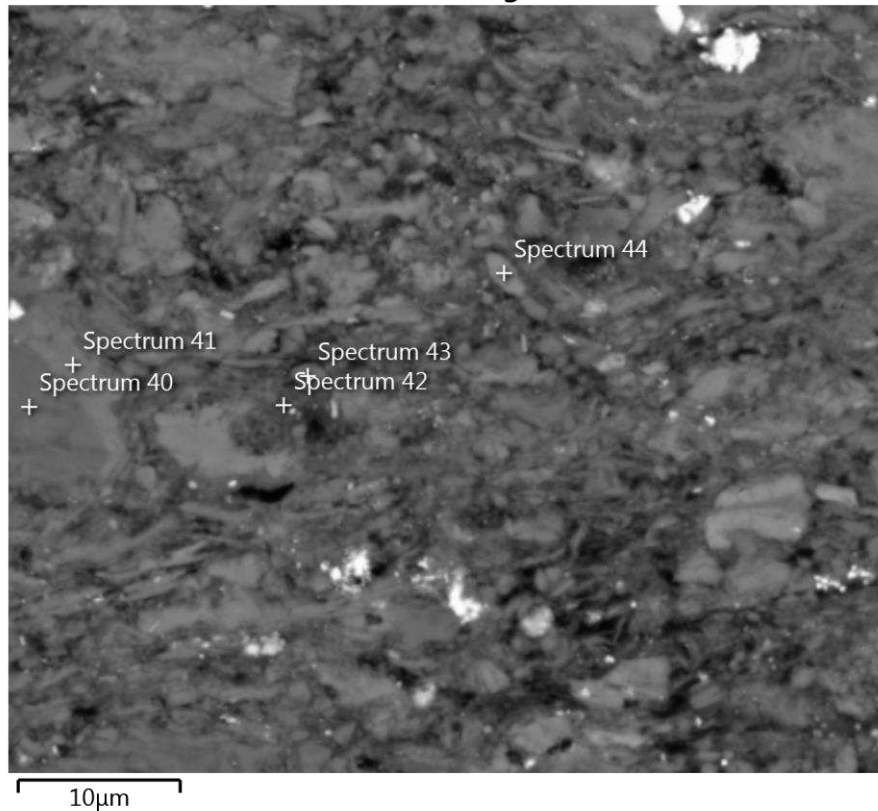
#12785-11276: Phycosiphon Fecal String in Facies 2a- More OM and slighlty finer grained. Appears that some clays are going perpendicular to clays on the side.

pt40   Dolomite
pt41   Dolomite-Fe-rich
pt42   Clay Mixture- With Vanadium
pt43   Quartz
pt44   Calcite

Electron Image 8
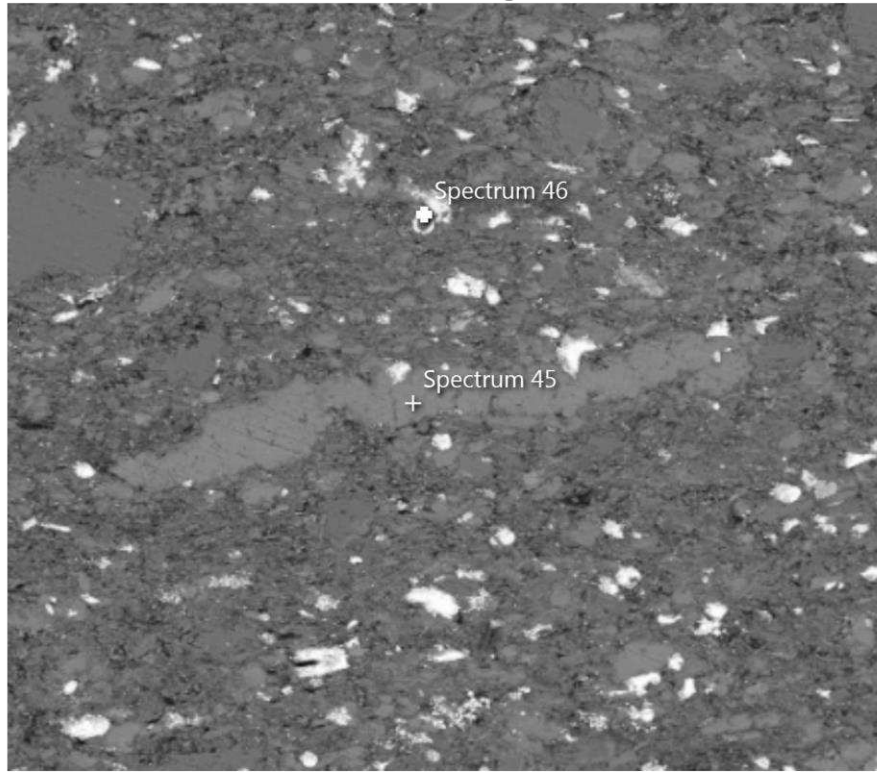
50μm

#12785-11275: Facies 2a cements
pt45   Calcite
pt46   Pyrite

Electron Image 9

10μm
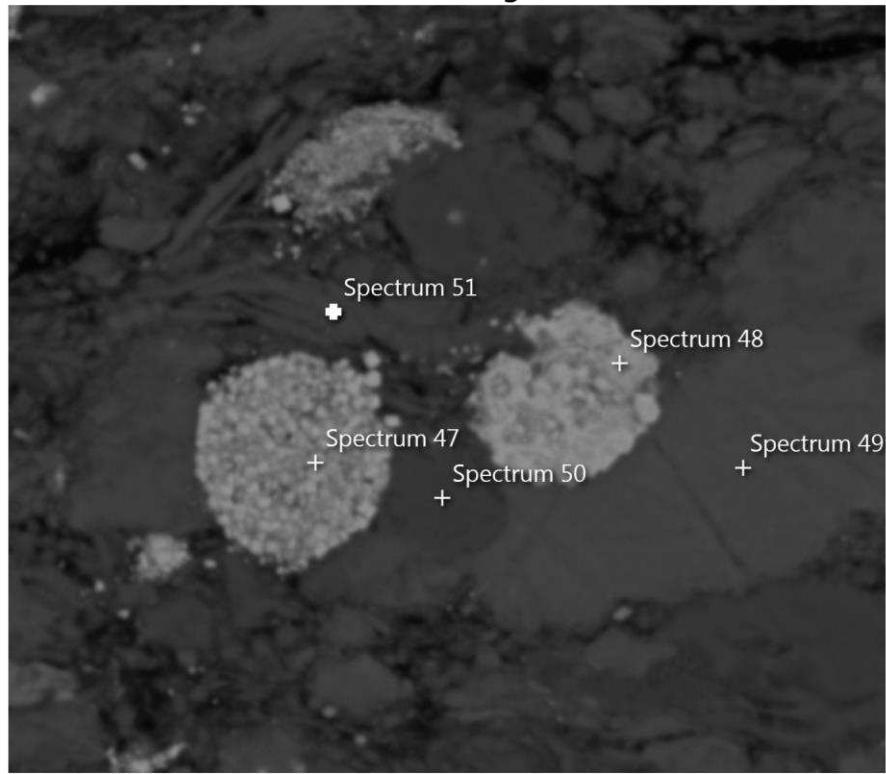
#12785-11275: Facies 2a cements and grains.

pt47   Pyrite
pt48   Pyrite
pt49   Calcite
pt50   Quartz
pt51   Illite

Electron Image 10

10μm
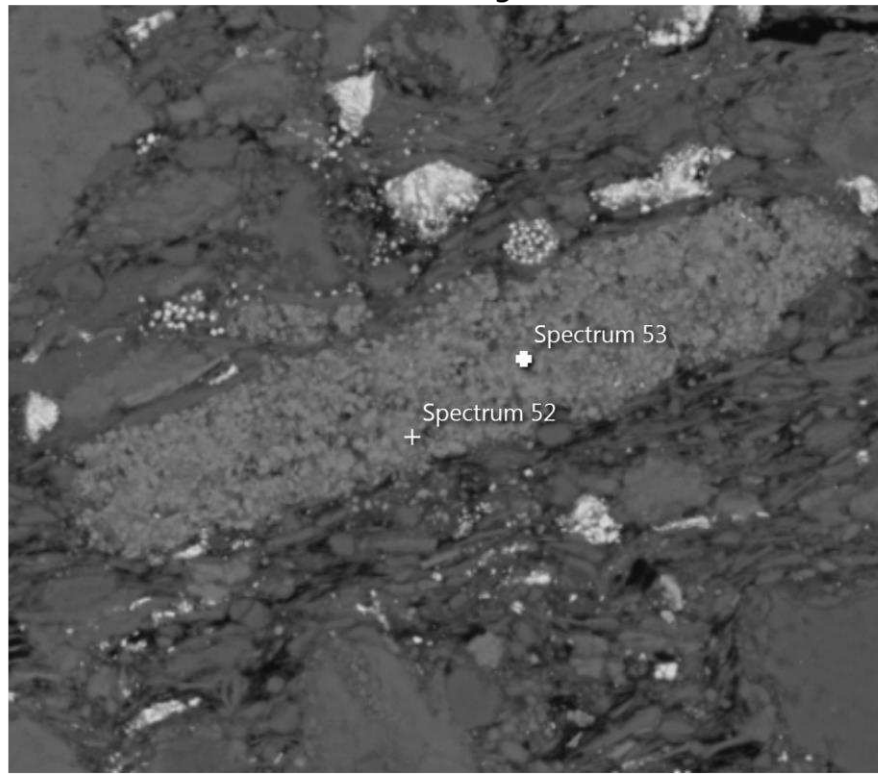
#12785-11275: Fecal pellet? In facies 2a
Pt52   Phosphate
Pt53   Phosphate

Electron Image 17

Spectrum 94

Spectrum 93

100μm
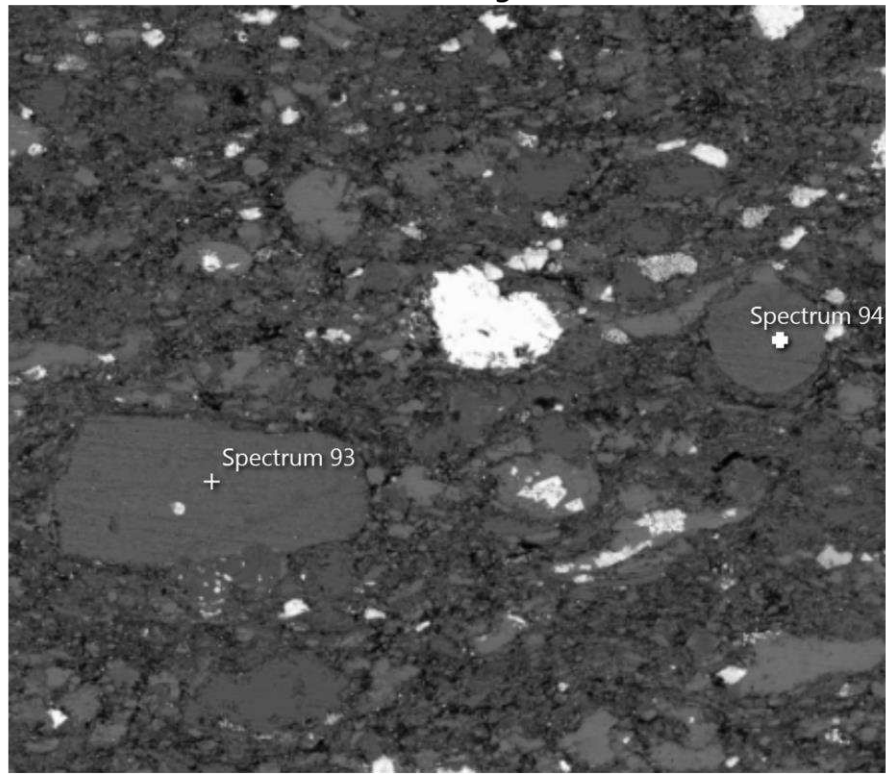
#12785-11275: Facies 2a
Pt92   Biotite
Pt93   Biotite

Facies 2b

Electron Image 11

Spectrum 6061
Spectrum 63
Spectrum 62
Spectrum 68
Spectrum 64
Spectrum 65
Spectrum 69
Spectrum 66
Spectrum 67

100μm
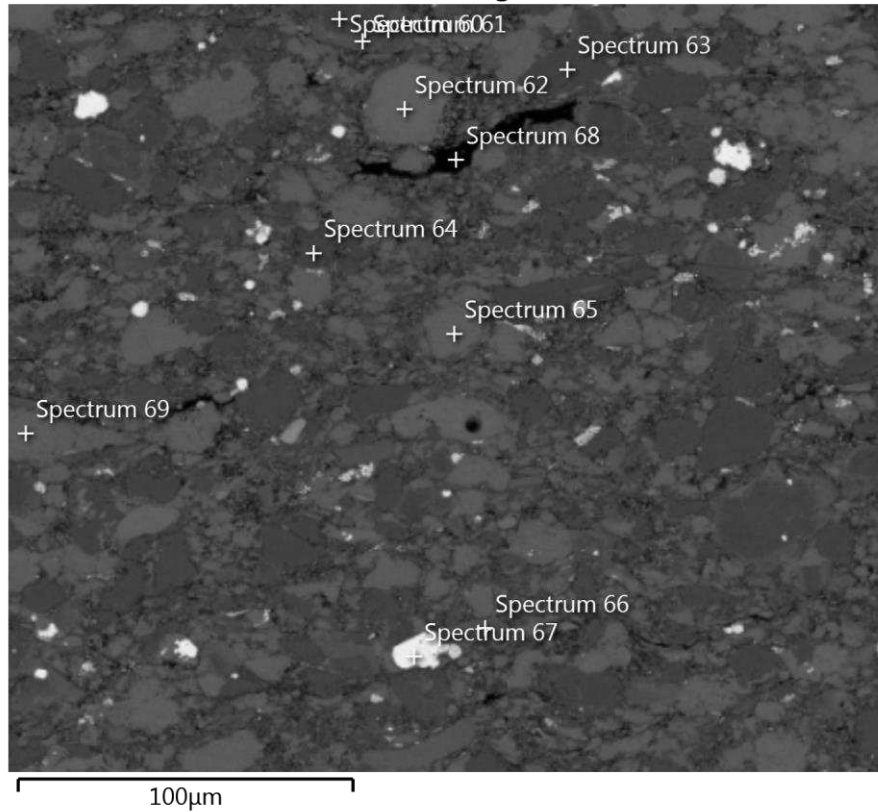
#8251-10369.6: Coarser grains of Facies 2b
Pt63   Quartz
Pt64   Quartz
Pt65   Calcite Mg-rich
Pt66   Illite
Pt67   Pyrite
Pt68   Epoxy
Pt69   Dolomite

Electron Image 12

100µm
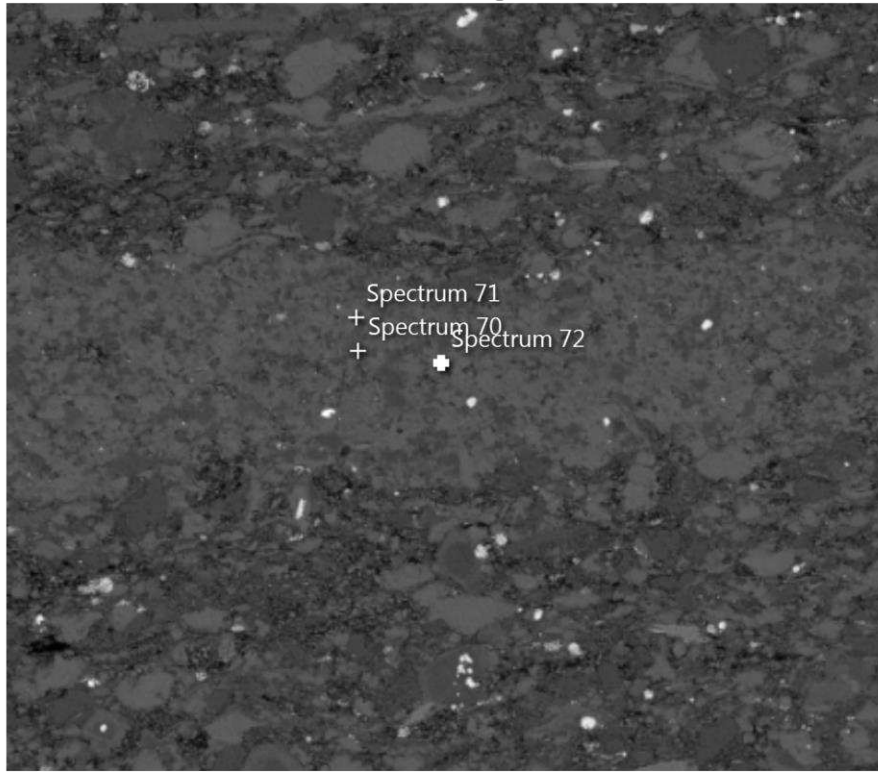
#8251-10369.6: Zoomed in on Planolites near the knotch at the top of thin section in Facies 2b

Pt70   Dolomite
Pt71   Calcite
Pt72   Calcite

Electron Image 13
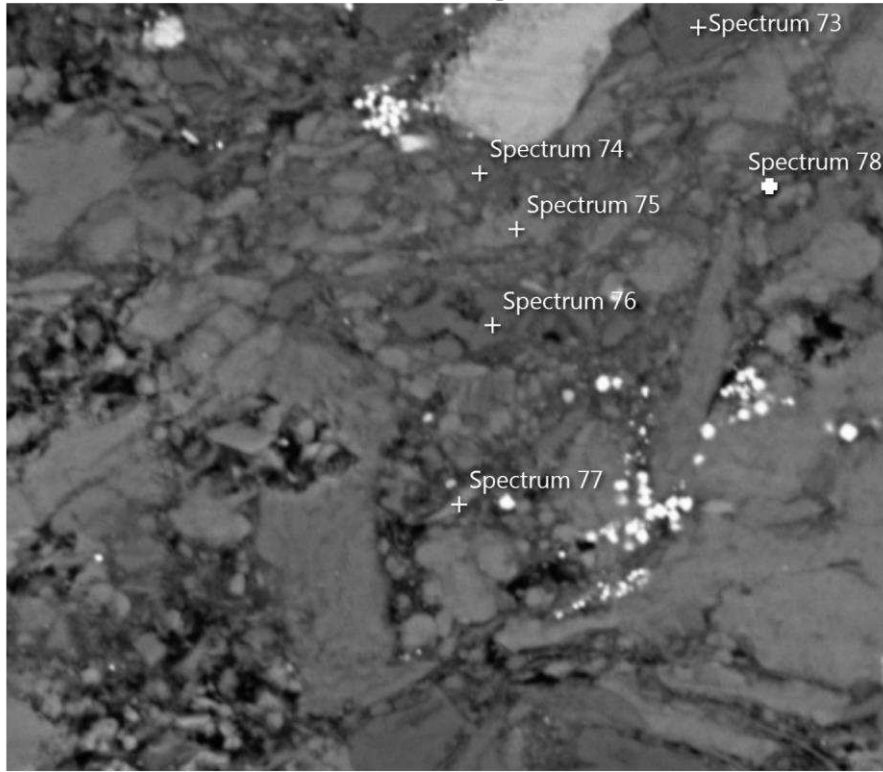
#8251-10369.6: Matrix of Facies 2b

pt73   Quartz
pt74   Dolomite
pt75   Calcite
pt76   Quartz
pt77   Chlorite
pt78   Clay-Calcite/Clay mix

Facies 3

Electron Image 14

Spectrum 82

Spectrum 79

Spectrum 83

Spectrum 81

Spectrum 80

10μm
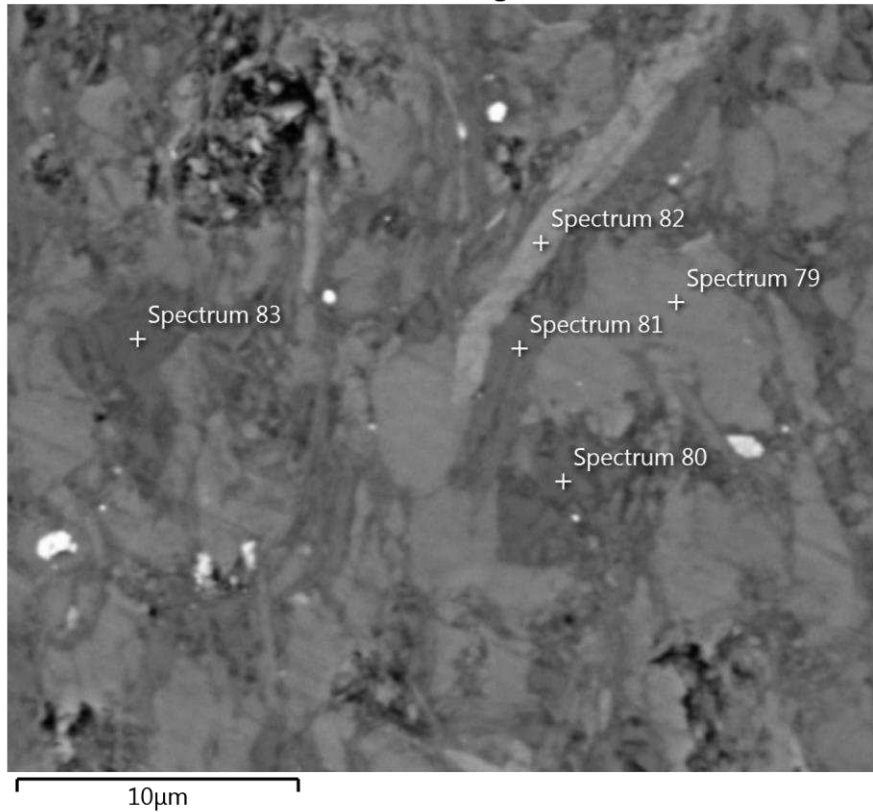
#12886-10509: Matrix of facies 3

pt79   Calcite

pt80   Quartz

pt81   Illite to Muscovite

pt82   Chlorite

pt83   Quartz

Electron Image 16

50µm
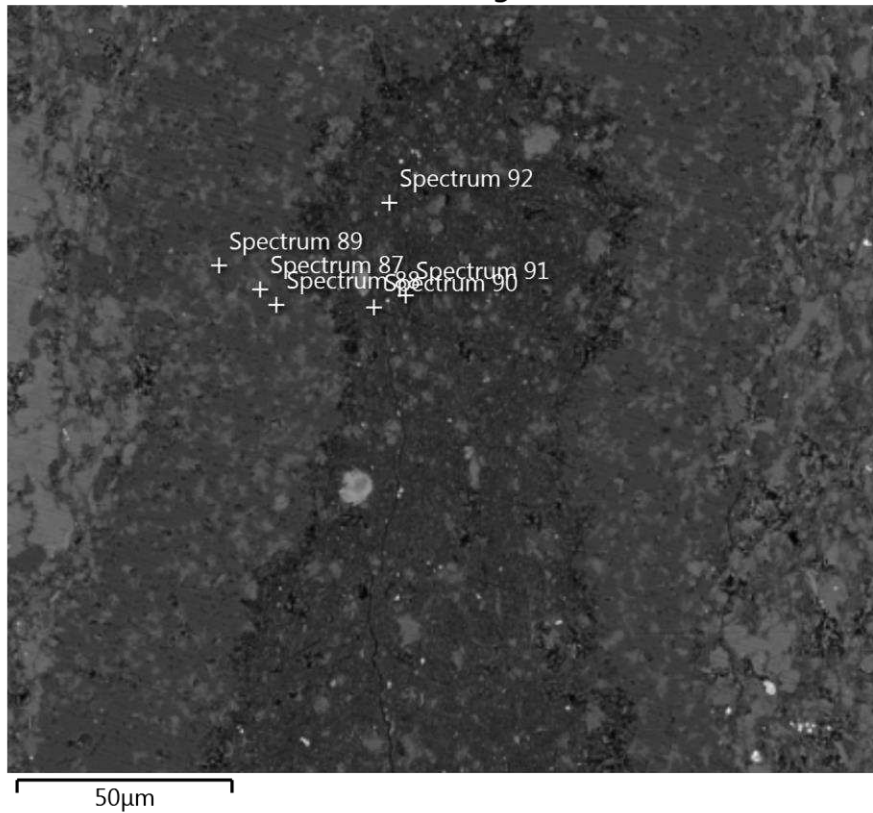
#12886-10509: Composition of agglutinated foraminifera in facies 3.

pt87   Kspar
pt88   Quartz
pt89   Quartz
pt90   Clay-Clay supported in matrix not much organic matter in the center
pt91   Clay
pt92   Quartz

Electron Image 18

50µm
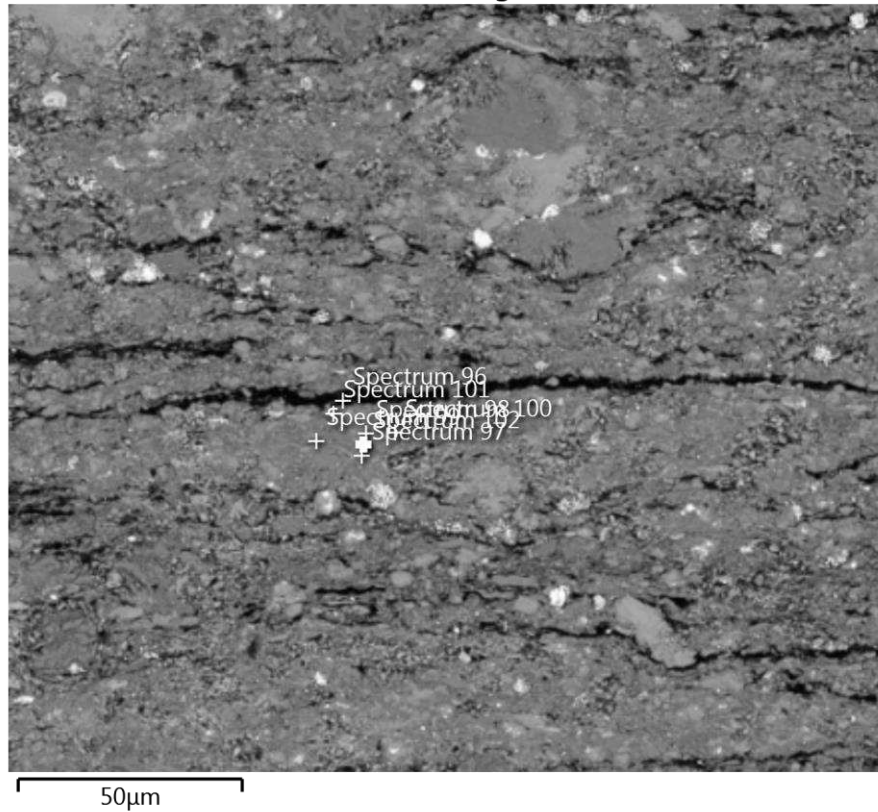
#26661-9327.3: Facies 4 with clay clast outlined by organic matter

pt96   Organic matter
pt97   Calcite with clays
pt98   Quartz with clays
pt99   Quartz
pt100   Calcite
pt101   Kspar
pt102   Pyrite

Electron Image 19
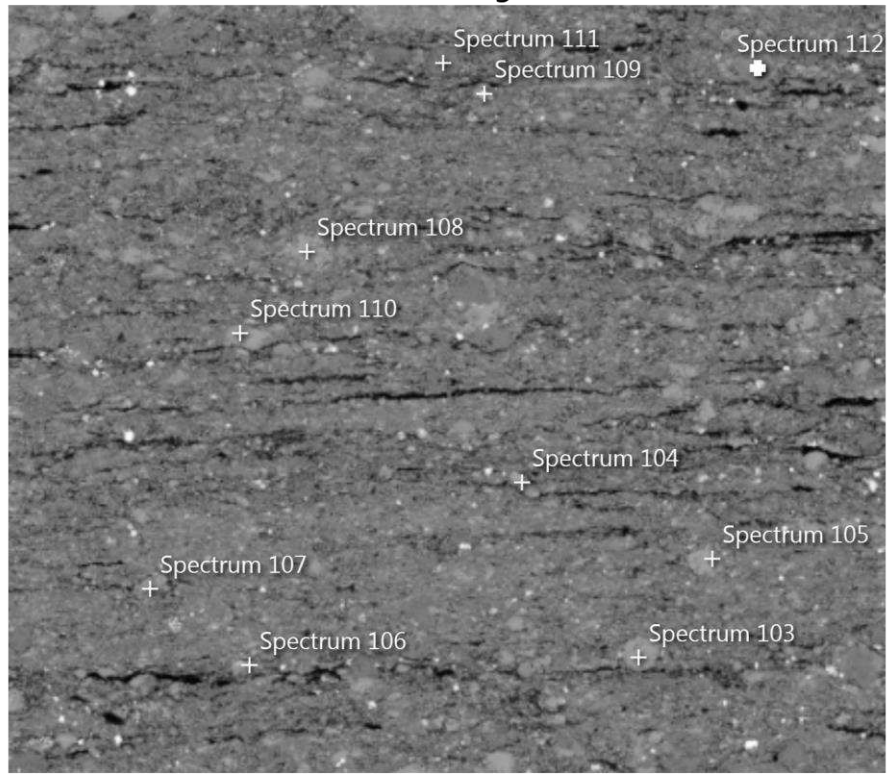
#26661-9327.3: Coarse grains within Facies 4 lamina

pt103   Calcite
pt104   Calcite
pt105   Calcite
pt106   Chlorite
pt107   Calcite
pt108   Calcite
pt109   Pyrite
pt110   Calcite
pt111   Quartz
pt112   Dolomite

Electron Image 20
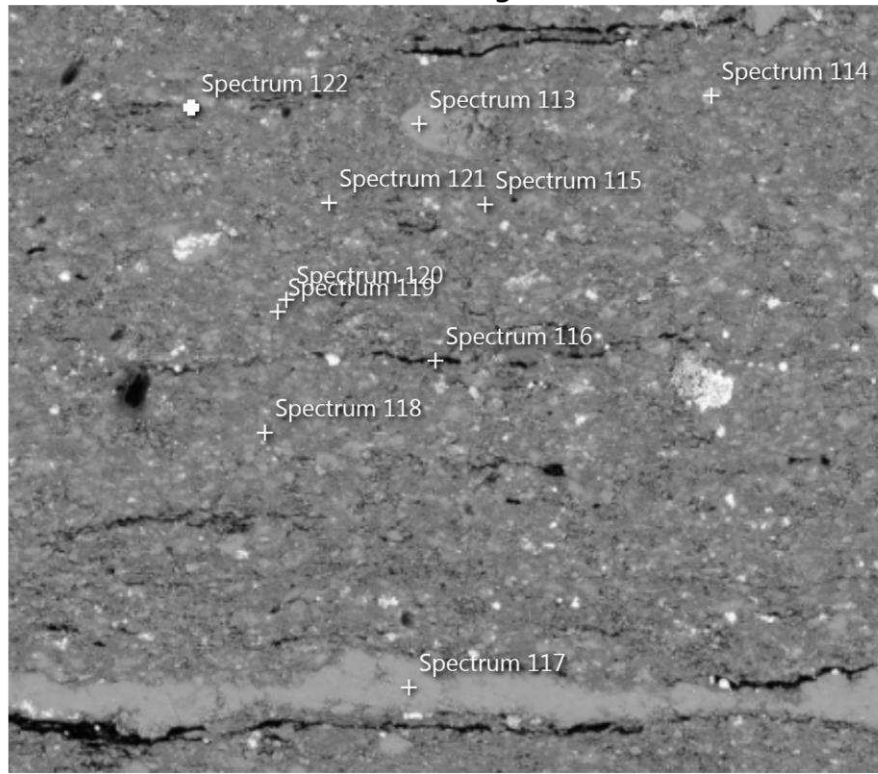
#26661-9327.3: Light band just above dark clay lamina under knotch in facies 4

pt113   Calcite
pt114   Apatite
pt115   Dolomite
pt116   OM
pt117   Calcite
pt118   Illite
pt119   Rutile
pt120   Calcite
pt121   Chlorite
pt122   Chlorite

Electron Image 21
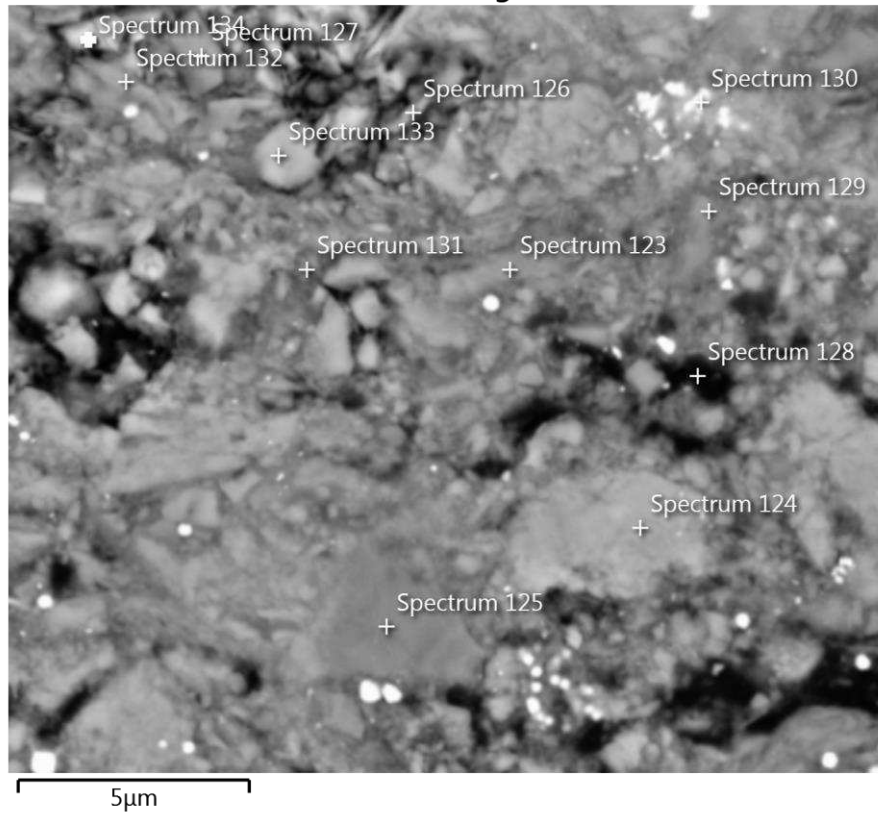
#26661-9327.3: Matrix of facies 4

pt123   Clay
pt124   Calcite
pt125   Dolomite
pt126   Clay
pt127   Quartz
pt128   OM
pt129   Quartz
pt130   Pyrite
pt131   Clay
pt132   Clay
pt133   Kspar
pt134   Calcite

Electron Image 30

10μm
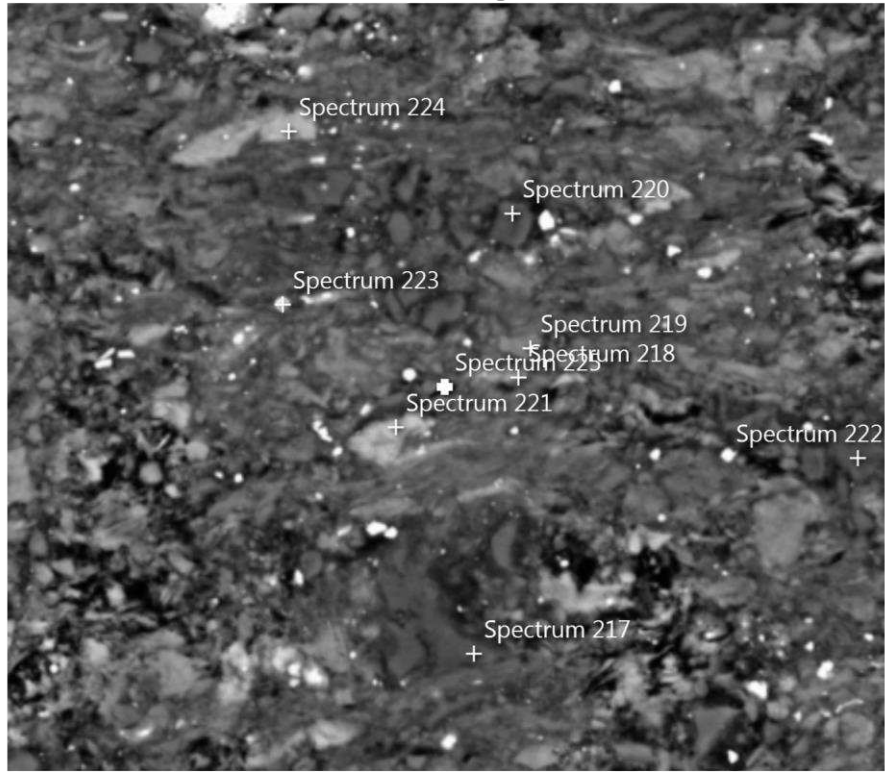
#22092-9879: Composition of matrix in facies 4.

pt217   Quartz
pt218   Clay
pt219   Calcite
pt220   Quartz
pt221   Clay
pt222   Quartz
pt223   Pyrite
pt224   Clay
pt225   Clay

Electron Image 32
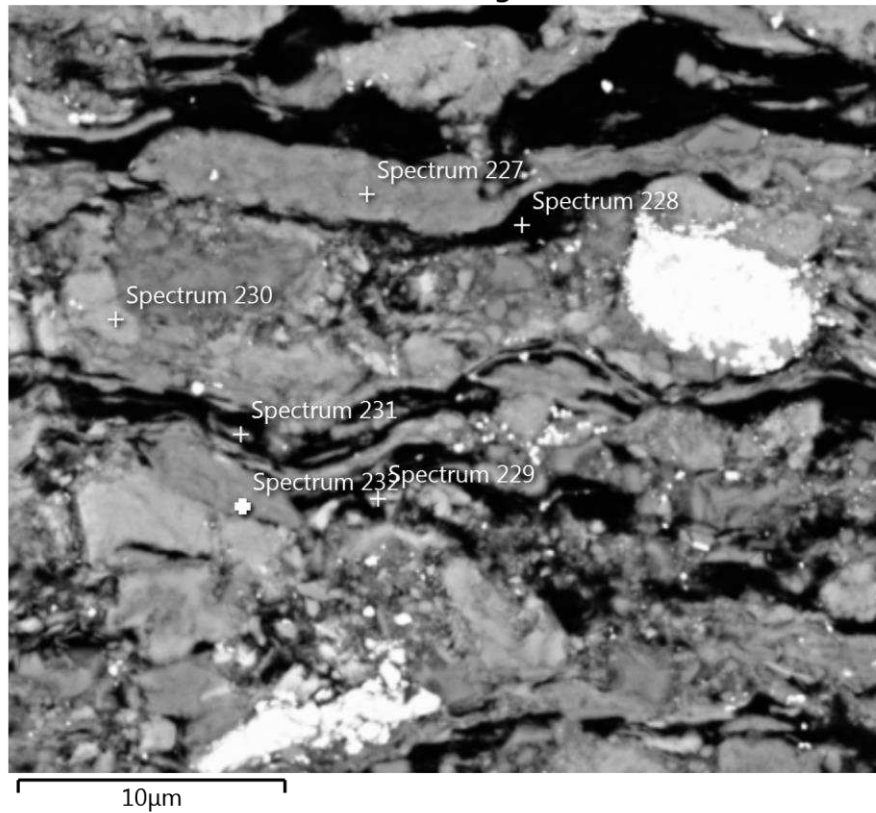
#22092-9879: Within Facies 4 lamina

pt227   Clay
pt228   Organic matter
pt229   Calcite and Clay
pt230   Calcite
pt231   Quartz
pt232   Clay

Electron Image 33
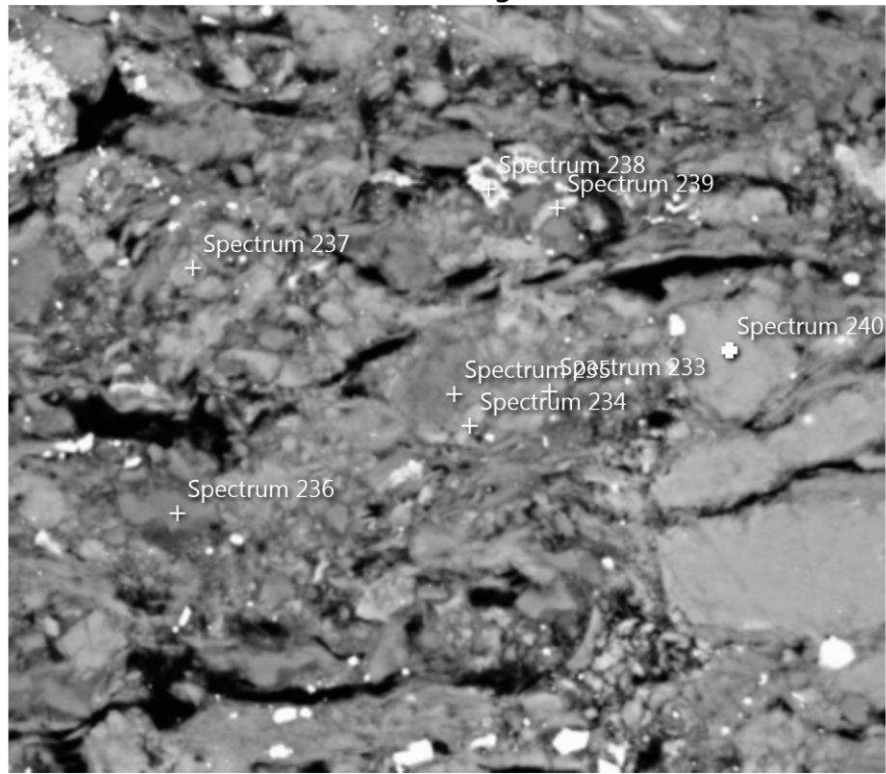
#22092-9879: Matrix of Facies 4 laminae

pt233   Kspar
pt234   Dolomite
pt235   Dolomite
pt236   Quartz
pt237   Calcite
pt238   Rutile
pt239   Chlorite
pt240   Calcite
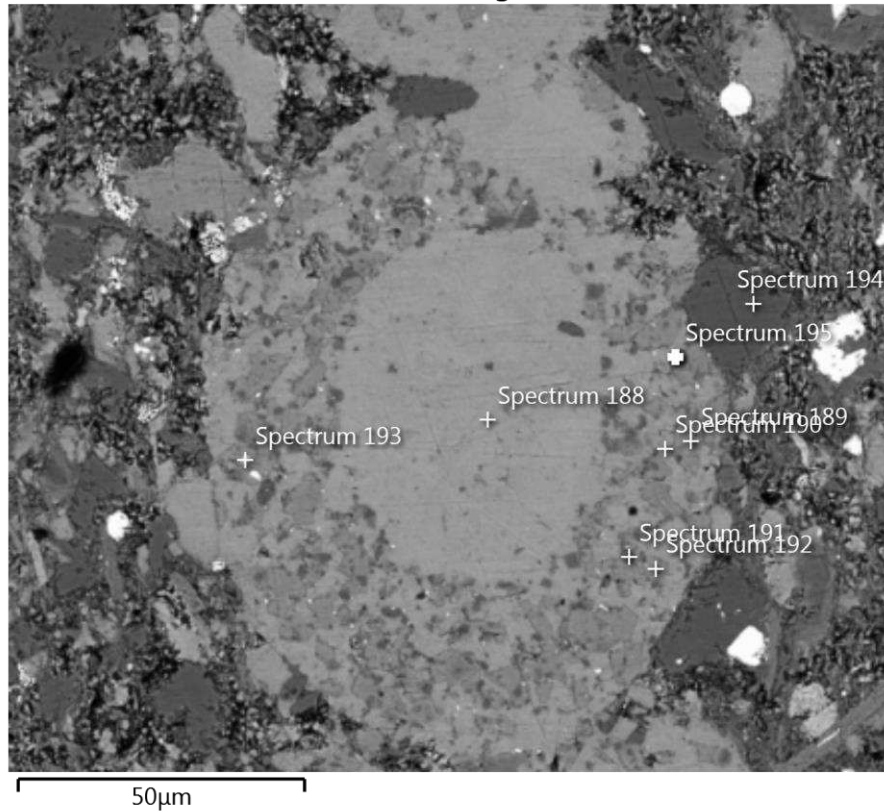
Electron Image 27

#19709-9250.3: Calcisphere in facies 5

pt188   Calcite
pt189   Kspar
pt190   Calcite And Kspar
pt191   Quartz
pt192   Kspar
pt193   Pyrite
pt194   Quartz
pt195   Quartz

Electron Image 28
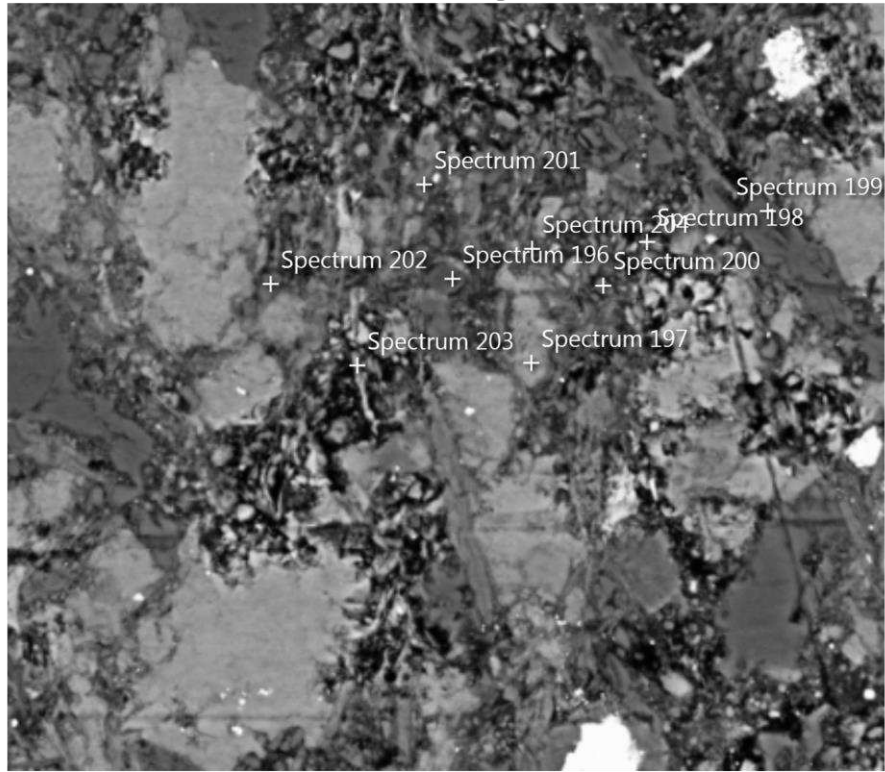
10μm

#19709-9250.3: Matrix in upper lighter half of thin section of facies 5

pt196   Quartz
pt197   Calcite
pt198   Clay
pt199   Quartz
pt200   Albite
pt201   Illite and Muscovite
pt202   Quartz
pt203   Clay
pt204   Clay and Calcite

Electron Image 29
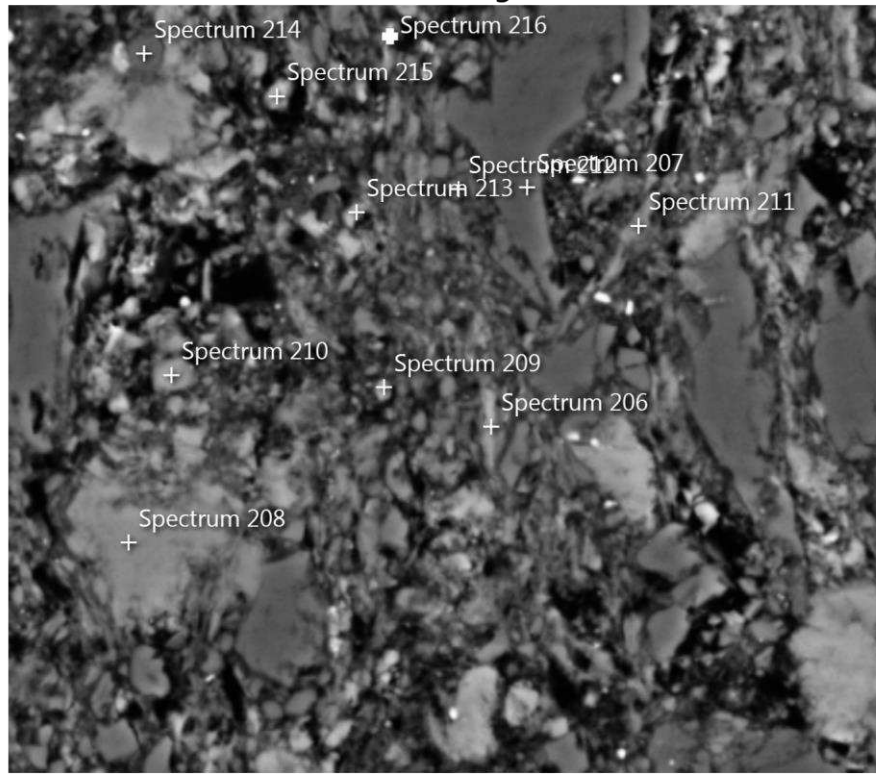
#19709-9250.3: Matrix in bottom darker half of facies 5

pt206   Calcite and Clays
pt207   Quartz
pt208   Kspar
pt209   Calcite and Clays
pt210   Kspar
pt211   Illite
pt212   Quartz
pt213   Kspar
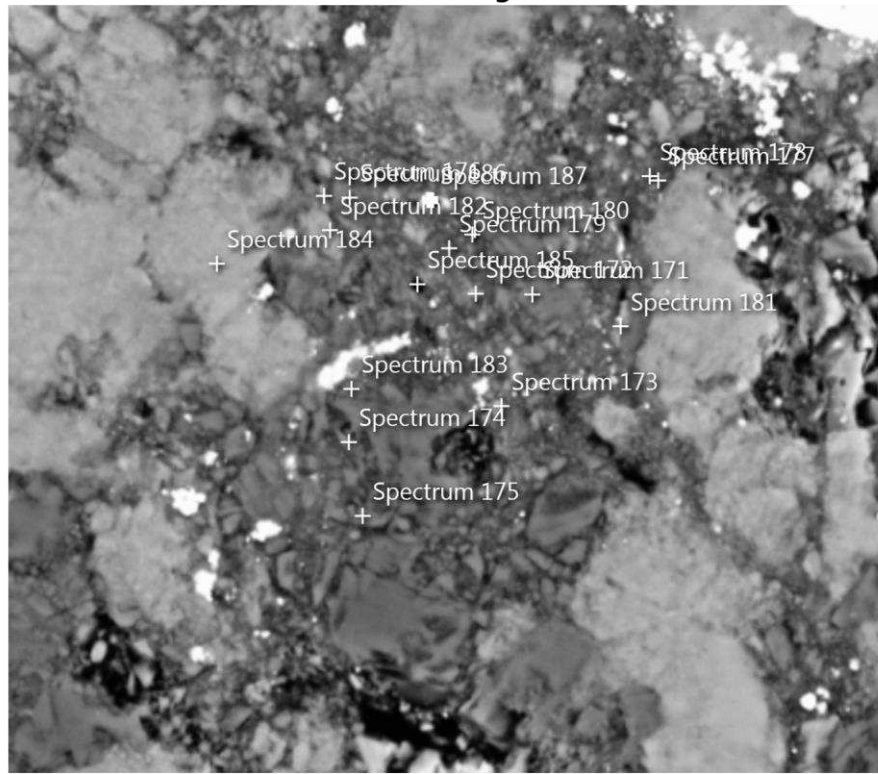pt214   Quartz
pt215   Calcite and Chlorite
pt216   Clay

Electron Image 24
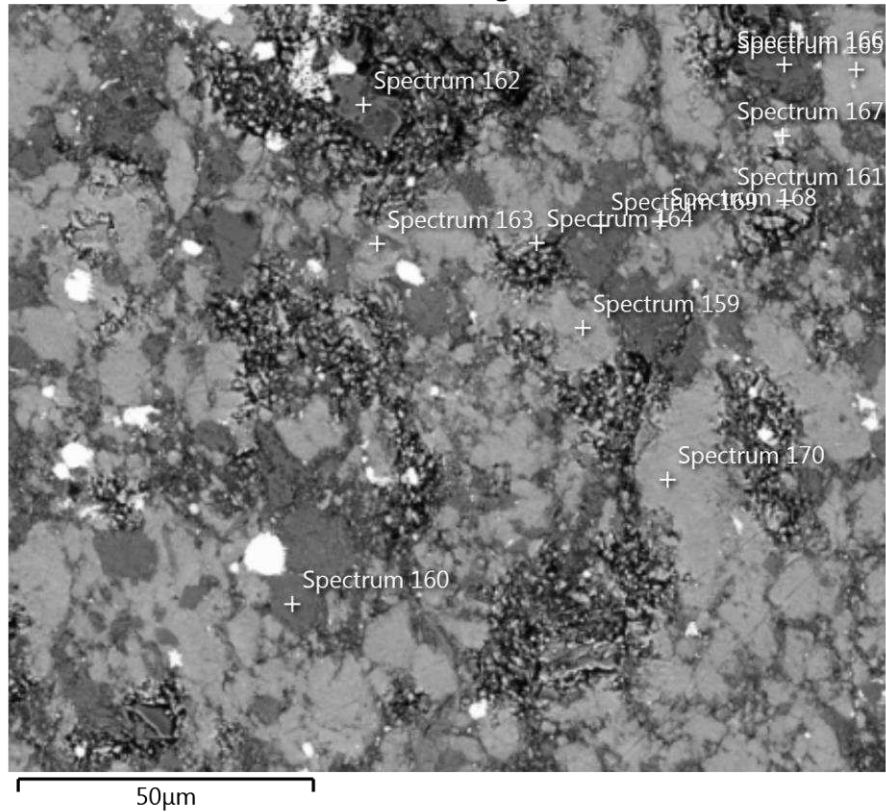
#17396-7915.8: Coarse grains within the lower half of this thin section in facies 6

pt159   Calcite
pt160   Dolomite
pt161   Calcite
pt162   Quartz
pt163   Calcite
pt164   Calcite
pt165   Calcite
pt166   Quartz
pt167   Pyrite
pt168   Calcite
pt169   Dolomite
pt170   Dolomite

Electron Image 26

10μm

#17396-7915.8- Matrix of lower half of the thin section within facies 6.

pt171   Dolomite
pt172   Everything- Calcite/Clay/Pyrite
pt173   Clay-Calcite
pt174   Quartz
pt175   Quartz
pt176   Rutile-Clay and Calcite
pt177   Chlorite and Calcite
pt178   Chloriteand Calcite
pt179   Clay
pt180   Clay
pt181   Calcite
pt182   Calcite
pt183   Quartz
pt184   Calcite
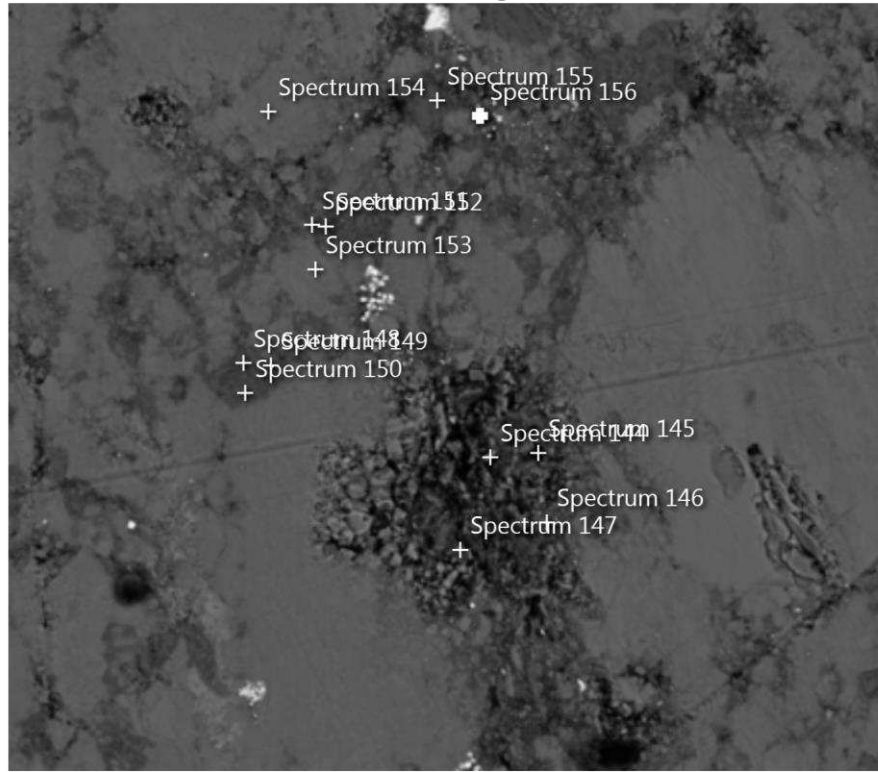pt185   Clay
pt186   Dolomite
pt187   Rutile
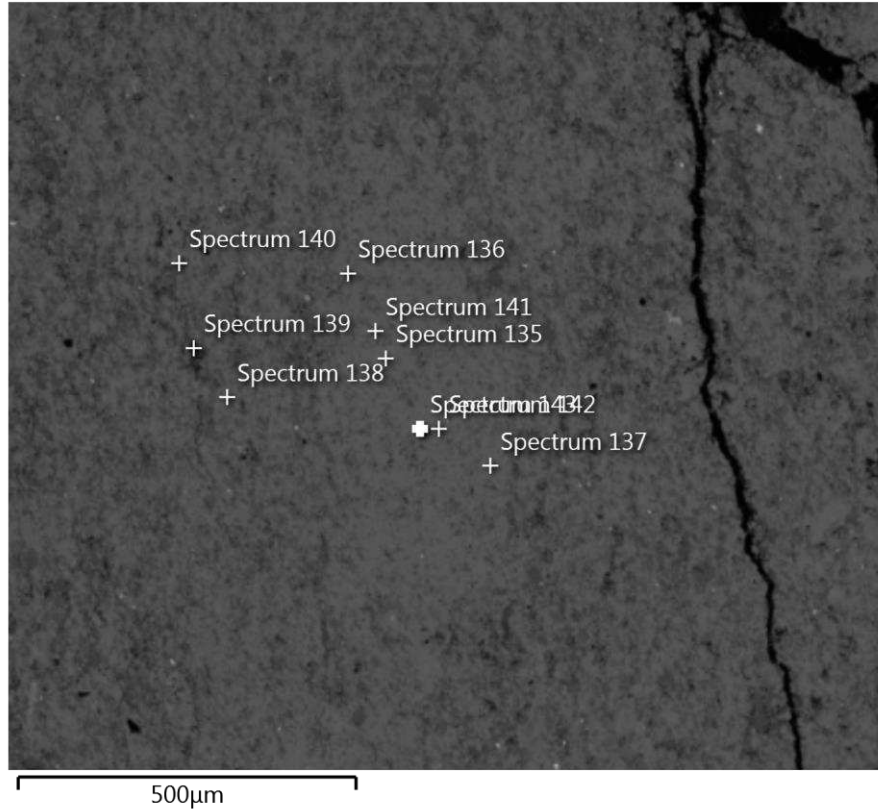
Electron Image 22

#17396-7915.8: Planolites burrow within Facies 8.

pt135   Calcite
pt136   Quartz
pt137   Calcite
pt138   Calcite
pt139   OM
pt140   Dolomite
pt141   Quartz
pt142   Calcite
pt143   Calcite

Electron Image 23

25μm

#17396-7915.8: Matrix within facies 8

pt 144   Calcite
pt 145   Calcite
pt 146   Pyrite
pt 147   Calcite
pt 148   Quartz
pt 149   Calcite
pt 150   Quartz
pt 151   Calcite
pt 152   Quartz
pt 153   Calcite
pt 154   Calcite
pt 155   Dolomite
pt 156   Rutile